



**University of Natural Resources  
and Life Sciences, Vienna**

DISSERTATION

APPLICATION POTENTIAL AND OPTIMIZATION OF  
HIGH TEMPERATURE HEAT PUMP SYSTEMS FOR  
PROCESS HEAT SUPPLY

ausgeführt zum Zwecke der Erlangung des akademischen Grades eines Doktors  
der Bodenkultur unter der Leitung von

Univ. Prof. Dipl.-Ing. Dr. techn. Tobias Pröll

am Institut für Verfahrens- und Energietechnik  
eingereicht an der Universität für Bodenkultur Wien,  
Department für Materialwissenschaften und Prozesstechnik

von  
Dipl. Ing. Magdalena Wolf  
Matrikelnummer: 0740214  
Grüngasse 9/14  
1050 Wien

Vienna, August 10, 2017

.....  
Magdalena Wolf



# Abstract

Heat pumps may play an important role in a sustainable energy system based on renewable electricity. While heat pumps are already widely used in the field of building technology, they still play a menial role in industrial heat supply. This is due to both technological and economic reasons.

The present work focuses on the technical process design of mechanically driven high temperature heat pumps (HTHP) and shows optimization potentials, which can be applied to increase the efficiency of these systems. The aim is to provide process heat at a temperature level between 120°C and 150°C<sup>1</sup>. The methodology bases on experimental heat pump testing, thermodynamic analysis and process simulation. A tool for exergy-analysis of heat pump processes is presented and the relevant heat supply processes are modelled on a thermodynamic level.

As first part of this work, a high-temperature heat pump testing station was developed, which allows determination of efficiency parameters of HTHP. In contrast to conventional heat pump testing stations, the developed system is designed for temperatures up to 150°C and pressures up to 40 bar<sub>abs</sub> in the heat carrier streams. The design of the heat pump testing station enables a resource efficient operation because only the amount of heat according to the electric energy of the heat pump must be removed in a cooler. Operation of a commercially available heat pump on the testing station shows that the technical specifications are reached by the testing station and by the tested heat pump at least up to the tested temperatures of 60°C.

In the second part of this work, HTHP systems are optimized depending on the used working fluid. The working fluids are classified according to their behaviour during the compression into two groups. The first group shows a superheating behaviour during the compression process. The reason for this is a bell-shaped two-phase area. In the second group suction gas superheating after evaporation step is necessary to prevent condensation during the compression process. These working fluids belong to the group with re-entrant saturation line. Depending on the process design, an efficiency improvement between 13% and 63% can be achieved with the proposed optimization measures.

In the third part of this thesis, a potential application case for HTHP in the field of pulp and paper industry is investigated. A HTHP system is compared with state of the art gas and steam turbine systems for low-pressure steam supply. Beside thermodynamic performance, economic factors are considered. For the period from January 2013 to June 2016 an optimization calculation with the target function of minimum costs of heat production was carried out, based on real electricity and gas prices from the European Energy Exchange (EEX). The share of the supply through HTHP varies between 45% and 76%, depending on the assumed investment costs.

In conclusion, the results show that the developed testing environment is suitable

---

<sup>1</sup>The unit of the temperature in all calculations accord to the SI-Unit [K]. Only for readability the temperatures are denoted in [°C].

for heat pump performance testing. Further, a significant efficiency increase can be achieved, especially if excess suction gas superheating is applied with re-entrance working fluids while wet compression could be interesting for HTHP using water (R718) as working fluid.

The investigated case study shows that installation of HTHP systems may represent an economic alternative to common fossil fuel-based heat generation methods, depending on the price relation of electricity and (fossil) fuels. The expected future development towards renewable electricity generation and cost penalties for CO<sub>2</sub> emissions from fossil fuels will make the installation of heat pumps for process heat supply more attractive.

# Kurzfassung

In einem nachhaltigen Energiesystem spielen Wärmepumpen eine wichtige Rolle. Während im gebäudetechnischen Bereich diese Technologie bereits breite Anwendung findet, kommt ihr im industriellen Wärmebereitungssektor noch eine untergeordnete Rolle zu. Gründe dafür sind einerseits technologische, aber auch wirtschaftliche Faktoren.

Die vorliegende Arbeit fokussiert daher die technische Prozessauslegung von elektrisch betriebenen Hochtemperaturwärmepumpen (HTHP) und zeigt Optimierungspotenziale auf, mit der die Effizienz dieser Systeme gesteigert werden kann. Als Ziel wird die Bereitstellung von Prozesswärme auf einem Temperaturniveau zwischen  $120^{\circ}\text{C}$  und  $150^{\circ}\text{C}^2$  angestrebt. Mittels Prozesssimulation werden die relevanten Prozesse abgebildet und, auf Basis thermodynamischer Stoffdaten, die Effizienzparameter bestimmt. Zudem wurde ein Wärmepumpenprüfstand entwickelt, mit dem die Effizienz von Hochtemperaturwärmepumpen bestimmt werden kann.

Im ersten Teil der Arbeit wird der entwickelte Hochtemperaturwärmepumpenprüfstand beschrieben. Im Gegensatz zu herkömmlichen Wärmepumpenprüfständen ist die entwickelte Anlage auf Temperaturen bis zu  $150^{\circ}\text{C}$  und Drücke bis zu  $40\text{ bar}_{\text{abs}}$  im Wärmeträgermedium ausgelegt. Ein zyklischer Aufbau ermöglicht einen ressourcenschonenden Betrieb, da über das Kühlsystem nur ein kleiner Teil der Heizleistung abgeführt werden muss. Die Funktion des Prüfstandes wurde mit einer Heizungs-Wärmepumpe, die auch die Bereitstellung von Warmwasser ermöglicht, evaluiert.

Im zweiten Teil der Arbeit wird auf die Optimierung von Wärmepumpenprozesse eingegangen. Bei der Optimierung der HTHP-Systeme wird nach eingesetztem Kältemittel unterschieden. Diese werden entsprechend ihrem Verhalten während des Verdichtungs Vorganges in zwei Gruppen eingeteilt. Die erste Gruppe zeigt ein überhitzendes Verhalten während des Verdichtungs Vorganges. Grund dafür ist ein glockenförmiges Zweiphasengebiet. Bei der zweiten Gruppe hingegen ist ein Überhitzen nach dem Verdampfen zwingend nötig, um während des Verdichtungs Vorganges Kondensation zu verhindern. Bei diesen Kältemitteln liegt ein überhängendes Zweiphasengebiet vor. Je nach Prozessdesign kann mit den vorgeschlagenen Optimierungsmaßnahmen eine Effizienzsteigerung zwischen 13% und 63% erzielt werden.

Im dritten Teil wird ein potenzieller Anwendungsfall für HTHP zur Prozesswärmebereitung in einem industriellen Betrieb untersucht. Dabei werden neben exergetischen Größen auch wirtschaftliche Faktoren berücksichtigt. Verglichen wird eine HTHP mit derzeit eingesetzten Gas- und Dampfturbinensystemen zur Prozesswärmebereitung in einem papierverarbeitenden Betrieb. Für die Periode von Jänner 2013 bis Juni 2016 wurde eine Optimierungsrechnung mit der Zielfunktion der minimalen Wärmegestehungskosten auf Basis realer Strom- und Gaspreise durchgeführt. Der Erzeugungsanteil der HTHP schwankt in Abhängigkeit der angenommenen Investitionskosten zwischen

---

<sup>2</sup>Die Temperaturen sind in der SI-Einheit [K] angegeben und in dieser Einheit in die Formeln einzusetzen. Für eine fließende Lesbarkeit werden die Temperaturen in [ $^{\circ}\text{C}$ ] angegeben.

45% und 76%.

Die Ergebnisse dieser Arbeit zeigen, dass der entwickelte Wärmepumpenprüfstand den Anforderungen zur Bestimmung der Effizienzparameter gerecht wird. Zudem zeigen die Ergebnisse, dass mit den untersuchten Optimierungsmaßnahmen eine signifikante Effizienzsteigerung erzielt werden kann. Kältemittel mit einem überhängenden Kältemittel profitieren von exzessiver Sauggasüberhitzung, während bei Einsatz von Wasser (R718) Nassdampfkompensation zur Optimierung eingesetzt werden kann. Der untersuchte Anwendungsfall zeigt, dass HTHP-Systeme eine wirtschaftliche Alternative zu gängigen fossilen Wärmebereitstellungsmethoden, in Abhängigkeit von vorherrschenden Energiepreisen, darstellen. In einem zukünftigen Energiesystem basierend auf einem hohen Anteil an erneuerbarer Stromerzeugung und steigenden Kosten für CO<sub>2</sub> Emissionen stellen Wärmepumpen eine attraktive Alternative zur Prozesswärmebereitung dar.

# Preface and Acknowledgements

The present thesis is divided into three parts, which are in this sense stand-alone sections. All parts contain a short literature overview, a methodical approach and conclusions of the obtained results. The first part describes the developed heat pump testing station with focus on testing high temperature heat pump systems. The second chapter examines the different optimization technologies for high temperature heat pump systems according to the used working fluid. The third part introduces a application case of high temperature heat pump systems for process heat supply in the field of pulp and paper industry.

First of all, I like to thank my supervisor Univ. Prof. Dipl.-Ing. Dr. Tobias Pröll for giving me the opportunity to work in the research group Energy Technology and Energy Management. He motivated me to write my dissertation thesis in the section of HTHP. Furthermore, I like to thank him for encouraging my personal way of working and for his support during finalisation of this work.

I would like to extend my sincerest gratitude to Ao. Univ. Prof. Dipl.-Ing. Dr. Herbert Braun for supporting me during my studies and for the trust he put in me. I also say thank you for evaluating my dissertation.

I would also like to thank Ao. Univ. Prof. Dipl.-Ing. Dr. Andreas Werner for assessing this thesis.

I would like to express a very warm thank you to all my colleagues in the research group Energy Technology and Energy Management for the interesting, inspiring and enjoyable talks!

My thanks also go to my graduate students, DI Andreas Leitner, DI Benedikt Kogler, DI Tobias Kalthoff, Anna Austaller, BSc., Thomas Detzlhofer, BSc., and Norbert Heinrich, BSc., who supported me with their activities in my research work.

The present work was developed during my research work at the Institute for Chemical and Energy Engineering at the University for Natural Resources and Life Sciences, Vienna. Thanks to all those responsible and the state of Austria, who gave me an eminent education and for the opportunity to work in this institution.

I would like to thank my mother Veronika, who always stood by me with help and advice and she always supported me with all my decisions. All I can say is thank you!

I also would like to thank my father Manfred, who enabled me my education, and who gave me the opportunity to develop my strengths. I am thinking of you every day!

Finally, my deepest and greatest gratitude to Peter! This thesis would simply not exist without you and your support. Thank you so much for lifting me up whenever I'm down, for your good advices and your understanding in work-intensive hours!



# Nomenclature

## Abbreviations

<i>CHP</i>	combined heat and power
<i>CoH</i>	costs of heat
<i>EEX</i>	European energy exchange
<i>FL</i>	Fuzzy logic
<i>GT – CC</i>	gas turbine and steam combined cycle
<i>GT</i>	gas turbine process
<i>GWP</i>	Global Warming Potential
<i>HFC</i>	Hydro Fluorocarbons
<i>HFC</i>	hydrofluorocarbon
<i>HFO</i>	Hydro Fluoroelaines
<i>HTHP</i>	high temperature heat pump process
<i>HX</i>	heat exchanger
<i>IHX</i>	internal heat exchanger
<i>LHV</i>	lower heating value
<i>MDK</i>	Model Development Kit
<i>NIST</i>	National Institute of Standards and Technology
<i>NPV</i>	net present value
<i>ODP</i>	Ozon Depletion Potential
<i>PSE</i>	Process Simulation Environment
<i>R114</i>	1,2-Dichlorotetrafluoroethane
<i>R11</i>	Trichlorofluoromethane
<i>R1233zd</i>	1-chloro-3,3,3-Trifluoroprop-1-en
<i>R1234yf</i>	2,3,3,3-Tetrafluoroprop-1-en
<i>R1234ze(E)</i>	trans-1,3,3,3-Tetrafluoroprop-1-en
<i>R134a</i>	1,1,1,2-Tetrafluoroethane
<i>R22</i>	Chlorodifluoromethane
<i>R236fa</i>	1,1,1,3,3,3-Hexafluoropropane
<i>R245fa</i>	1,1,1,3,3-Pentafluoropropane
<i>R290</i>	Propane
<i>R365mfc</i>	1,1,1,3,3-Pentafluorobutane
<i>R600a</i>	Isobutane
<i>R717</i>	Ammonia
<i>R718</i>	Water
<i>R744</i>	CO <sub>2</sub>
<i>ST</i>	steam turbine
<i>TEV</i>	Thermostatic expansion valve
<i>TEWI</i>	Total Equivalent Warming Impact

## Greek

$\alpha_{recovery}$	recycling factor working fluid
---------------------	--------------------------------

[–]

$\beta$	emission intensity of electric energy	$[kg_{CO_2}/kWh_{el}]$
$\Delta\vartheta_{LM}$	logarithmic mean temperature difference	$[^{\circ}C]$
$\eta_{Compr}$	isentropic efficiency of the compressor	$[-]$
$\eta_{el,GT-CC}$	net electric efficiency of the GT – CC process <sup>3</sup>	$[-]$
$\eta_{el,GT}$	net electric efficiency of the GT process <sup>3</sup>	$[-]$
$\eta_{heat}$	heat utilization efficiency of the process <sup>3</sup>	$[-]$
$\eta_{Mech}$	mechanical conversion efficiency	$[-]$
$\eta_{motor}$	conversion efficiency from the motor	$[-]$
$\eta_{s,C}$	isentropic efficiency of a compressor	$[-]$
$\eta_{s,T}$	isentropic efficiency of a turbine	$[-]$
$\eta_{SGT-800}$	gross efficiency of the SGT-800 GT process <sup>3</sup>	$[-]$
$\eta_{total}$	total fuel utilization efficiency	$[-]$
$\eta_{Turb}$	single cycle efficiency of the gas and the steam turbine	$[-]$
$\kappa$	isentropic exponent	$[-]$
$\rho$	density	$[kg/m^3]$
$\varepsilon^+$	efficiency surplus	$[-]$
$\varepsilon_{Carnot}$	ideal efficiency of the HTHP system	$[-]$
$\vartheta''_C$	outlet temperature secondary side of a HX	$[^{\circ}C]$
$\vartheta''_H$	inlet temperature secondary side of a HX	$[^{\circ}C]$
$\vartheta'_C$	outlet temperature primary side of a HX	$[^{\circ}C]$
$\vartheta'_H$	inlet temperature primary side of a HX	$[^{\circ}C]$
$\vartheta_{acc}$	temperature accuracy	$[^{\circ}C]$
$\xi$	stoichiometric index of complete combustion reaction	$[-]$
$\zeta$	exergetic efficiency of the process	$[-]$
$\zeta_{GT-CC}$	exergetic efficiency of the GT – CC process	$[-]$
$\zeta_{GT}$	exergetic efficiency of the GT process	$[-]$
$\zeta_{HP}$	exergetic efficiency of the heat pump system	$[-]$

### Latin

$\dot{n}_{in}$	molar flow in	$[mol/s]$
$\dot{n}_{out}$	molar flow out	$[mol/s]$
$H$	enthalpy of a substance	$[kJ]$
$H^*(T, p)$	conventional enthalpy of a pure substance	$[kJ]$
$H_{f,298}^0$	standard formation enthalpy of a substance	$[kJ]$
$\Delta h$	difference of specific enthalpy of the used process heat	$[kJ/kg]$
$\Delta H_{f,298,CO_2}^0$	molar standard enthalpy of carbon dioxide at 298.15 K	$[kJ/mol]$
$\Delta H_{f,298,H_2O(g)}^0$	molar standard enthalpy of water (gaseous) at 298.15 K	$[kJ/mol]$
$\Delta H_{f,298,SO_2}^0$	molar standard enthalpy of sulphur dioxide at 298.15 K	$[kJ/mol]$
$\Delta h_{f,298}^0$	spec. standard enthalpy of formation at 298.15 K	$[kJ/kg]$
$\Delta H_{R,298}^0$	reaction enthalpy at standard conditions	$[kJ/mol]$
$\Delta h_{evap,298}$	spec. evaporation enthalpy of water at standard conditions	$[kJ/kg]$
$\Delta p$	pressure drop	$[bar_{abs}]$
$\Delta p_1$	pressure drop of mass flow 1 in a HX	$[bar_{abs}]$
$\Delta p_2$	pressure drop of mass flow 2 in a HX	$[bar_{abs}]$
$\Delta T_{SH}$	temperature difference of superheating	$[K]$
$\dot{B}_Q$	anergy stream of the heat	$[MW]$

<sup>3</sup>referred to the lower heating value (LHV)

$\dot{E}$	exergy stream	[kW]
$\dot{E}_{air}$	exergy of an air stream	[kW]
$\dot{E}_{chem}$	chemical exergy of a stream	[kW]
$\dot{E}_{exh,gas}$	exergy of an exhaust gas stream	[kW]
$\dot{E}_{Fuel}$	exergy stream of the fuel	[MW]
$\dot{E}_{Heat\ source}$	exergy stream of the heat source	[MW]
$\dot{E}_{in}$	entrant exergy stream	[kW]
$\dot{E}_{loss}$	exergy losses	[kW]
$\dot{E}_{out}$	outgoing exergy stream	[kW]
$\dot{E}_{phys}$	physical exergy of a stream	[kW]
$\dot{E}_Q$	exergy stream of the heat	[MW]
$\dot{m}$	mass flow	[kg/s]
$\dot{m}_1$	first mass flow of HX	[kg/s]
$\dot{m}_2$	second mass flow of HX	[kg/s]
$\dot{m}_{Fuel}$	mass flow of the fuel	[kg/s]
$\dot{m}_{in}$	entrant mass flow	[kg/s]
$\dot{m}_{out}$	outlet mass flow	[kg/s]
$\dot{m}_{Ref}$	mass flow of the working fluid	[kg/s]
$\dot{m}_{Steam}$	mass flow of the steam used as process heat	[kg/s]
$\dot{Q}$	heat stream	[MW]
$\dot{Q}_C$	cooling power of the heat pump	[kW]
$\dot{Q}_H$	heating power of the heat pump	[kW]
$\dot{Q}_{in}$	heating power of the heat source of the HTHP	[kW]
$\dot{Q}_{Loss}$	thermal losses	[kW]
$\dot{Q}_{Process}$	heating power used as process heat	[MW]
$\dot{Q}_{Rec}$	heating power of the recuperator of the HTHP with IHX	[kW]
$\dot{S}_Q$	entropy stream prop. to transported heat	[kJ/sK]
$\dot{V}_{nom}$	nominal mass flow	[L/s]
$A$	area	[m <sup>2</sup> ]
$a$	amplification factor fuzzy logic control	[-]
$c$	velocity	[m/s]
$c_1$	entrant velocity	[m/s]
$c_2$	outlet velocity	[m/s]
$c_p$	spec. isobaric heating capacity	[kJ/kgK]
$C_{Break\ Even}$	costs of heat at point of break even	[EUR/MWh]
$C_{Capital}$	capital costs	[EUR/MWh]
$C_{el,Break\ Even}$	electricity price at point of break even	[EUR/MWh]
$C_{El}$	electricity price	[EUR/MWh]
$C_{Gas}$	gas price	[EUR/MWh]
$C_{Personnel}$	personal costs for operating the HTHP	[EUR/a]
$C_{Service}$	service costs of the HTHP	[EUR/a]
$CO_2$	global CO <sub>2</sub> emissions	[kg]
$CoH_{f,HTHP}$	(fixed) capital costs of heat for the HTHP	[EUR/MWh]
$CoH_{GT-CC}$	costs of heat for the GT-CC process	[EUR/MWh]
$CoH_{GT}$	costs of heat for the GT process	[EUR/MWh]
$CoH_{HTHP}$	costs of heat for the HTHP process	[EUR/MWh]
$CoH_{v,HTHP}$	(variable) consumption related costs for the HTHP	[EUR/MWh]

$COP$	coefficient of performance	$[-]$
$D_C$	imputed depreciation	$[EUR/a]$
$E$	global energy consumption	$[PJ]$
$e$	specific isobaric heat capacity	$[kJ/kg]$
$e_0$	specific exergy of the stream at standard conditions	$[kJ/kg]$
$e_{1,in}$	spec. exergy in of mass flow 1 in a HX	$[kJ/kg]$
$e_{1,out}$	spec. exergy out of mass flow 1 in a HX	$[kJ/kg]$
$e_{2,in}$	spec. exergy in of mass flow 2 in a HX	$[kJ/kg]$
$e_{2,out}$	spec. exergy out of mass flow 2 in a HX	$[kJ/kg]$
$E_{annual}$	annual electric energy demand	$[kWh_{el}]$
$e_{Fuel}$	specific exergy of the fuel	$[kJ/kg]$
$e_{in}$	entrant spec. exergy	$[kJ/kg]$
$e_{out}$	outlet spec. exergy	$[kJ/kg]$
$F$	volume flow	$[m^3/s]$
$g$	Newton's constant	$[m/s^2]$
$GDP$	gross domestic product	$[EUR]$
$h$	specific enthalpy of the stream	$[kJ/kg]$
$h_0$	specific enthalpy at environment conditions	$[kJ/kg]$
$h_4$	specific enthalpy of the working fluid at compressor outlet	$[kJ/kg]$
$h_6$	specific enthalpy of the working fluid after condensation	$[kJ/kg]$
$H_H$	higher heating value	$[MJ/kg]$
$H_L$	lower heating value	$[MJ/kg]$
$h_{1,in}$	spec. enthalpy in of mass flow 1 in a HX	$[kJ/kg]$
$h_{1,out}$	spec. enthalpy out of mass flow 1 in a HX	$[kJ/kg]$
$h_1$	entrant specific enthalpy	$[kJ/kg]$
$h_{2,in}$	spec. enthalpy in of mass flow 2 in a HX	$[kJ/kg]$
$h_{2,out}$	spec. enthalpy out of mass flow 2 in a HX	$[kJ/kg]$
$h_2$	outlet specific enthalpy	$[kJ/kg]$
$h_{in}$	entrant specific enthalpy	$[kJ/kg]$
$h_{out,ideal}$	ideal outlet specific enthalpy	$[kJ/kg]$
$h_{out}$	outlet specific enthalpy	$[kJ/kg]$
$i$	required rate of return	$[\%]$
$I_0$	acquisition costs	$[EUR]$
$I_C$	imputed interests	$[EUR/a]$
$k$	heat transfer coefficient	$[W/m^2K]$
$L$	leakage rate of working fluid	$[kg/a]$
$m$	mass working fluid	$[kg]$
$M_{H_2O}$	molar mass water	$[kg/mol]$
$M_H$	molar mass hydrogen	$[kg/mol]$
$M_S$	molar mass sulphur	$[kg/mol]$
$n$	expected life time	$[a]$
$P$	global population	$[-]$
$P$	power	$[kW]$
$p$	pressure	$[bar_{abs}]$
$p_0$	pressure at standard conditions	$[bar_{abs}]$
$P_M$	mechanical power	$[kW]$
$p_{1,in}$	entrant pressure of mass flow 1 in a HX	$[bar_{abs}]$

$p_{1,out}$	outlet pressure of mass flow 1 in a HX	$[bar_{abs}]$
$p_{2,in}$	entrant pressure of mass flow 2 in a HX	$[bar_{abs}]$
$p_{2,out}$	outlet pressure of mass flow 2 in a HX	$[bar_{abs}]$
$p_{Cond}$	condensation pressure of the HTHP	$[bar_{abs}]$
$P_{el,GT-CC}$	electric power of the GT – CC	$[MW]$
$P_{el,GT}$	electric power of the gas turbine	$[MW]$
$P_{el,ST}$	electric power of the steam turbine	$[MW]$
$P_{el}$	electric power of the compressor	$[MW]$
$p_{Evap}$	evaporation pressure of the HTHP	$[bar_{abs}]$
$p_{in}$	entrant pressure	$[bar_{abs}]$
$p_{out}$	outlet pressure	$[bar_{abs}]$
$p_{ratio\ SGT-800}$	pressure ratio of the SGT-800 GT process	$[-]$
$p_{ST,HP}$	high-pressure level of the steam turbine	$[bar_{abs}]$
$p_{ST,LP}$	low-pressure level of the steam turbine	$[bar_{abs}]$
$p_{Steam,out}$	minimum pressure level of the process steam	$[bar_{abs}]$
$P_{therm}$	thermal power of a fuel <sup>4</sup>	$[MW]$
$q_{12}$	specific heat	$[kJ/kg]$
$Q_{Process}$	process heat	$[MW]$
$q_{th}$	volumetric heating capacity	$[kJ/m^3]$
$R_W$	liquidity receipts	$[EUR]$
$s$	specific entropy of the stream	$[kJ/kgK]$
$s_0$	specific entropy at environment conditions	$[kJ/kgK]$
$T$	temperature	$[K]$
$t$	annual operating time	$[h/a]$
$T_0$	environmental temperature	$[K]$
$T_1$	entrant temperature	$[K]$
$T_2$	outlet temperature	$[K]$
$T_Q$	temperature of the heat	$[K]$
$T_{1,in}$	entrant temperature of mass flow 1 in a HX	$[K]$
$T_{1,out}$	outlet temperature of mass flow 1 in a HX	$[K]$
$T_{2,in}$	entrant temperature of mass flow 2 in a HX	$[K]$
$T_{2,out}$	outlet temperature of mass flow 2 in a HX	$[K]$
$T_{Compr,in}$	superheated temperature at compressor inlet	$[K]$
$T_{Compr}$	temperature at compressor outlet	$[K]$
$T_{Cond}$	condensation temperature of the HTHP	$[K]$
$T_{Evap}$	evaporation temperature of the HTHP	$[K]$
$T_{exh,gas}$	temperature of the exhaust gas in the chimney	$[K]$
$T_{Feedwater}$	feedwater temperature of the used process steam	$[K]$
$T_{in}$	inlet temperature of the process heat	$[K]$
$T_{out}$	temperature out	$[K]$
$T_{SGT-800,out}$	turbine outlet temperature of the SGT-800 GT process	$[K]$
$T_{ST,HP}$	steam temperature of the high-pressure level of the ST	$[K]$
$T_{ST,LP}$	steam temperature of the low-pressure level of the ST	$[K]$
$T_{steam,out}$	outlet temperature of the used process steam	$[K]$
$u$	intrinsic energy	$[kJ/kg]$
$v$	specific volume	$[m^3/kg]$

<sup>4</sup>referred to the lower heating value (LHV)

$v_3$	specific volume of working fluid at compressor inlet	$[m^3/kg]$
$w_C$	mass fraction carbon	$[kg/kg]$
$w_H$	mass fraction hydrogen	$[kg/kg]$
$w_N$	mass fraction nitrogen	$[kg/kg]$
$w_O$	mass fraction oxygen	$[kg/kg]$
$w_S$	mass fraction sulphur	$[kg/kg]$
$w_{t12}$	specific technical work	$[kJ/kg]$
$y/T$	COP improvement in percent per 1 K	$[\%/K]$
$y_{min,max}$	improvement of COP from $\Delta T_{SH,min}$ to $\Delta T_{SH,max}$	$[\%]$
$z$	geodesic hight	$[m]$
$z_1$	geodesic hight entrance	$[m]$
$z_2$	geodesic hight outlet	$[m]$

# Contents



# 1 Introduction

## 1.1 The challenge of sustainable energy supply

One of the greatest challenges of this time is the conversion of the current energy system, which is mainly based on fossil fuels, to a sustainable energy system to counteract climate change. Therefore, the use of resource-efficient technologies and the switch to renewable resources are indispensable to overcome this challenge. Kaya and Yokobori [1] declared that CO<sub>2</sub> emissions only decrease, if, in case of increased population and increased gross domestic product, the energy intensity of the industry and the CO<sub>2</sub> intensity of energy supply decrease. Therefore, the energy efficiency and the share of renewable energy needs to be increased. In 2015, the European final energy consumption amounted 45 383 PJ, whereas 65.7% were provided by fossil fuels (solid fuels, oil and gas) and 21.7% by electricity. In contrast, the share of total renewable energy reached 8.0%. ?? shows the distribution of the final energy consumption

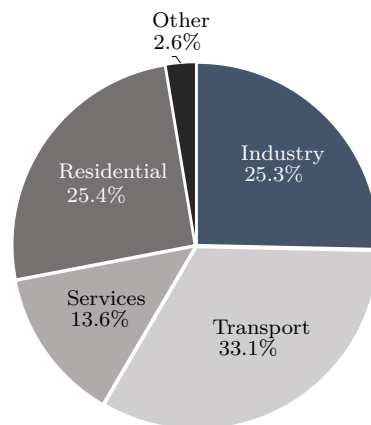


**Figure 1.1:** Distribution of the European final energy consumption 2015 according to different sectors, based on Eurostat data [2].

of different sectors for the European countries in 2015. Beside the transport and the residential sector the industrial sectors plays an major role in European energy consumption with about 11 503 PJ. The energy demand of the industrial sector is divided into electricity (31.2%) and heat (68.8%), as illustrated in ??. The industrial demand of heat is covered mainly by fossil fuels. The share of natural gas rates about 31.5%, followed by solid fuels (12.7%) and oil (10.1%). Renewable energy sources (7.8%), derived heat (5.5%) and wastes (1.2%) play an subordinate role.

In the industrial field, the demand of heat is very high. A closer look shows that industrial processes are operated across a wide temperature range. The energy intensity of process heat production is decisively influenced by the required temperature levels. Therefore, the industrial heat demand can be classified according to the required

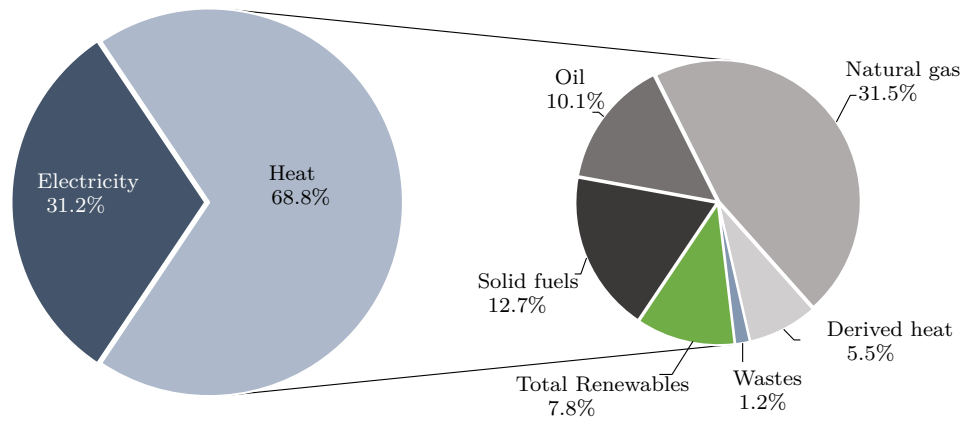


**Figure 1.2:** Distribution of industrial final energy consumption 2015 according to different energy sources [2].

**Table 1.1:** Classification and share of process heat demand in industry at different temperature levels [3].

Classification	Temperature [°C]	Share [%]
low temperature heat	<100°C	25.5
middle temperature heat	100°C – 400°C	27.2
high temperature heat	>400°C	47.3

temperature levels. Naegler et al. [3] distinguishes between three different process heat temperature levels. The shares of heat according to the temperature classifications are shown in ??.

Depending on different branches and applied technologies, the shares of process heat at different temperature levels differs significantly. The highest demand for high temperature process heat (>400°C) is in the iron and steel production as well as in the sector of non-metallic minerals. Process heat with temperature levels between 100°C and 200°C is required in the sectors pulp and paper, food and textile. Especially in this field, high temperature heat pump systems may contribute to decrease CO<sub>2</sub> emissions in the industry sector. Therefore, heat pumps can provide process heat at a certain temperature level by utilizing waste heat. However, the efficiency of heat pumps is mainly influenced by the required temperature levels of the process heat, what is introduced in detail in ??.

## 1.2 Energy efficiency in industrial processes

In general, industrial processes require large amounts of heat and electricity. During the manufacturing process, energy is lost due to equipment inefficiencies and mechanical and thermal limitations. ?? shows an exemplary industrial plant with its general energy flows. Energy is taken up, transformed and released in the single processes.

A detailed examination of the energy flows shows that the input energy is provided mainly in form of electricity, fuels (solid and liquid) and energy of the raw materials. A high amount of energy is used for the production of process heat, but energy is also needed for refrigeration applications, engines, space heating or lightening. In the end, the energy input is in the product and the waste heat released to the environment.

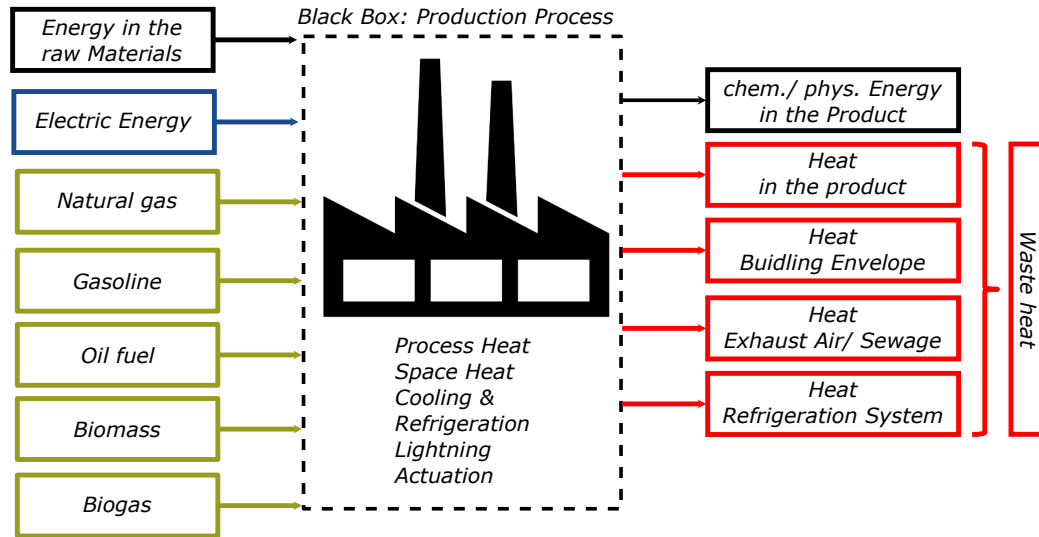


**Figure 1.3:** General energy flows in a production process.

Currently the high demand of heat is covered with (fossil) fuel fired boiler systems. However, large amounts on unused waste heat below 100°C are emitted from afterwards. Currently, this waste heat is released via chillers to the environment. As a result, significant losses and inefficiencies during the process occur. The utilization of this waste heat can make an important contribution to considerably increase the energy efficiency. Cascade heat utilization is an attempt to recover as much of the waste heat as possible. Our approach is to recovery a high share of waste heat, to increase the energy efficiency and to reduce CO<sub>2</sub> emissions. Beside direct heat integration, for processes requiring heat at a lower temperature level than the waste heat temperature, we conclude active heat integration. Heat pumps for active heat integration lift the temperature level of waste heat to a certain temperature level and can therefore supply process heat. If waste heat from the product, the building envelope, exhaust air and sewage and heat from refrigeration systems can be recovered and utilized with heat pumps, the amount of input fuels can be decreased significantly.

### 1.3 Aim and scope of this thesis

With regard to the high share of fossil fuels on energy production, de-carbonisation of the industry sector is a major challenge for future climate protection. Heat pumps for process heat supply may be an opportunity to reduce CO<sub>2</sub> emissions in the industrial field. Thus, we hypothesize that heat pump systems can contribute to increase the efficiency of industrial processes and can be integrated in future energy supply systems based on renewable energy sources.

## *1 Introduction*

Against the introduced background, the central questions that motivates this thesis are, on the one hand, the optimization and evaluation of this technology and, on the other hand, the economic application of heat pumps. Therefore, we deduce detailed aims for this work:

The development and evaluation of a test station for high temperature heat pump systems to determine the efficiency parameters at defined conditions.

The examination of different optimization measures of heat pump systems depending on the used working fluid.

Execution of a case study of a heat pump application in the industrial field including performance evaluation with focus on thermodynamic and economic factors.

## 2 Fundamentals of high temperature heat pump systems

### 2.1 Thermodynamic basics

In order to provide heat at a certain temperature level from waste heat, we can imagine theoretical process according to ???. Waste heat  $Q_0$  is absorbed by our process at temperature level  $T_0$  and heat  $Q_1$  with an increased temperature level  $T_1$  is released. It can be easily shown that, if no additional power  $P$  is supplied to the process ( $P = 0$ ), the second law of thermodynamic is not fulfilled if  $T_1 > T_0$  because  $\Delta\dot{S}_{irr}$  would be negative in this case (compare ??).

$$1^{st}\text{Law} : \dot{Q}_1 = \dot{Q}_0 + P \quad (2.1)$$

$$2^{nd}\text{Law} : \frac{\dot{Q}_1}{T_1} = \frac{\dot{Q}_0}{T_0} + \Delta\dot{S}_{irr} \quad (2.2)$$

On the other hand we can determine from this set of equations (????) the minimum power requirement in case of a theoretical reversible process ( $\Delta\dot{S}_{irr}$ ). ?? represents the efficiency of an ideal Carnot cycle and is called Carnot efficiency.

$$\eta_C = \frac{P_{min}}{\dot{Q}_1} = 1 - \frac{T_0}{T_1} \quad (2.3)$$

For heat pump systems, we see  $P$  as the effort and  $\dot{Q}_1$  as the useful energy stream. Based on this relation we define the maximum (Carnot) efficiency of performance according to ??.

$$\epsilon_C = COP_C = \frac{\dot{Q}_1}{P_{min}} = \frac{T_1}{T_1 - T_0} \quad (2.4)$$

Based on this relations we conclude from fundamental thermodynamic that

1. we need to supply a certain amount of power to increae the temperature level of the heat stream from  $T_0$  to  $T_1$  and
2. the minimum amount of power required depends on the temperature levels of the heat reservoirs according to the Carnot cycle efficiency  $\epsilon_C$ .

Real heat pump systems can only approach the Carnot cycle efficiency to a certain level of about 50 to 60%.

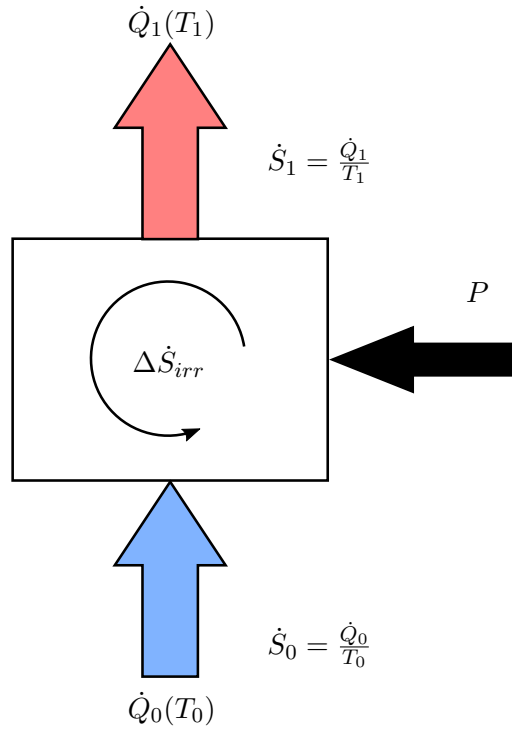


**Figure 2.1:** Basic thermodynamic of a heat pump process.

## 2.2 The exergy concept

In order to get to a simplified description of entropic processes, the exergy concept can be applied. Energy is neither created nor destroyed during a process. Energy changes from one form to another according to the first law of thermodynamics, but the first law gives no statement whether a particular energy conversion at all is possible. In contrast, the second law of thermodynamics limits the convertibility of energy. Energy is the sum of exergy and anergy and constant in a system(?). According to Baehr and Kabelac [4] the exergy is the part of energy which is convertible to any other form of energy. Irreversible processes transform exergy to anergy, whereas the destruction of exergy is proportional to the entropy increase of the system.

$$Energy = Exergy + Anergy \quad (2.5)$$

Technical work, electrical energy, potential and kinetic energy are per definition pure exergy. Whereas the conversion of enthalpy, heat and chemical energy is limited. The limits of the conversion depend on the thermodynamic environment. Deduced from the power balance equation the exergy stream of a heat stream can be calculated as shown in ?? . It is the product of the heat stream and the Carnot factor. The Carnot factor includes parameters of ambient temperature and the temperature of the heat

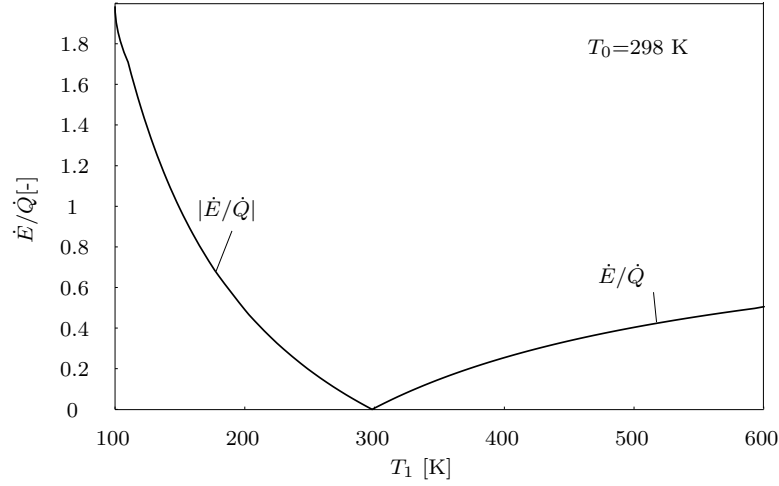


**Figure 2.2:** Correlation of exergy of the heat and temperature.

stream crossing the system.

$$\dot{E}_Q = \eta_C * \dot{Q} = \left(1 - \frac{T_0}{T_1}\right) * \dot{Q} \quad (2.6)$$

The anergy stream  $\dot{B}_Q$  of a heat stream is described by ??.

$$\dot{B}_Q = \dot{Q} - \dot{E}_Q = \dot{Q} * \frac{T_0}{T_1} = T_0 * \dot{S}_Q \quad (2.7)$$

?? shows, that the exergy of heat is mainly influenced by environmental temperature  $T_0$  and the temperature of the outgoing heat stream  $T_1$ . Therefore, ?? illustrates the correlation of exergy and the temperature of the heat stream  $T_1$  with an environmental temperature  $T_0=298$  K. For exergy no general law of conservation exist. In irreversible processes ( $\Delta\dot{S}_{irr} > 0$ ) the exergy decreases, whereas the anergy increases. This transformation of exergy into anergy is called exergy losses of irreversible processes and described by ??.

$$\dot{E}_{Loss} = \sum_{in} \dot{E}_{in} - \sum_{out} \dot{E}_{out} \quad (2.8)$$

In general, the exergy stream can be calculated as the product of specific exergy and mass flow described by ??.

$$\dot{E} = \dot{m} * e \quad (2.9)$$

If no material exchange with the environment happens, only the pyhsical exergy needs to be considered. The specific physical exergy is described in ?? (the parts of kinetic

and potential energy are neglected).

$$e = e_0 + (h - h_0) - T_0 * (s - s_0) \quad (2.10)$$

The specific exergy of a material flow, which is transported into the control volume, consists of the chemical and physical exergy. In ??,  $e_0$  represents the chemical exergy, which considers the chemical composition. According to Ahrendts [5] the components must be in state of complete thermodynamic equilibrium and no mixing or separation processes may occur. For the calculations an equilibrium environment based on Diederichsen [6] is chosen. Based on this considerations we introduce the exergetic efficiency  $\zeta$ . The exergetic efficiency relates in and outlet exergy respectively the inlet exergy and the exergy losses according to ??.

$$\zeta = \frac{\dot{E}_{out}}{\dot{E}_{in}} = 1 - \frac{\dot{E}_{loss}}{\dot{E}_{in}} \quad (2.11)$$

### 2.2.1 Exergy concept of heat pump systems

The described exergy concept can be applied to the basic heat pump process according to ??. Heat pumps uses exergy to lift the temperature level of a heat stream. For this purpose different forms of exergy sources (mechanical power, electrical power, chemical power or heat at increased temperature) can be exploited. ?? shows the connections between exergy  $E$  and anergy  $A$  in a heat pump system.

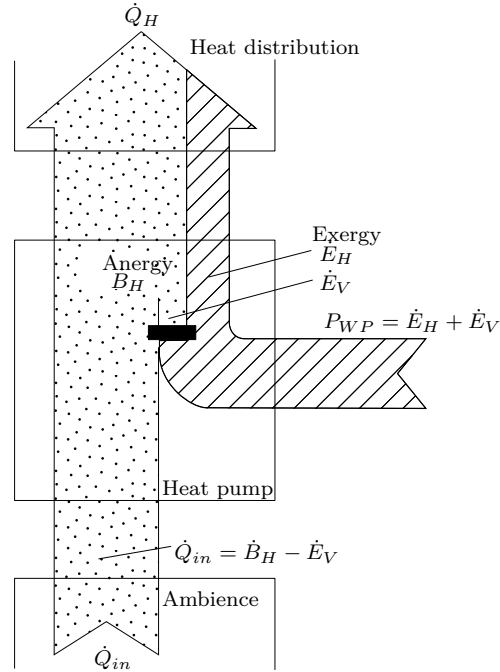


**Figure 2.3:** Anergy and exergy flow in a heat pump system.

The energy efficiency of a heat pump system can be described with several performance

## 2.3 System components of high temperature heat pumps

factors. The most important factor is the COP. It relates the heating power in the heat sink to the power input. In case of electrically driven heat pumps the input power is the electrical power brought into the system (??).

$$COP = \frac{\dot{Q}_H}{P_{el}} \quad (2.12)$$

The COP is a time depending factor and shows only temporary relations. To evaluate a heat pump system over a longer period, the seasonal performance factor (??) is used.

$$SPF = \frac{\int Q_H}{\int Q_{el}} \quad (2.13)$$

Based on the described exergetic considerations the exergetic efficiency of heat pump systems can be defined according to ??.

$$\zeta = \frac{\eta_C * \dot{Q}_H}{P_{el} + \dot{E}_{Heat\ source}} \quad (2.14)$$

If the heat source temperature is higher than the temperature of the equilibrium environment according to Diederichsen [6], the exergy of the heat source needs to be regarded. For electrically driven heat pump systems using anergy as heat source (e.g. geothermal heat, ambient heat) only the electrical power needs to be considered ( $\dot{E}_{Heat\ source} = 0$ ), as shown in ??.

$$\zeta = \frac{\eta_C * \dot{Q}_H}{P_{el}} = \frac{\eta_C}{COP} \quad (2.15)$$

Summarizing, exergy is the part of energy that can be converted to any other energy form. Exergy is lost in irreversible processes, and for the ideal case of a reversible process, the exergy loss is zero. The exergetic efficiency describes the deviation of a process from reversibility.

Heat pump systems require exergy to lift the temperature level of the heat stream. Different exergy sources such as mechanical power or heat at increased temperature level can be exploited for this purpose. For electrically driven heat pumps using anergy as heat source, the exergetic efficiency is equal to the ratio of real COP and ideal Carnot efficiency performance evaluated at the source temperature level.

## 2.3 System components of high temperature heat pumps

This work focusses mechanically driven systems, especially the electrically driven vapor compression process, because for high temperature heat production this system is technologically and economically more favourable.

High temperature heat pumps may be defined in many different ways, according to

the literature. In this work, high temperature heat pumps (HTHP) mean that heat with a temperature level higher than  $100^{\circ}\text{C}$  can be produced. Heat pumps in the building sector for space and water heating usually reach temperature levels up to  $70^{\circ}\text{C}$ . In contrast, the main application field for high temperature heat pump systems is, therefore, in the industry to substitute fossil fuels for process heat production.

The general process of high temperature heat pumps is similar to heat pumps for space heating. However, because of the higher temperatures, the technological requirements for the system components are more pretentious and systems design has an important impact on the efficiency of the system (as shown in ??). Mechanically driven heat pumps typically base on the vapor compression cycle, where a working fluid is circulated. The basic cycle for an electrical driven vapor compression heat pump is shown in ??. In the evaporator (4–1) the working fluid gets evaporated by taking up heat at a low temperature level (heat source). In the compression step (1–2) the working fluid gets compressed. Pressure and temperature increase. In the condensation step (2–3) the working fluid is condensed and heat with a higher temperature level is released towards to a heat sink. In the last step (3–4), the working fluid is expanded in an expansion valve and pressure and temperature decrease.

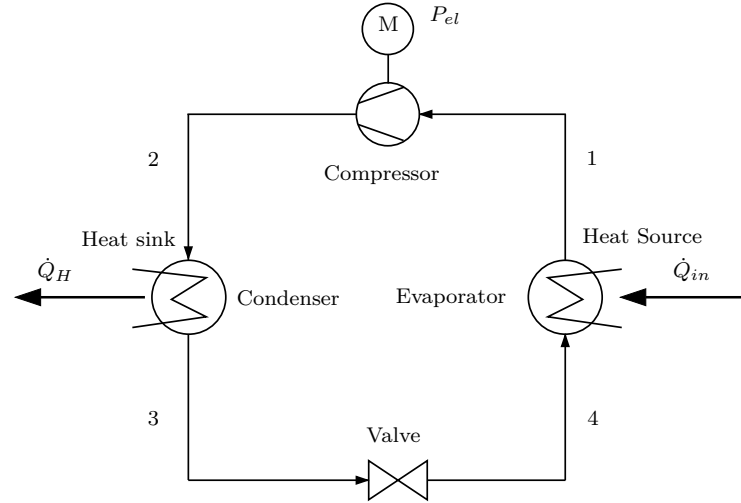


**Figure 2.4:** Basic process scheme of a vapor compression heat pump cycle.

### 2.3.1 Compressor for HTHP systems

The compressor is a very important component of a heat pump system. The design of the compressor has a significant impact on the efficiency of the whole system. Especially for high temperature heat pumps with reachable higher temperature levels, the design and type of compressor are very important. Not every type of compressor is applicable, and in many times standard compressors must be adapted for high temperature usage. Typical types of compressor systems for HTHP are:

- Reciprocating piston compressor
- Rotation piston compressor

- Screw compressor
- Scroll compressor
- Turbo compressor

The selection of a compressor is mainly influenced by the achieved pressure ratio and the volumetric flow rate. ?? illustrates the application fields of different compressor types. Piston compressors reach high pressure ratios, but are limited in the discharge. Rotation compressors, including screw and scroll compressors, ranges between. If high flow-rates are required, fluid machines like turbo compressors are applied. In the following, compressor types for high temperature heat pump applications are introduced.

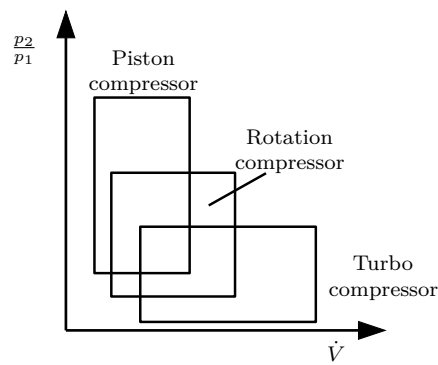


**Figure 2.5:** Scope of different compressor types depending on pressure ratio and volumetric flow-rate (according to Maurer [7]).

For choosing compressors for HTHP applications, several specifications must be considered. The temperature after the compressor must be in a tolerable range, because of the used lubricants. Typical lubricants for refrigeration processes would not bear the temperature ranges of HTHP and start to disintegrate. This reduces the lubricating performance and could damage the compressor. To increase the efficiency of the compressor an additional cooling of the cylinder head, working fluid injection or inter-cooling in case of a multi-stage system can be installed.

**Reciprocating piston compressor** The piston compressor is one of the oldest compressor systems for refrigeration applications. Its application field ranges from a few Watt (household refrigeration systems  $< 1 \text{ kW}_{\text{el}}$ ) to large scale applications ( $> 100 \text{ kW}_{\text{el}}$ ). For small applications hermetic systems are used. This means that the whole compressor (including working chamber, cylinder, lubrication, engine and electrical motor) is in a closed housing. The advantage of those system is that no severice efforts and no leakage losses occur. The generated heat in the hermetic systems is lead off with the working fluid In contrast in open systems the working chamber and the electrical drive are separated. Special dynamic sealings are required to connect the static and the rotating components of the compressor. Open systems enable the application of a cooling system to the cyclinder head or the working chamber. Piston compressor for larger refrigeration applications are designed as open systems. The third construction form are semi-hermetic compressor systems. Therefore, the housing of the compressor

can be opened for service efforts. The electrical drive of the compressor is located outside the housing, only the egde runner is inside. The waste heat from the motor is dissipated to the ambient.

**Rotation compressor** In a rotation compressor a cylindrical piston is driven with an eccentric in a cylindrical working chamber. A flexible barrier separates the working chamber in a suction and discharge chamber. The rotating piston enlarges the suction chamber, until the piston reaches the bar. Simultaneously the discharge chamber volume is decreased and the pressure increases.

**Screw compressor** The screw compressor exists of two geared screws, which rotate inside the working chamber. The compression happens in the decreased space between the screws. Compared to piston compressors, the design of screw compressors is more compact and less service intensive because of missing valves for gas change. The pressure ratio of screw compressors depends on the design of the working chamber and the space between the geared screws. The regulation is done with a flexible bar, which regulates the position of admission/ exhaust edge. Screw compressors are constructed in an open or semi-hermetic form and used for medium and large scale refrigeration systems.

**Scroll compressor** A scroll compressor consists of two interlocking spirals. One spiral is fixed, whereas the other spiral fulfils a rotary movement. The suction gas moves from outside into the sickle-shaped chamber between the spirals. The rotary movements increase the pressure and the gas is discharged in the middle of the spirals. Because of low radial forces on the shaft the system is insensitive to slugging. Common heat pumps for hot water and space heating are driven with scroll compressor systems, but also HTHP application is conceivable.

**Turbo compressor** Turbo compressor belong to the group of fluid machines and work like a reverse turbine. A wheel with shovels rotates and transfers mechanical work on the suction gas. Turbo compressor base on a continuous flow process and the advantage of this system is its oil-free operation mode, if a magnetic bearing of the shaft is applied. The system is suitable for working fluids with a vapor density  $> 1 \text{ kg/m}^3$  and water. Currently, the lower limits for turbo compressors are about  $75 \text{ kW}_{\text{el}}$ .

### 2.3.2 Heat exchanger for HTHP systems

Typical heat exchanger systems for heat pumps are:

- Plate heat exchanger
- Tube bundle heat exchanger
- Vertical tube evaporator
- Fin coil evaporator
- Coaxial tube-in-tube heat exchanger

The heat exchanger for HTHP application doesn't really differ to common heat pump systems. The chosen material (copper, stainless steel) must bear the higher temperature levels. The material choice is not that problem, because in many large scale refrigeration systems still stainless steel is used. In further consequence this systems are not examined in detail.

### 2.3.3 Thermostatical expansion valve

In most heat pump applications a thermostatical expansion valve (TEV) is used for pressure release. The System consists of a membrane, a feather, a temperature sensor to the evaporator outlet, an inlet from the condenser and an outlet to the evaporator as shown in ???. The temperature sensor is connected to the bottom of the membrane, at the top side of the membrane the evaporation pressure acts. If the temperature at the evaporator outlet increases or the evaporation pressure decreases, the valve opens and the flow rate to the evaporator is increased. This lowers the suction gas superheating. Typically, the system is adjusted to a suction gas superheating temperature of 1 – 2 K.

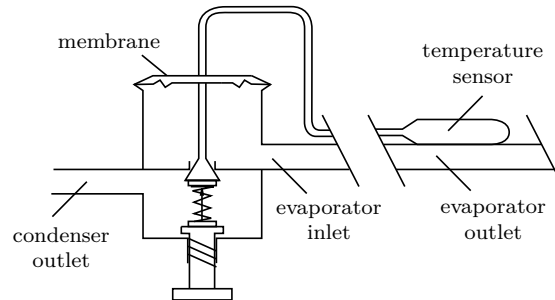


**Figure 2.6:** Scheme of thermostatical expansion valve (according to Maurer [7]).

The TEV is applied in household refrigeration system or small refrigeration application. For large scale applications, electronic valves are used to adjust the working mass flow in the evaporator. Therefore, slide valves or magnetic valves with electrical actuator are applied. The electric expansion valves are controlled via superheating controller, which measure temperature and pressure at the evaporator outlet.



## 3 Process simulation and methodical approach

### 3.1 Physical basis

This chapter introduces into thermodynamic basics, which are required for understanding the heat pump process. Additionally, the process simulation is based on the introduced thermodynamic principles.

#### 3.1.1 Mass and Energy balance

The first law of thermodynamics postulates that neither energy can be produced nor be destroyed. Based on this theorem mass and energy balances for processes are formulated. Technical applications often bases on a flow process, where in- and outgoing streams traverse a defined control volume. ?? show the mass balance of a stationary flow process. The mass in the control volume is constant over time ( $dm/d\tau$ ) and so the mass balance can be described as ??:

$$\sum_{i=1}^n \dot{m}_{in} = \sum_{i=1}^n \dot{m}_{out} \quad (3.1)$$

In a stationary flow process the amount of energy in the control volume stays constant.

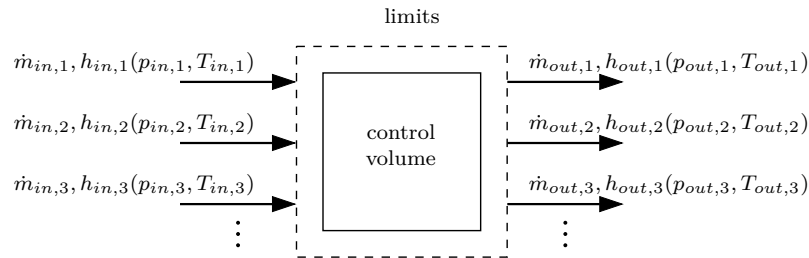


**Figure 3.1:** Balance limit and control room of a stationary flow process.

Deduced from the conservation of mass and energy the steady flow energy equation is shown in ?.  $\dot{Q}$  and  $P$  are the heat and the mechanical power. Energy input shows a positive sign, energy release a negative sign.

$$\dot{Q} + P = \sum_{i=1}^n \dot{m}_{out} * \left( h + \frac{c^2}{2} + g * z \right)_{out} - \sum_{i=1}^n \dot{m}_{in} * \left( h + \frac{c^2}{2} + g * z \right)_{in} \quad (3.2)$$

If only one stream flows through the control volume, ?? can be simplified to ??, also called power balance equation:

$$\dot{Q} + P = \dot{m} \left[ \left( h + \frac{c^2}{2} + g * z \right)_{out} - \left( h + \frac{c^2}{2} + g * z \right)_{in} \right] \quad (3.3)$$

In assumption, that a stream traverse several control units, the indices 1 for the incoming and 2 for the outgoing stream are used. ?? can be transformed in a mass-specific form by dividing through the mass flow  $\dot{m}$ . This leads to a specific energy balance equation (??):

$$q_{12} + w_{t12} = h_2 - h_1 + \frac{1}{2}(c_2^2 - c_1^2) + g(z_2 - z_1) \quad (3.4)$$

?? combines the heat ( $q_{12}$ ) and the technical work ( $w_{t12}$ ) with the specific enthalpy, the specific kinetic energy and the specific potential energy. The amount of energy in form of heat and technical work, which traverses the control volume, is described with the change of specific enthalpy, specific kinetic energy and specific potential energy.

#### 3.1.2 Enthalpy

Per definition the specific enthalpy  $h$  includes the intrinsic energy  $u$  and the product of the pressure  $p$  and the specific volume  $v$  (??):

$$h := u + p * v \quad (3.5)$$

The specific enthalpy  $h$  is an intensive state parameter and depends on two independent parameters. In the caloric state equation the enthalpy is affected by the pressure  $p$  and the temperature  $T$ . The partial differential equation to pressure and temperature is shown in ??

$$dh = \left( \frac{\partial h}{\partial T} \right)_p dT + \left( \frac{\partial h}{\partial p} \right)_T dp, \quad (3.6)$$

were the specific isobaric heat capacity can be deduced:

$$c_p := \left( \frac{\partial h}{\partial T} \right)_p \quad (3.7)$$

Based on ??, for small temperature lifts and under neglecting the temperature dependence of  $c_p$ , an approximation for the change of specific enthalpy is formulated according to (??). For ideal gases and incompressible streams, the pressure dependency can be neglected. For working fluids of HTHPs, which undergo state changes, enthalpy

has to be evaluated as a function of pressure and another suitable quantity of state.

$$h(T_2, p) - h(T_1, p) = cp * (T_2 - T_1) \quad (3.8)$$

The previous considerations base on the formation of enthalpy differences, were the undefined constant factor of the enthalpy is left out. For the consideration of chemical reactions, as e.g. in combustion processes, the constant factor of the enthalpy of the different streams must be calculated at coordinated conditions. The so called conventional enthalpy of pure substances is described in ?? at reference conditions. The thermodynamic standard conditions  $T_0 = 298.15 \text{ K}$  ( $t_0 = 25^\circ \text{C}$ ) and  $p_0 = 100 \text{ kPa}$  are an appropriate reference state. The conventional enthalpy of a pure substance  $H^*(T, p)$  is calculated as the sum of the of standard formation enthalpy of the substance  $H_{f,298}^0$  and the enthalpy difference of state condition  $(T, p)$  and reference condition  $(T_0, p_0)$  according to Baehr and Kabelac [8].

$$H^*(T, p) = H_{f,298}^0 + [H(T, p) - H(T_0, p_0)] \quad (3.9)$$

The conventional enthalpy allows the calculation of balance equations for chemical reactions similar to stationary flow processes in molar form (??):

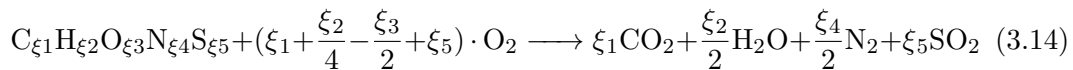
$$\dot{Q} + P = \sum_{i=1}^N \dot{n}_{i,out} * H^*(T_{out}, p_{out}) - \sum_{i=1}^N \dot{n}_{i,in} * H(T_{in}, p_{in}) \quad (3.10)$$

### 3.1.3 Lower heating value

The lower heating value  $H_L$  of a fuel is the specific reaction enthalpy of the oxidation reaction of a combustion process ( $H_L = \Delta H_{R,298}^0$ ). Per definition, the lower heating value is the energy released by complete combustion of a fuel with free oxygen. Fuels bases on a matrix consisting C, H<sub>2</sub>, S, O<sub>2</sub>, N<sub>2</sub> and H<sub>2</sub>O, whereas the products of combustion are CO<sub>2</sub>, H<sub>2</sub>O, SO<sub>2</sub> and N<sub>2</sub>. The general reaction processes in a combustion are shown in ??????:



For fuels with defined molecular structure the complete combustion reaction can be described compared to ??, according to Pröll and Hofbauer[9]:



### 3 Process simulation and methodical approach

Per definition, the water content of the stoichiometric exhaust gas is in a gaseous state. In contrast, the higher heating value  $H_H$  is defined as the reaction enthalpy of a oxidation reaction, were the product  $H_2O$  is completely condensed, according to ??.

$$H_L = H_H - w_H * \frac{M_{H_2O}}{2 * M_H} * \Delta h_{evap,298} \quad (3.15)$$

The lower heating value of a fuel (water and ash free basis) can also be deduced from ultimate analysis by the Boije formula, according to ??.

$$H_L = 34835 * w_C + 93870 * w_H - 10800 * w_O + 6280 * w_N + 10465 * w_S \quad (3.16)$$

If  $H_L$  and the elementary composition of the fuel are known, the specific formation enthalpy can be calculated according to ??

$$\Delta h_{f,298}^0 = H_L + \frac{w_C}{M_C} * \Delta H_{f,298,CO_2}^0 + \frac{w_H}{2 * M_H} * \Delta H_{f,298,H_2O(g)}^0 + \frac{w_S}{M_S} * \Delta H_{f,298,SO_2}^0 \quad (3.17)$$

With the lower heating value the chemical energy of a fuel is defined and the fuel power (based on the lower heating value) can be calculated (??):

$$P_{therm} = \dot{m}_{Fuel} * H_L \quad (3.18)$$

## 3.2 Process simulation

In general, process simulation is the description of chemical and mechanical processes with computer programs based on mathematical correlations, e.g. mass and energy balances. The equation systems are solved numerically. Process simulation allows a prognosis of the behaviour and the efficiency of different processes.

In order to obtain consistent and interpretable results, a suitable model description, model parameters, reaction mechanisms and specific data of the used materials are necessary. Most commercially available simulation environments obtain the specific data from reference databases, like the NIST Standard Reference Database. In this work the process simulation software IPSEpro is used.

### 3.2.1 The process simulation environment IPSEpro

The simulation environment IPSEpro is a flexible environment, which allows the simulation of stationary processes. The structure of IPSEpro is shown in ??. The main modules of IPSEpro are the Model Development Kit (MDK) and the Process Simulation Environment (PSE).

PSE is the graphical user interface to create process flow diagrams based on components from the Model Libraries. PSE adopts a 2-phase equation oriented approach. In the analysis phase, PSE checks the models for errors and in case of correct specifications the optimum solution method is determined. In the numerical

solution phase PSE solves the equations with the numerical methods defined in the analysis phase [10].

MDK allows the mathematical and graphical description of process units, process streams and the definition of global specifications. The main parts of MDK are the Model Editor and the Model Compiler. The Model Editor allows the graphical design of icons and symbols to represent the models and combines them with the mathematical description. The Model Editor uses a Model Description Language MDL. The Model Compiler translates the model descriptions into a format that can be solved from the equation solver in the PSE. In the libraries, standard models are available, the existing models can be customized and new models can be built.

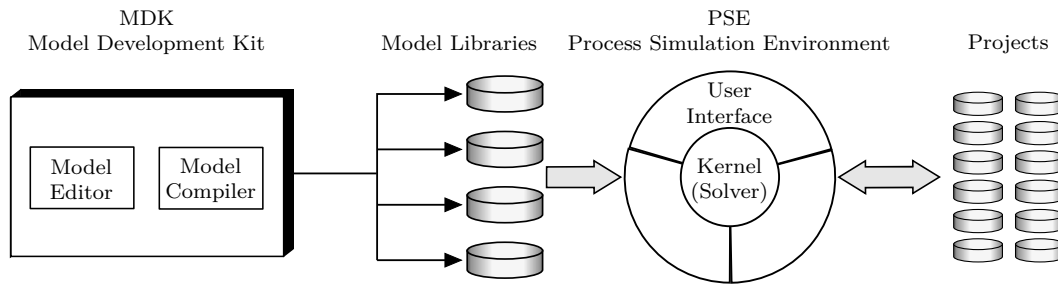


**Figure 3.2:** Architecture of the process simulation program IPSEpro [11].

### 3.2.2 Model Libraries

IPSEpro comes in a standard version with a library for modeling thermal power systems (Advanced Power Plant Library - APP), but this library is not used in the present work. In the following, the libraries that are used for the present work are introduced.

**Low Temperature Process Library - LTP** The Low Temperature Process Library for IPSEpro has been designed for modelling low temperature energy conversion processes like the Organic Rankine Cycle or the Kalina Cycle. The library contains data of established and new working fluids obtained from the NIST Reference Fluid Thermodynamic and Transport Properties (REFPROP) Version 9.1. A detailed description of the reference data from the analysed working fluids is declared in ???. The observed heat pump and refrigeration systems were built with this library.

**Pyrolysis and Gasification Process Library - PGP** The Pyrolysis and Gasification Process Library focuses on the design of biomass gasification and biomass-fuelled plants. The library also allows the modeling of gas and steam turbines. The physical property data are obtained from the PPPGPSys.dll. The modeling of the gas turbine process and the gas and steam turbine combined cycle process are based on this library.

### 3.2.3 Model classes

This part introduces the used model classes for modeling processes with IPSEpro

**Units** Units represent with specific icons the mathematical description of devices and process components. The mathematical description is based on mass- and energy balances and variables from global definitions can be referenced. Connections allow linking single units.

**Connections** Connections link single units and transfer informations. Connections can reference variables from global definitions and thermal state equations are implemented.

**Globals** Globals are global definitions of streams and material flows. The chemical composition or predefined substances (e.g. working fluids, thermal oils, lubricants, etc...) can be defined and referenced by units and connections.

#### 3.2.4 Model Units

In the following, the used units for the process simulation are summarized and shortly introduced.

**Compressor and Pump** The model for compressors and pumps is shown in ??.

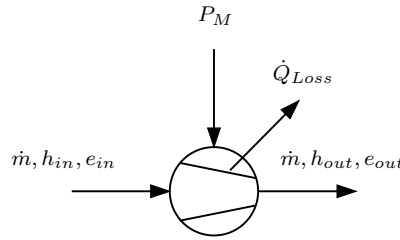


**Figure 3.3:** Unit icon of a compressor.

???? show the energy balance of a compressor and the occurring losses.

$$\dot{m} * (h_{out} - h_{in}) = \eta_{Mech} * P_M \quad (3.19)$$

$$\dot{Q}_{Loss} = (1 - \eta_{Mech}) * P_M \quad (3.20)$$

The exergy balance includes the in and outgoing exergy stream, the mechanical power and the occurring exergy losses  $\dot{E}_{Loss}$ .

$$\dot{E}_{Loss} = \dot{m} * (e_{in} - e_{out}) + P_M \quad (3.21)$$

To describe the change of enthalpy in a real compression process, the correlation of an ideal adiabatic isentropic compression is adopted. The isentropic efficiency  $\eta_{s,C}$  ?? describes the connection of in and outgoing enthalpy of an adiabatic compressor system.

$$\eta_{s,C} = \frac{h_{out,ideal} - h_{in}}{h_{out} - h_{in}} \quad (3.22)$$

**Heat exchanger** In a heat exchanger heat from a hot stream is exchanged to a colder stream without changing the composition of the stream (see ??). The energy balance is described in ??.

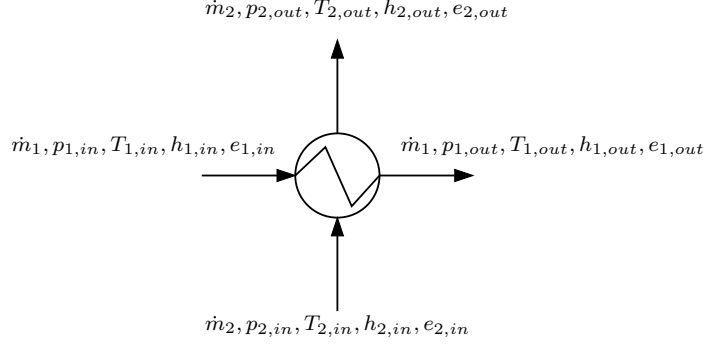


**Figure 3.4:** Energy balance of a heat exchanger.

$$\dot{m}_1 * (h_{1,out} - h_{1,in}) = \dot{m}_2 * (h_{2,in} - h_{2,out}) \quad (3.23)$$

The exergy balance includes the in and outgoing exergy stream and the exergy losses of the heat exchange process. The losses are caused by irreversible heat exchange (??) and pressure losses (????).

$$\dot{m}_1 * e_{1,in} + \dot{m}_2 * e_{2,in} = \dot{m}_1 * e_{1,out} + \dot{m}_2 * e_{2,out} + \dot{E}_{Loss} \quad (3.24)$$

$$\Delta p_1 = p_{1,in} - p_{1,out} \quad (3.25)$$

$$\Delta p_2 = p_{2,in} - p_{2,out} \quad (3.26)$$

**Valve** The valve, as shown in ??, is used to throttle a stream and to decrease the pressure. The pressure drop  $\Delta p$  is shown in ??. It is assumed that the throttling process is adiabatic ( $h_{in} = h_{out}$ ).

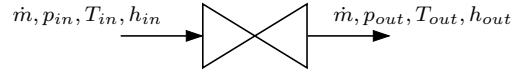


**Figure 3.5:** Valve Unit.

$$\Delta p = p_{in} - p_{out} \quad (3.27)$$

**Turbine** The energy and exergy balance of a turbine (??) are similar to these of a compressor system. For the sake of completeness, the balances for a turbine are shown in ????.

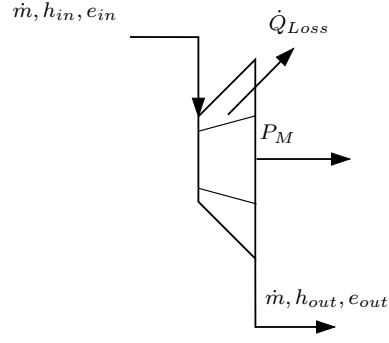


**Figure 3.6:** Turbine unit model.

$$P_M = \eta_{Mech} * \dot{m} * (h_{in} - h_{out}) \quad (3.28)$$

$$\dot{Q}_{Loss} = (1 - \eta_{Mech}) * (h_{in} - h_{out}) \quad (3.29)$$

The exergy balance follows ??:

$$\dot{E}_{Loss} = \dot{m} * (e_{in} - e_{out}) - P_M \quad (3.30)$$

The adiabatic expansion in the turbine is described by ??:

$$\eta_{s,T} = \frac{h_{in} - h_{out}}{h_{in} - h_{out,ideal}} \quad (3.31)$$

**Combustion chamber** In a combustion chamber a fuel is oxidized with oxygen. Most of the time air is used as oxygen carrier. ?? shows the scheme of a combustion process. The mass balance of a combustion includes fuel and air as input streams and exhaust gas and ash as reaction products. A combustion is an exergetic chemical reaction

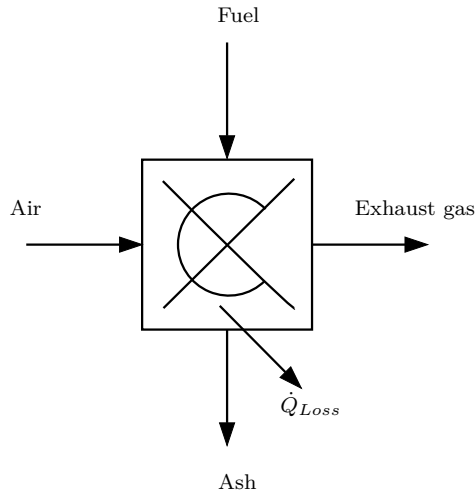


**Figure 3.7:** Model of a combustion chamber.

process which emits thermal heat to the outgoing exhaust gas stream. A complete combustion occurs, if all combustible fuels are oxidized completely to  $\text{CO}_2$ ,  $\text{H}_2\text{O}$  and  $\text{SO}_2$ . Whereas a lack of oxygen causes an incomplete combustion, where the reaction products still contain combustibles and the associated chemical energy leaves the process. In practice incomplete combustion should be avoided [12]. To calculate the chemical reaction of a combustion process the fuels are classified into two groups:

- Fuels with a defined chemical structure: Hydrogen ( $\text{H}_2$ ), Methanol ( $\text{CH}_3\text{OH}$ ) or Methane ( $\text{CH}_4$ )
- Fuels with a heterogeneous chemical structure: mostly all liquid and solid fuels as biomass, coal or oil fuel

The combustion of homogeneous fuels, e.g. natural gas (main component:  $\text{CH}_4$ ), can be calculated with the mass fractions of the pure substances. For heterogeneous fuels an elementary analysis gives results about the mass fractions of C, H, S, O, N,  $\text{H}_2\text{O}$  and ash of the used fuel. For the thermal energy of a combustion chamber ?? is used. The exergy losses are formulated as ??:

$$\dot{E}_{\text{loss}} = \dot{E}_{\text{air}} + \dot{E}_{\text{fuel}} - \dot{E}_{\text{exh, gas}} \quad (3.32)$$

### 3.3 Working fluids

The working fluid is one of the most important factors of a heat pump system. In case of vapor compression systems, the working fluid is evaporated, compressed, condensed and expanded in a closed cycle. The thermodynamic properties of the used working fluid distinctly influence the efficiency of a heat pump system. There are several types of working fluids, which are state of the art in refrigeration technology and introduced in the following section.

Beside temperature and pressure range of a working fluid, ecologic and economic factors play a role for selecting a suitable working fluid. The most important selection parameters for working fluids depend on thermophysical, chemical, physiological, ecological and economic factors, summarized in ??.

#### 3.3.1 Ecological impact

Since the introduction of chlorofluorocarbons (CFC) in the early 1930, the ecologic impact on the environment caused by refrigeration systems has increased dramatically. The negative effects of CFC on the ozone layer caused a ban on them, fixed in the Montreal Protocol in 1987. Afterwards, several restrictions became law to regulate the deployment of environmentally critical substances in refrigeration and heat pump systems. At least the regulation Nr.517/2014 on fluorinated greenhouse gases [14] fixed a phase-out for working fluids with environmental impact. To characterise the impacts of working fluids on the environment several parameters were defined, which are described below.

**Table 3.1:** Parameters for selection of a suitable working fluids according to Pohlmann [13].

<b>Thermophysical properties</b>	<ul style="list-style-type: none"> <li>• high phase-change enthalpy</li> <li>• steep saturation vaporization curve</li> <li>• high volumetric cooling capacity</li> <li>• low compressor outlet temperatures</li> <li>• high thermal conductivity</li> <li>• high critical pressure and temperature levels</li> </ul>
<b>Chemical properties</b>	<ul style="list-style-type: none"> <li>• thermal and chemical stability</li> <li>• not flammable nor explosive</li> <li>• compatibility with piping material and lubricant</li> <li>• miscibility with lubricant</li> </ul>
<b>Physiological properties</b>	<ul style="list-style-type: none"> <li>• low or even no toxicity</li> <li>• no hazardous degradation products</li> </ul>
<b>Ecological properties</b>	<ul style="list-style-type: none"> <li>• no Ozon Depletion Potential (ODP)</li> <li>• low Global Warming Potential (GWP)</li> </ul>
<b>Economic properties</b>	<ul style="list-style-type: none"> <li>• low costs</li> <li>• high availability</li> </ul>

### 3.3.1.1 Ozone Depletion Potential

The Ozone Depletion Potential (ODP) gives information about the impact on the ozone layer mainly caused by bromine and chlorine radicals. Because of their distinctive chemical stability, CFC get into the stratosphere, stay there and damage the ozone layer [15]. The ODP is calculated as ratio to a reference substance (Trichlorfluoromethane R11), which has a value of ODP=1.

### 3.3.1.2 Global Warming Potential

The Global Warming Potential (GWP) describes the impact of a working fluid on the climate and its share on the greenhouse effect. Over a defined time period the impact on the greenhouse effect is determined and related to carbon dioxide, which has a GWP=1 [7].

### 3.3.1.3 Total Equivalent Warming Impact

The Total Equivalent Warming Impact TEWI describes the complete direct and indirect greenhouse effect of a refrigeration system over its life time. It includes the direct emissions caused by leakage losses and recovery losses and indirect emissions, caused by the operation energy of the refrigeration or heat pump system. ?? shows the formulation of TEWI.

$$TEWI = (GWP * L * n) + (GWP * m [1 - \alpha_{recovery}]) + (n * E_{annual} * \beta) \quad (3.33)$$

## 3.3.2 Classification of working fluids

Based on the chemical structure and the synthesizing process, working fluids are classified in different groups:

- Natural working fluids
- Hydrocarbons
- Hydrofluoroolefines
- Halogenated hydrocarbons

### 3.3.2.1 Natural working fluids

They all have a low or even no impact on the environment and, depending on the application field, good thermodynamic properties for refrigeration and heat pump systems.

**Ammonia - R717** Ammonia is one of the oldest and cheapest working fluids. The benefits of ammonia are its favourable thermodynamic properties and no impact on the environment (ODP=0, GWP=0). In refrigeration and heat pump system it can reach high COP's, which causes a generous TEWI balance. It has a very high phase-change enthalpy, a high volumetric cooling capacity and a high heat conductivity. This leads to compact systems with high cooling and heating capacities. Therefore,

ammonia is used in large refrigeration systems in food and chemical industry. The disadvantages of ammonia are its toxicity and flammability. This requires higher security measure and specific instructions for the plant operators. Ammonia also has high saturation pressures, which leads to high absolute condensation pressures ( $T_{cond} = 120^\circ\text{C}$  conforms  $p_{cond} = 91.1 \text{ bar}_{abs}$ ). Because of its corrosive effect on copper and tin materials, stainless steel must be used as piping material.

**Water - R718** Water as working fluid has the best ecological properties. It also has a high phase change enthalpy, is highly available and cheap. The disadvantage of water is the low saturation pressure in a temperature range  $< 90^\circ\text{C}$ . For applications with evaporation temperatures at  $40^\circ\text{C}$ – $50^\circ\text{C}$  the saturation pressure varies between 0.074–0.124  $\text{bar}_{abs}$ . ?? shows the saturation curve of water. For refrigeration systems water is not suitable, but for HTHP systems it is an potential working fluid, because of higher heat source temperatures. For multi-stage heat pump systems water is suitable as working fluid for the second stage, were higher evaporation temperatures occur. Disadvantages of R718 are the low volumetric cooling capacity and the low heat conductivity. This causes large equipment dimensioning and additional cooling systems for the compressor, if the compressor outlet temperature exceeds the upper temperature limit, must be applied.

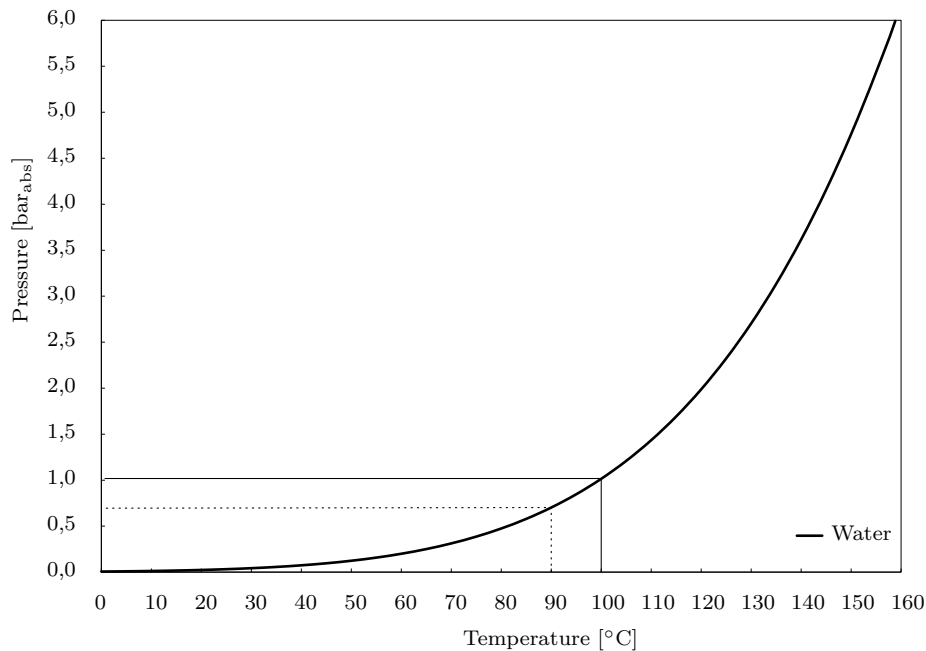


**Figure 3.8:** Saturation line of water in a T-p-Diagram according to Linstrom and Mallard [16].

**CO<sub>2</sub> - R744** Carbon dioxide is an old working fluid and has been used since the 19<sup>th</sup> century. The critical temperature of CO<sub>2</sub> is  $31^\circ\text{C}$ . For heat pump applications working with CO<sub>2</sub> the process is transcritical. Because of the low critical temperature the return temperature of the heat sink must be lower than  $31^\circ\text{C}$ . This restricts applications to cases with high temperature spreads in the sink. In general the operation pressures

of CO<sub>2</sub> are quite high, which requires special demand on the technical construction of the system. From an economic point of view it is a good working fluid, because it is cheap (compared to other working fluids) and highly available on market. It is not flammable, the toxic concentration is quite low and it also has a high volumetric cooling capacity.

**Hydrocarbons** Hydrocarbons have low ecological impact (GWP<10). Depending on their chemical structure (number of carbon atoms, saturated carbon connections, unsaturated carbon connections) the hydrocarbons have broad spectrum of thermodynamic properties. Therefore, they are used as substitutes for out-phased working fluids like R22. Typical hydrocarbon working fluids are Isobutane (R600a) and Propane (R290). Isobutane gets an important working fluid for household refrigerators whereas propane is used in air conditioning and air-source heat pump systems. The disadvantage of hydrocarbons are their high flammability (classified as A3). Other hydrocarbon working fluids are Ethane (R170), Butane (R600), Cyclopropane (RC270) and Propylene (R1270).

### 3.3.2.2 Synthetic working fluids

**Hydrofluoroolefines - HFO** As new "Low-GWP" working fluid fluorinated olefines, with a GWP < 10, were developed. Mostly used are R1234yf and R1234ze(E). The performance of R1234yf closely matches that of R134a and it is used in aircondition systems in the automotive sector. It has a similar pressure as R134a. The disadvantages are its flammability and its moderate volumetric cooling capacity.

The volumetric cooling capacity of R1234ze(E) is quite a bit lower than for R1234yf, but also the production costs are lower than for R1234yf. Because of its high molecular weight R1234ze(E) is used in large aircondition and ventilation systems.

There exist also several mixtures of the mentioned working fluids, called blends. By mixing the working fluids, the thermodynamic, ecological and physical properties should be optimized and adjusted to the application case. Especially the HFO are promising ingredients for future low-GWP blends.

**Halogenated Hydrocarbons** The halogenated hydrocarbons are mainly derivatives from alkane and alkene, where hydrogen atoms were substituted with halogen atoms. As halogens chlorine and fluorine were used. This stabilizes the whole molecule and decreases its reactivity, whereas the flammability is decreased. In the Montreal protocol and the regulation Nr.517/2014 on fluorinated greenhouse gases [14] the phase-out of these working fluids is regulated. First of all the Montreal protocol limited the usage of chlorinated fluorocarbons, like R12, and chlorinated hydro fluorocarbons, like, R22.

Substituting working fluids were hydro fluorocarbons (HFC), like R134a. On 1<sup>st</sup> January 2015 started the phase-out process for this type of working fluids. Until 2030 the number of sales should be reduced to 21% based on the reference year 2015.

For high temperature application at least working fluids from Organic Rankine Cycle processes (ORC) were analysed. Hydrofluorocarbons, like R245fa and R236fa, were in the focus of several research works. Based on their high critical temperature and pressure levels they can be applied in HTHP systems.

**Table 3.2:** Summary of references for thermodynamic state equations for common working fluids for heat pump applications.

Abbreviation	Chemical structure	Reference
R717	Ammonia	Wagner and Tillner-Roth [18]
R718	Water	Wagner and Pruß [19]
R744	CO <sub>2</sub>	Span and Wagner [20]
R600a	Isobutane	Bücker and Wagner [21]
R290	Propane	Lemmon et al. [22]
R134a	1,1,1,2-Tetrafluoroethane	Tillner-Roth and Baehr [23]
R245fa	1,1,1,3,3-Pentafluoropropane	Lemmon and Span [24]
R236fa	1,1,1,3,3,3-Hexafluoropropane	Pan et al. [25]
R365mfc	1,1,1,3,3-Pentafluorobutane	Lemmon and Span [26]
R1234yf	2,3,3,3-Tetrafluoroprop-1-en	Richter et al. [27]
R1234ze(E)	trans-1,3,3,3-Tetrafluoroprop-1-en	Thol and Lemmon [28]
R1233zd	1-chloro-3,3,3-Trifluoroprop-1-en	Mondéjar et al. [29]

### 3.3.2.3 Reference data for thermodynamic properties of working fluids

?? summarizes the chemical structure and reference data sources of common working fluids. The thermodynamic state equations for the process simulation of the heat pump cycles base on the NIST Reference Fluid Thermodynamic and Transport Properties (REFPROP) Version 9.1 [17].

### 3.3.3 Behaviour during compression

In general, the working fluids behave differently during compression depending on the look of the saturation line. The shape of the phase boundary in this space differs from one material to another, depending on the molecular structure of the substance [30]. For example, Ammonia or water become superheated during compression. Ammonia has a large isentropic coefficient ( $\kappa_{NH_3} = 1.31$ ), which causes high compressor outlet temperatures [7]. This type of working fluid shows a *bell-shaped saturation line*. For Ammonia the log(p)-h-diagram is shown in ??.

The second group are the working fluids with *re-entrant saturation line*. These working fluids enter the two-phase region during compression. HFC, like R245fa, R236fa, R365mfc or hydrocarbons like R600a, are part of this group. ?? shows Isobutane (R600a) with a re-entrant saturation line.

???? present solutions for an optimized operation of a HTHP depending on the used working fluid.

## 3.4 Summary

This chapter introduces the chosen methodology. There are some promising working fluids for HTHP applications. Depending on their thermodynamic properties during compression, the design of the HTHP must be adapted. ?? summarizes interesting

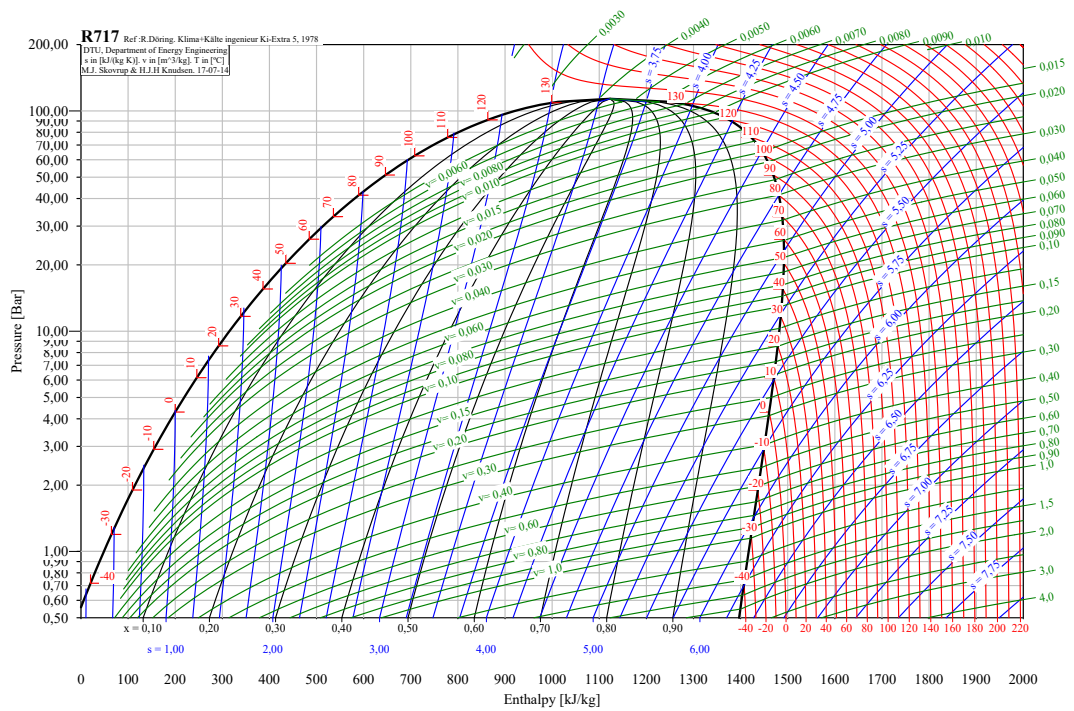


**Figure 3.9:** Log(p)-h-diagramm of Ammonia. It has a bell-shaped saturation line, which results in high superheating temperatures during compression.

working fluids for heat pump applications and classifies them depending on the saturation curve shape. Especially water could be a good working fluid for HTHP, if heat source temperatures above  $90^{\circ}\text{C}$  ( $\cong 0.7 \text{ bar}_{abs}$  saturation pressure of water) are available.

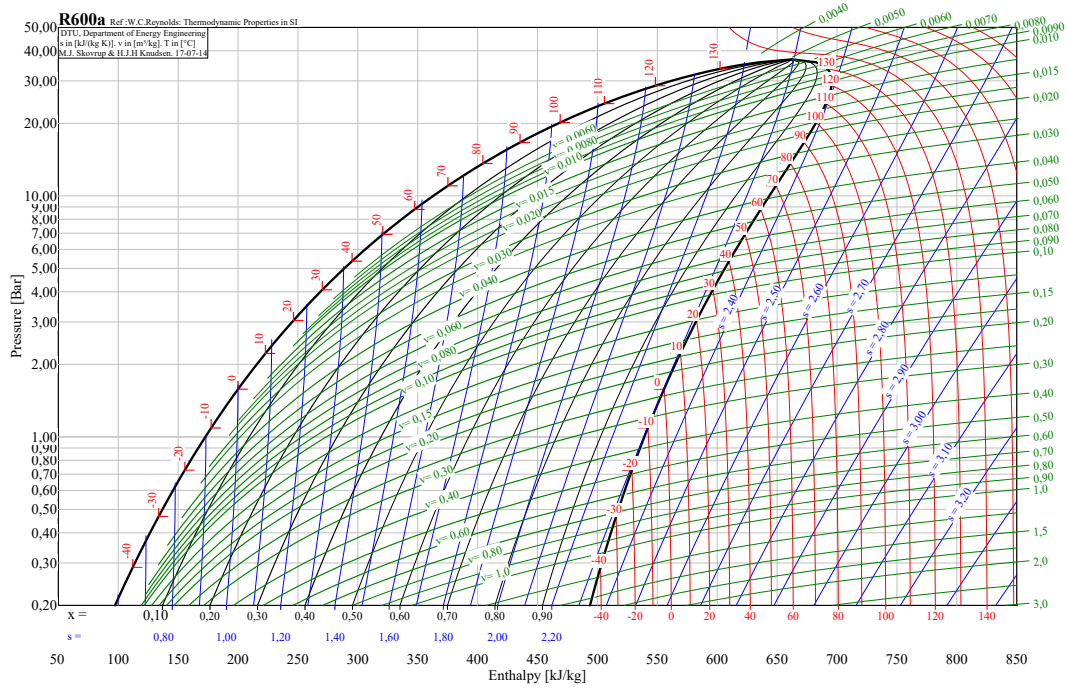


**Figure 3.10:** Log(p)-h-diagramm of R600a with a re-entrant saturation line.

**Table 3.3:** Classification of working fluids according to their behaviour during compression. The table also includes the critical temperature  $T_c$ , the critical pressure  $p_c$  and the specific vapor volume at 70°C.

Working fluid	$T_c$ [°C]	$p_c$ [bar <sub>abs</sub> ]	$v''_{70^\circ C}$ [m <sup>3</sup> /kg]	bell-shaped saturation line	re-entrant saturation line
R717	132	113.3	0.038	✓	—
R718	374	220.6	5.040	✓	—
R134a	101	40.6	0.009	✓	—
R245fa	154	36.5	0.030	—	✓
R236fa	125	32.0	0.015	—	✓
R365mfc	187	32.7	0.066	—	✓
R600a	135	36.3	0.002	—	✓
R1234yf	95	33.8	0.008	—	✓
R1234ze(E)	109	36.3	0.011	—	✓
R1233zd(E)	166	35.7	0.037	—	✓

## 4 Heat pump testing station

This chapter describes into the developed high temperature heat pump test station, which enables the determination of performance parameters of HTHP systems. The heat pump testing station is built as a multifunctional test bench. The test station is developed and designed for testing high temperature heat pumps as well as heat exchangers. It differs from conventional heat pump test stations, because no active heating or cooling system is applied. Because of increased requirements of HTHP systems, the heat pump testing station is designed for temperature levels up to 150°C and a pressure limit for the heat carrier in the heat sink of 40 bar<sub>abs</sub>.

### 4.1 Detailed function description of the heat pump test station

The heat pump testing station is designed for testing HTHP and allows the measurement of important efficiency parameters. The test station has several specifications, which are described in this part. In general the test station consists of the following measurements:

- 14 temperature measurements
- five pressure measurements
- four flow meters
- five pumps with frequency converters
- two valves with actuators

The test station is built up with different cycles, which are combined together. The detailed piping and instrumentation scheme with the functional cycles is shown in ???. The measurement components are listed in ??.

The first cycle is the heat source cycle. The heat source cycle provides the heat pump with heat. This cycle is constructed to run with water or brine. This allows also testing heat pumps with heat source temperatures lower than 0°C.

The intermediate cycle protects HX 2 against freezing, if the temperature gets below 4°C. Therefore the temperature is checked by sensor T2. If the temperature drops below 4°C an actuator opens a three-way-valve (M1). As a result the heat exchanger HX 1 is not working, until the temperature rises above 4°C. This cycle is also constructed to run with brine, whereas the connection cycle and the heat sink cycle are filled with water.

The heat sink cycle takes up the heat from the heat pump system. In the heat sink cycle the flow temperature is hold constant because of the temperature sensor T4 and the actuator 2 (M2). M2 controls the flow across the external chiller HX 3 by

creating a bypass over a ball valve, as shown in ???. As long as the temperature T4 is lower than the desired temperature, the ball valve stays opened. If the temperature rises above the desired temperature, M2 closes the bypass line until enough heat is withdrawn by the HX 3. All control elements use fuzzy logic, which is described in ??.

With the connection cycle heat from the heat sink of the heat pump is exchanged with the heat source. The heat pump's supply temperature in the heat source cycle T13 is held constant by controlling the mass flow of the recirculation with pump 3. If the temperature drops below the set point, the pump increases the volumetric flow rate so more heat gets back to the source cycle.

The whole system bases on the fundamental energy balance  $\dot{Q}_H = P_{el} + \dot{Q}_C$ . The amount of heat according to the cooling capacity  $\dot{Q}_C$  of the heat pump, is exchanged back to the heat source cycle via the connection cycle. The surplus heat brought into the system conforms to the electric power  $P_{el}$  of the heat pump. This surplus needs to be discharged out of the system. Two options are integrated:

1. Providing the local heating system with this heat using HX 4
2. Emitting the surplus heat with a chiller to the surroundings using HX 3

An additional function of the test station is the possibility to measure the behaviour of heat exchangers. In this function the heat pump provides the heat sink cycle with heat. This heat is exchanged from the primary side of the heat exchanger to the secondary side. The temperature levels, the pressure levels and the volume flows of both sides are measured and so the heat transfer coefficient  $k$  can be calculated. In case of heat exchanger testing, HX 5 marks the tested heat exchanger.

The heat sink cycle and the connection cycle are designed for temperatures up to 150°C and for a nominal pressure of 40 bar<sub>abs</sub>. These features allow to test high temperature heat pumps and heat exchanger with higher temperature levels, if the heat pump can provide them.

The description of the measurement points is summarized in ??. In the following, the construction parameters of important components of the test station are described.

### 4.1.1 Heat exchanger

In this test station the heat will be transferred by Alfa Laval stainless steel plate-heat-exchangers. For testing the heat pump HX 1, HX 2 and HX 3 are relevant. In ?? the relevant technical data are listed. For the construction of the test station an inlet temperature of 35°C and an outlet temperature of 40°C has been set at the warm side. The temperatures at the cold side are 10°C and 15°C. The area of the heat exchanger can be calculated by multiplication of the length and width with the amount of plates. According to the entry and outlet temperature the logarithmic mean of the temperature difference ( $\Delta\vartheta_{LM}$ ) is calculated in ??. The heat transfer coefficient  $k$  can be calculated out of ??.

$$\Delta\vartheta_{LM} = \frac{(\vartheta'_H - \vartheta''_C) - (\vartheta''_H - \vartheta'_C)}{\ln(\vartheta'_H - \vartheta''_C)/(\vartheta''_H - \vartheta'_C)} \quad (4.1)$$

$$\dot{Q} = k * A * \Delta\vartheta_{LM} \quad (4.2)$$

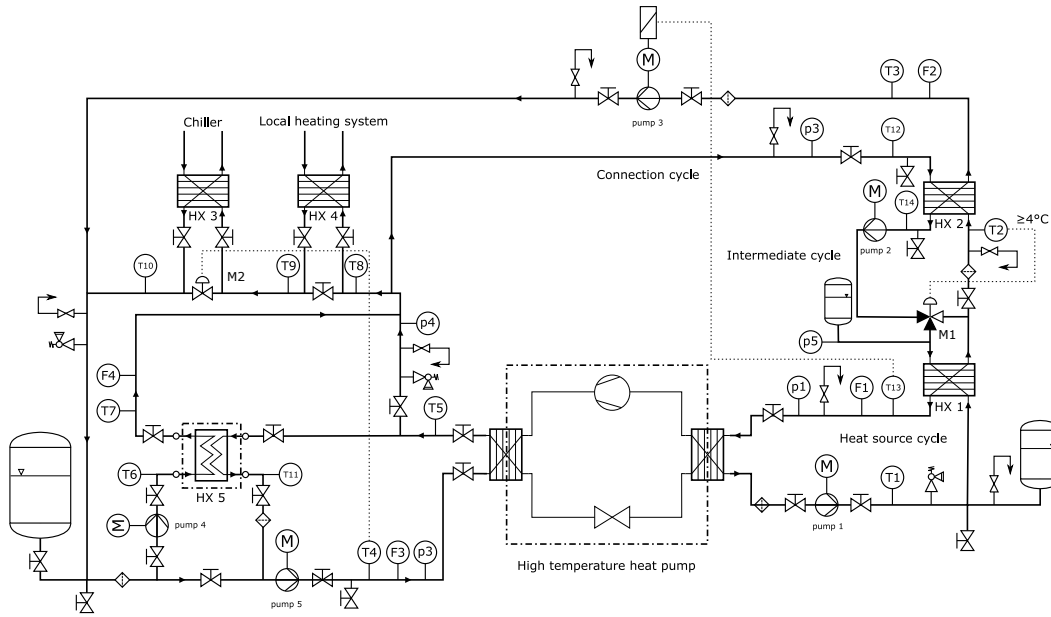


**Figure 4.1:** Instrumentation scheme of the test bench for high temperature heat pumps

#### 4.1.2 Programmable logic controller PLC

The programmable logic control systems gathers all necessary data (temperature, flow rate, pressure, power consumption). Furthermore, components like pumps and engines are controlled from here. The system is provided with an three-phase 380 V electrical supply. As safety measures, a residual current circuit breaker is installed, followed by 10 A fuses. These 10 A fuses, made for 230 V, should protect both power supplies (24 V/ 10 A, 5 V/ 5 A), the pumps, the ventilation and both engines. The PLC has been provided by the company *Bernecker & Rainer*.

**I/O System** The I/O System (Input/ Output) bases on the X20-System from *Bernecker & Rainer*, which is an automation system for plants and machineries. The system is alimented by a 24 V power supply. The PLC is built up in several modules, which are combined via a field bus system. The first module is the processor unit (CPU - Central Processing Unit) working with a frequency of 1.33 GHz. Apart from the CPU, the PLC includes digital in- and outputs, analog in- and output units, PT100-temperature modules, a counting module and an electric power measurement module.

**Power Panel** The operation of the PLC is done by a *Power Panel 500*, which is a touch screen display including three USB-connections, as well as an Ethernet connection and an RS232 connection. The *Power Panel 500* is the graphical interface and allows controlling and surveillance of the test station.

**Table 4.1:** Detailed measurement points of the description of the heat pump test set- up.

Measurement Point	Description
T1	Temperature heat source - out of the heat pump
T2	Temperature intermediate cycle
T3	Temperature connection cycle
T4	Temperature heat sink - into the heat pump
T5	Heat exchanger test - primary inlet temperature
T6	Heat exchanger test - secondary inlet temperature
T7	Heat exchanger test - secondary outlet temperature
T8	Temperature local heating system in
T9	Mixing Temperature local heating system out and heat sink cycle
T10	Mixing Temperature chiller system out and heat sink cycle
T11	Heat exchanger test - primary outlet temperature
T12	Temperature connection cycle
T13	Temperature heat source - into the heat pump
T14	Temperature intermediate cycle
F1	Flow rate heat source cycle
F2	Flow rate connection cycle
F3	Flow rate heat exchanger primary side
F4	Flow rate heat exchanger secondary side
p1	Pressure heat source cycle
p2	Pressure connection cycle
p3	Pressure heat exchanger primary side
p4	Pressure heat exchanger secondary side

#### 4.1.3 Measuring technique

To control the heat pump test station, specific measurement equipment is necessary. Following the installed sensors and transmitter are summarized:

**Temperature sensor** To measure the temperature in the system 14 PT100 - temperature sensors are used. The PT100 have a accuracy of  $\vartheta_{acc}[^{\circ}C] = 0.1^{\circ}C + 0.0017 * |\vartheta|$ .

**Pressure transducer** The used pressure transmitter is a ceramic pressure transducer with a pressure range from -1 to 400 bar<sub>rel</sub>. The pressure transducer consists of a piezo-resistive thick film ceramic sensor and a stainless steel housing.

**Flow meter** For measuring the flow, two types of flow meter were used: rotating meter and ultrasonic meter. The flow counter F1 is a rotating meter. It works because of the rotation of the paddle wheel which is caused by the flow through a measuring tube. The sensor F1 is part of the heat source circle. It has a nominal flow of 400 L/min. The quantity of pulses is 33 impulses/liter. The signal is also evaluated in the PLC by the counter model. It has a temperature range from  $-10^{\circ}C$  to  $+110^{\circ}C$ . The measuring inaccuracy is given with  $\pm 2\%$ .

**Table 4.2:** Detailed measurement points of the description of the heat pump test set- up.

Heat Exchanger	Product number	$\dot{V}_{nom}$ [L/s]	$\Delta p_{nom}$ [bar]	$A$ [m <sup>2</sup> ]	$k$ [W/m <sup>2</sup> K]
HX 1, HX 2	CB110–20L	2.89	0.175	2.35	1035
HX 3	CB30–34L	1.44	0.175	1.20	1012

The flow counters F2, F3 and F4 are ultrasonic flow meters. The temperature limits range from 5°C –150°C . The minimum flow rate  $q_{min}$  is 0.6 m<sup>3</sup>/h, the nominal  $q_{nom}$  6.0 m<sup>3</sup>/h and the maximum flow through  $q_{max}$  is 12 m<sup>3</sup>/h. The quantity of pulses is 25 impulses/liter. The signal is processed by the counter module of the PLC.

For the first test runs, the used heat carrier medium was water. For the use of brine, calibration of the flow meters will have to be done.

**Power metering** The electric power consumption is measured with a power monitoring module in the PLC. This module allows for measuring active, reactive and apparent power individually for each phase and for all of them collectively. Measurement of the main frequency and the phase angle of the three phases complete the power measurement data. An additional integration function maps the immediate power requirements of the machine.

#### 4.1.4 Control components

The amount of control components is limited to six pumps, two engines and one three-way-valve.

**Three-way-valve and actuator M1** The model of the three-way-valve is called VMV 20 and is made out of red brass by the company *Danfoss*. It is designed for hot water with a pH level of 7 – 10 and a maximum pressure of 16 bar<sub>abs</sub>. The maximum flow-through is 4,0 m<sup>3</sup>/h and the maximum temperature is 120°C.

The actuator model AMV 150 is produced by *Danfoss* and it is installed in the intermediate circle and regulates the three-way-valve. The power supply is done by 24 V, alternating current and the time for regulation is 24 s/mm. According to the given data, a time of 50.4 s for the complete opening of the three-way-valve can be calculated.

**Ball valve and actuator M2** The model Sal 61.00T40 is produced by *Siemens*. It has a rotation angle of 90°, a torque of 40 Nm and a regulation time of 120 s. Every analogue value stands for a defined position of the ball valve. The engine can be controlled by a voltage-signal (DC 0-10 V), the current (DC 4-20 mA) or a resistor. In the test station, the second way is used. The current 4 mA stands for the position 1° at the ball valve. A position of 90° means a current of 20 mA. The position of the ball valve depends on the temperature sensor T4, which should be hold constantly during the heat pump evaluation.

**Pumps** In the test block, six pumps, supplied by the company *Grundfoss*, were used. The pumps have digital and analog entry and exit. Controlling can be done by voltage signals of 0-10 V or a current of 4-20 mA. The pumps are linear controllable in a voltage range from 2-10 V. From 0-2 V the pump works at its minimum and after that the rotation number raises proportional to the control-signal.

Five pumps of the type *MAGNA 3 – 32 – 100 – 180* (*MAGNA 3*: internal diameter = 32 [mm]; maximum discharge head = 100 [dm]; built-in length = 180 [mm]) are installed. They have the numbers 1, 2, 4, 5 and 6. This five pumps have a maximum volumetric flow rate of 13 m<sup>3</sup>/h. Pump number 3 was designed smaller and is called *MAGNA 3 – 32 – 40 – 180*. The smaller pump has a maximum volumetric flow rate of 9 m<sup>3</sup>/h. The actually reached volumetric flow rate depends on the pressure-losses in the system.

##### 4.1.5 Fuzzy logic control system

The actuators and pumps in the heat pump test station were controlled in the PLC with a fuzzy logic control system. Following the fuzzy logic is introduced.

A formal, logical statement can be solved by the values *true* or *false*. Since this is not often sufficient, the concept of the fuzzy-logic (FL) was implemented. With this concept, it is possible to picture imprecise statements as mathematically predictable values. For the correct implementation it is necessary to create a fuzzy logic function with consensus of input and fuzzy rules. First all input values  $X = \{x_1, x_2, \dots\}$  must be fuzzified into fuzzy membership functions. This process is called *fuzzification* which leads to a *fuzzy-set*. Fuzzy-sets deliver a fuzzylogical statement depending on strict input values. The *fuzzy-amount*  $\mu$  can be defined by the degree of belonging  $\mu(x)$ . Notice that there is only one degree of belonging  $\mu$  for each variable  $x$ . During the decision-making process logical operators like *and*, *or* and *not* were introduced. In a second step all applicable rules to compute the fuzzy output functions are executed. The last step includes a *de-fuzzification* where the fuzzy output functions deliver crisp output values.

In the heat pump test station the entry-temperature to the heat pump in the heat source cycle (T13) and the entry-temperature to the heat pump in the heat sink cycle (T4) are controlled. ?? shows the fuzzy-set for the temperature control of the heat pump test station. The amount  $X$  is the deviation of the set point temperature to the actually occurring temperature ( $\Delta T$ ). For programming the fuzzy-logic an *or*-operator is used. The maximum of divergence is defined by the limits called  $\Delta T_L$  and  $\Delta T_R$ . The fuzzy-function follows a linear correlation between  $\Delta T$  and  $\mu(x)$ . ?? shows the fuzzy-set with the fuzzy functions and the logical correlations. For the *de-fuzzification* the function value  $F_1$  and  $F_2$  are combined with an amplification factor  $k$ . This is added to the control signal of the pump 3 respectively the actuator M2, according to ??. The fuzzy-control system can be extended with additional limits and amplification factors, to achieve a very precise control system.

$$control_{new} = control_{old} + a * (F_1 - F_2) \quad (4.3)$$

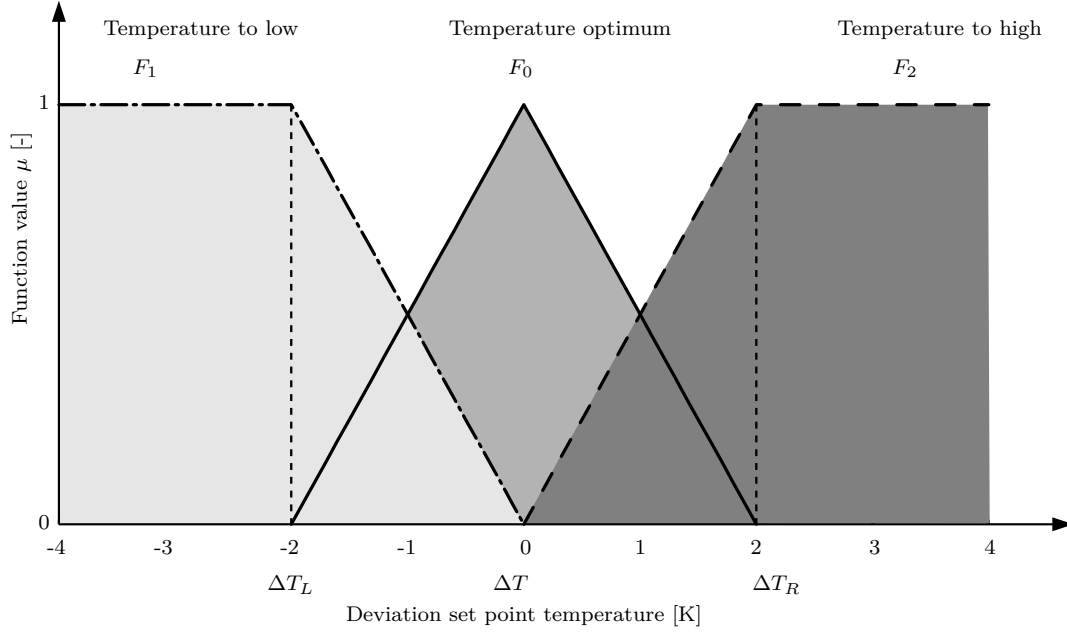


**Figure 4.2:** Defined fuzzy-set for the temperature control in the PLC of the heat pump station.

**Table 4.3:** Fuzzy-set for the temperature control pogramming.

	$F_0$	$F_1$	$F_2$
$\Delta T < \Delta T_L$	0	1	0
$\Delta T < \Delta T_L < 0$	$1 - \frac{\Delta T}{\Delta T_L}$	$\frac{\Delta T}{\Delta T_L}$	0
$0 < \Delta T < \Delta T_R$	$1 - \frac{\Delta T}{\Delta T_R}$	0	$\frac{\Delta T}{\Delta T_R}$
$\Delta T_R < \Delta T$	0	0	1

## 4.2 Evaluation of the heat pump test station

The experimental procedure is done, referring to the *EN 14511 – Air conditioners, liquid chilling packages and heat pumps with electrically driven compressors for space heating and cooling*. This standard is applied for hot-water heat pumps and space heating heat pumps and includes four parts:

- EN 14511-1:2013 Terms, definitions and classifications
- EN 14511-2:2013 Test conditions
- EN 14511-3:2013 Test methods
- EN 14511-4:2013 Operation requirements, marking and instructions

No specific standard for HTHP applications exists. In the following, the standard testing conditions and operation requirements of EN 14511 are introduced.

**Table 4.4:** Rated conditions for a water/water- and brine/water- setup.

		heat source in [°C]	heat source out [°C]	heat sink in [°C]	heat sink out [°C]
standard	water	10	7	30	35
conditions	brine	0	-3	30	35
nominal	water	15	b*	b*	35
operating	brine	5	b*	b*	35
conditions	brine	-5	b*	b*	35

\* operated with a volume flow which results from standard conditions

**EN 14511-2:2013 Test conditions** The test conditions for water/water and water/brine systems are summarized in ??.

**EN 14511-3:2013 Test methods** Apart from specifications about the correct testing and calculation of the power there are requirements from the testing equipment and the breadboard. The tested object should be built up like it is recommended by the manufacturer. Unless otherwise recommended by the manufacturer the temperature is set to the highest possible room temperature. Measurement uncertainties and test deviations are shown in ????.

**Table 4.5:** Allowed measurement accuracy according to EN 14511-3.

Monitoring point	Unit	Accuracy
temperature difference	[K]	$\pm 0.15$ K
temperature	[K]	$\pm 0.15$ K
volume flow	[m <sup>3</sup> /s]	$\pm 1\%$
static pressure difference	[kPa]	$\pm 1$ kPa or $\pm 5\%$
electric power	[W]	$\pm 1\%$
voltage	[V]	$\pm 0.5\%$
current	[A]	$\pm 0.5\%$
electric energy	[kWh]	$\pm 1\%$

The measurement of the delivered power is done in the so called steady state. This happens when all measuring sizes are constant over a period of time more than 30 minutes. The following chart shows the allowed deviations of the measuring sizes (??).

It is necessary to perform a continuous recording of all essential measuring data to guarantee a compliant test procedure. The recording period must be set in such a manner that every 30 seconds a complete data backup is produced. The test period has to be at least 35 minutes.

**Table 4.6:** Allowed deviations according to EN 14511-3.

Monitoring point	allowed averaged deviation of the measured data	allowed deviation of the single measured data
inlet temperature	$\pm 0.2 \text{ K}$	$\pm 0.5 \text{ K}$
outlet temperature	$\pm 0.3 \text{ K}$	$\pm 0.6 \text{ K}$
volume flow	$\pm 1\%$	$\pm 2.5\%$
static pressure difference	–	$\pm 10\%$
voltage	$\pm 4\%$	$\pm 4\%$

#### 4.2.1 Experimental procedure and data evaluation

The testing is done with the temperature-levels W10/W35, W10/W50 and W10/W60. This means an entry-temperature at the heat-source of  $10^\circ\text{C}$  and an exit temperature at the heat-sink of  $35^\circ\text{C}$ ,  $50^\circ\text{C}$  and  $60^\circ\text{C}$ . The data collection is done by the PLC and traced every second. For the heat pump testing, the temperature sensors T13 and T4 are the most important because the required temperature levels are controlled by them. According to the measured data for the flow rate (F1-F3), the pressure (P1-P4) and the temperature (T1, T3, T4, T8, T12 and T13), the calculation of performance parameter is possible(?????). The thermodynamic data for the evaluation of the test station bases on Wagner and Pruß [19].

$$\dot{Q}_C = F_1 * \rho(p_1, \bar{T}_{13\_1}) * c_p(p_1, \bar{T}_{13\_1}) * (T_{13} - T_1) \quad (4.4)$$

$$\dot{Q}_H = F_3 * \rho(p_3, \bar{T}_{8\_4}) * c_p(p_3, \bar{T}_{8\_4}) * (T_8 - T_4) \quad (4.5)$$

$$COP = \frac{\dot{Q}_H}{P_{el}} \quad (4.6)$$

#### 4.2.2 Heat pump for the evaluation of the test station

For the evaluation of the heat pump test station, a heat pump supplied by the company *Ochsner Wärmepumpen GmbH* was used. The model is called OWWP 54plus. The system is operated with the working fluid R410A and uses geothermal heat as energy source. The heat transmission fluid in the heat source and in the heat sink system is water (water-to-water heat pump). The heat pump works in a so called monovalent heating mode, which means that no other heat-producer is needed. The heating capacity reaches  $54 \text{ kW}_{\text{therm}}$  and a maximum heating temperature of  $60^\circ\text{C}$  is specified by the manufacturer (see ??).

**Table 4.7:** Manufacturer specification data of OWWP 54plus, a Water/Water heat pump from the company *Ochsner Wärmepumpen GmbH*.

Performance data heating	W10/W35	W10/W50	W10/W60	Unit
Heating power	53.9	49.7	46.5	[kW]
Cooling power	44.6	-	-	[kW]
Electric power	9.3	11.8	14.2	[kW]
COP	5.8	4.2	3.3	[-]
Current demand	16.8	21.4	25.8	[A]

### 4.3 Results of the heat pump testing

The following figures show the results at the different temperature-levels, as well as the average of the COP and the standard deviation. In ?????? the horizontal line shows the course of time. The axis on the left shows the temperature and the right axis shows the COP. For the trials, water is used as heat transfer medium in the heat pump test station.

#### 4.3.1 Test conditions W10/W35

The test results are shown in ??. The temperatures were hold on 10°C (heat source inlet) and 35°C (heat sink outlet). The minimum temperature of the source is 9.86°C and the maximum temperature is 10.20°C. The minimum temperature of the sink is 34.89°C and the maximum temperature is 35.29°C. This means that the required levels were maintained for about 35 minutes. The heat pump needs about 8.41 kW energy and delivers a heating-power of about 50.1 kW. The average of the COP is 5.95 and the related standard deviation is  $\pm 0.046$ . The minimum of the COP is 5.78 and the maximum is 6.09. The calculated cooling-performance is 40.9 kW. A slight oscillation of the COP, caused by temperature oscillations in the heat sink, is obtained.

#### 4.3.2 Test conditions W10/W50

?? shows the results for the temperature levels 10°C (heat source inlet) and 50°C (heat sink outlet). The minimum temperature of the source is 9.91°C and the maximum temperature is 10.12°C. The minimum temperature of the sink is 49.59°C and the maximum temperature is 50.25°C. This means again that the required levels were maintained for about 35 minutes. At a measured heating-performance of 46.32 kW, the electric power is 11.02 kW. This results in an average of the COP of about 4.20. The minimum COP is 4.00 and the maximum is 4.48. The standard deviation is  $\pm 0.078$ . Also this trial shows an oscillation of the COP, even more pronounced than in ??.

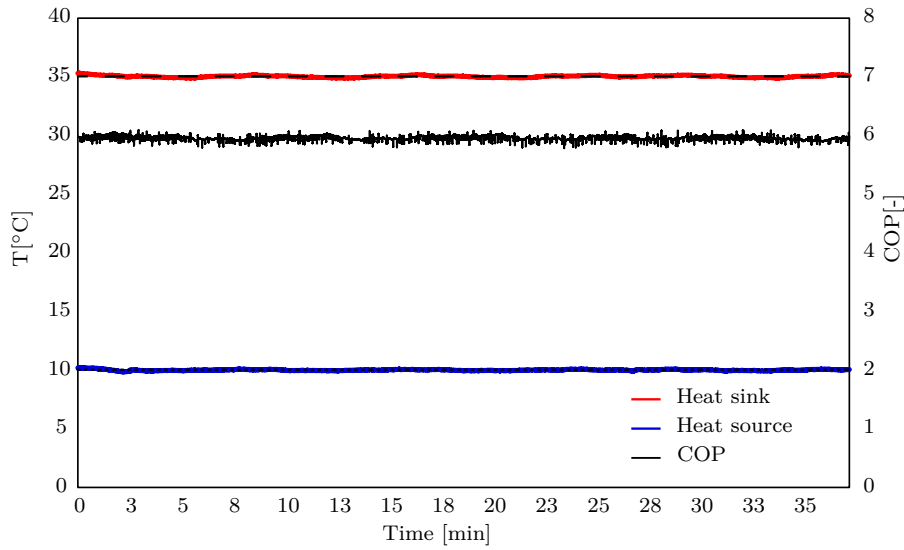


**Figure 4.3:** Test trial with heat source temperature of 10°C and heat sink cycle 35°C. The COP varies between  $5.95 \pm 0.046$

#### 4.3.3 Test conditions W10/W60

?? shows the last trial for the evaluation according to EN 14511. For the temperature levels 10°C (heat source inlet) and 60°C (heat sink outlet) the COP reached a value of 3.23 with a standard deviation of  $\pm 0.106$ . The standard deviation for this trial was higher than for the tests before. The heating performance is 43.83 kW and the electric power is 13.56 kW. The minimum temperature of the heat source inlet is 9.93°C and the maximum temperature is 10.08°C. The minimum temperature of the sink is 60.93°C and the maximum temperature is 59.69°C. This trial shows the most pronounced oscillation, compared to the other test trials.

## 4.4 Summary

The high temperature heat pump test station is a tool to assess performance parameters of heat pump systems, even if the temperature levels are higher than state of the art. Some prototypes of HTHP exist [31–33], but currently such systems are hardly available on the market. To test the heat pump test station, a common heat pump for space and hot water heating is used.

For all trials an oscillation of the measured COP was obtained. The oscillations of the COP are caused by oscillations in the heat sink temperature caused by a limited performance of the ball valve and the actuator M2 in the temperature control loop. With increased heat sink temperatures, also the oscillation increased. Despite the oscillations, the obtained results correlate well with manufacturer's specifications (??).

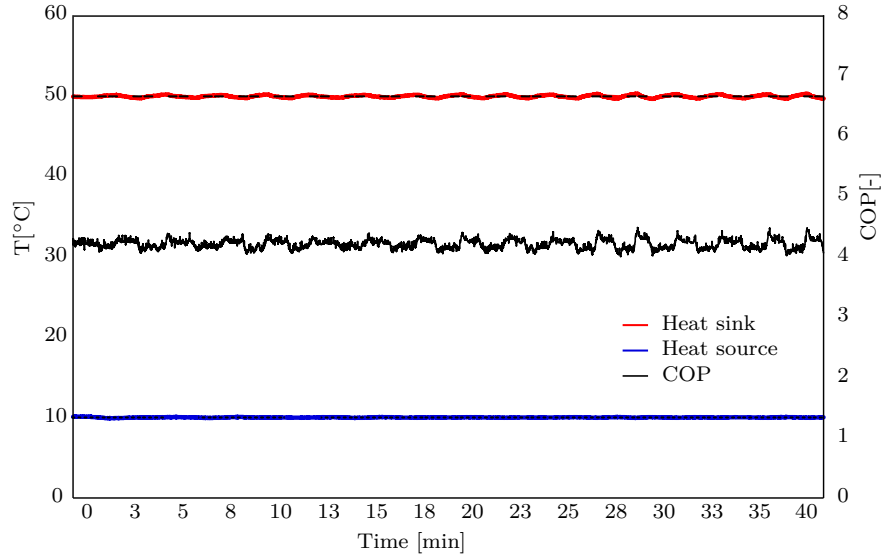


**Figure 4.4:** Test trial with heat source temperature of 10°C and heat sink cycle 50°C. The COP varies between  $4.20 \pm 0.078$

**Table 4.8:** Comparison of the COP obtained from the heat pump test station and the manufacturer's specification data.

Temperature levels [°C]	Manufacturer's data [-]	Test station [-]	Deviation [-]
W10/W35	5.80	5.95	$\pm 0.046$
W10/W50	4.20	4.20	$\pm 0.078$
W10/W60	3.30	3.23	$\pm 0.106$

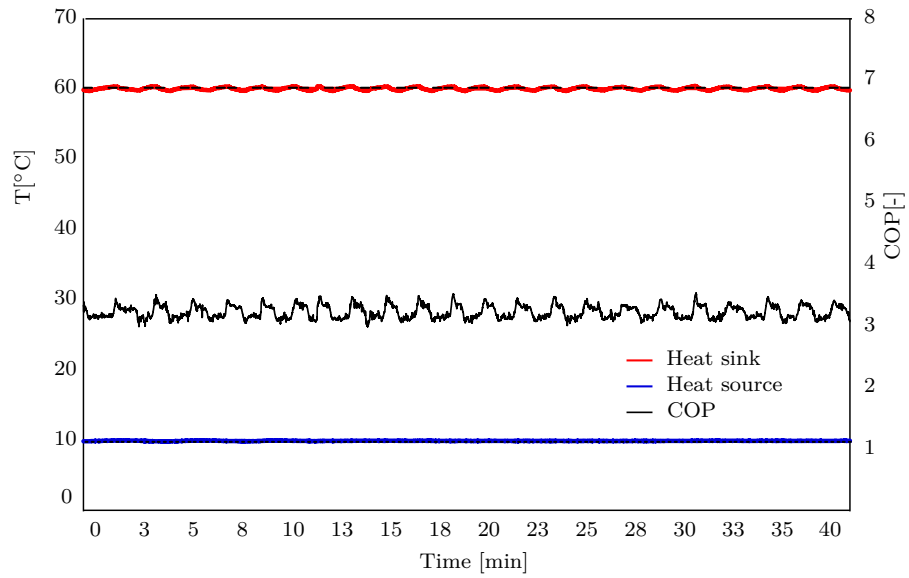


**Figure 4.5:** Test trial with heat source temperature of  $10^{\circ}\text{C}$  and heat sink cycle  $60^{\circ}\text{C}$ . The COP varies between  $3.23 \pm 0.106$



## 5 Optimization potential of high temperature heat pump systems

In the building sector, heat pump technology is well developed and widely used, but for industrial applications heat pump systems are not widely adopted. Reasons for this are special demands on technology and working fluids, because for industrial use, higher condensation temperatures are necessary. The installation of heat pump systems is also driven by economic factors, which are directly connected to the efficiency of the heat pump system. To establish heat pumps for industrial applications, two major challenges must be met: The system technology, including all components like compressor, lubricants and working fluids, must withstand higher temperatures, and simultaneously the efficiency of the system must be as high as possible. Useful working fluids for high temperature applications are natural working fluids like ammonia, or synthetic working fluids like R245fa. The working fluids show different behavior during compression, depending on their thermodynamic properties, as described in ???. For optimizing HTHP systems several process adaptations can be applied. The optimization depends on the used working fluid and its behavior during compression.

### 5.1 Optimization through extended suction gas superheating

For working fluids with re-entrant saturation line, the working fluid is superheated after the evaporator to avoid condensation during the compression. This is either done with the thermostatical expansion valve, which sets the evaporation temperature or with an internal heat exchanger (IHX). The internal heat exchanger, also called a recuperator, exploits heat from the hot liquid fluid between the condenser and the expansion valve and superheats the vapor exiting the evaporator. Superheating the working fluid after evaporation is necessary because of technical requirements and state-of-the-art. In heat pump and refrigeration systems, the cold vapor at the compressor inlet is superheated, between 3K - 8K [15, 34], to avoid condensation during compression.

However, superheating the cold vapor also influences the efficiency of the system, because as much heat is exchanged from the high-pressure side to superheat the working fluid at compressor inlet, as much the working fluid after condensation gets subcooled. The subcooling step directly influences the efficiency of the system. Especially for industrial heat pump systems an efficiency increase is very important, to increase their applications in practice. This part examines the change in energetic and exergetic efficiencies of selected working fluids for high temperature heat pump applications influenced by excess superheating and subcooling. The central question is: how much can internal heat exchange increase the efficiency of heat pump systems for the selected working fluids under given requirements?

### 5.1.1 Suction gas superheating in the literature

It is generally agreed that, downstream of the evaporator, superheating is necessary for certain fluids to avoid condensation during compression. It is not only necessary, in many cases it increases the efficiency of the heat pump or refrigeration system, which is obtained in several works. Radermacher and Hwang [35] and Maurer [7] describe vapor compression systems with internal heat exchangers in general. Subcooling the working fluid increases the specific cooling power. Concurrently, the suction gas gets superheated, and the density of the gas decreases. According to the working fluid and the slope of the isentropes in the  $\log(p)$ - $h$ -diagram, the specific work for compression increases. Maurer [7] explores the relation between increase of cooling capacity and technical work and describes the efficiency increase as follows:

$$\varepsilon^+ = \frac{1}{\frac{p_{Cond}}{p_{Evap}}^{\frac{\kappa-1}{\kappa}} - 1} \quad (5.1)$$

In this simplified relation, the gaseous working fluid is assumed to behave like an ideal gas. Moreover, superheating working fluids in heat pump cycles is investigated in several works. Kiss and Infante Ferreira [36] investigate the effect of superheating and subcooling to high temperature heat pumps to provide hot water with 120°C. They observed the effect for e.g. ammonia, butane and R245fa.

Selbaş et al. [37] also describe the effect of efficiency increase through superheating in refrigeration systems. For the superheated cycle, the mass flow rate is lower than for the saturated cycle, and the COP for superheated cycles is higher than that of saturated cycles. The authors describe in general the advantages of superheating refrigerant and heat pump cycles, but they do not differentiate between the types of working fluids, depending on their behavior of superheating or partial condensation along compression. To distinguish the two types, Felbab [38] developed a simple criterion to determine whether pure saturated vapor will be superheated or partially condensed during compression. To categorize the working fluids, the model only requires the compressor suction temperature, the ideal gas heat capacity and the enthalpy of vaporization at that temperature level.

Mastrullo et al. [39] analyzed refrigeration systems with 19 ozone friendly fluids, varying evaporation and condensation temperatures in the range of  $-40^\circ\text{C}/100^\circ\text{C}$  and  $25^\circ\text{C}/50^\circ\text{C}$ . The adoption of the suction/liquid heat exchanger is a profitable choice to prevent flash gas formation. A benefit on the performance depends on the combination of operating conditions and fluid properties. Klein et al. [40] concluded that liquid-suction heat exchangers are most useful at high temperature lifts and with a relatively small value of the fraction evaporation enthalpy to specific heating capacity and condensation temperature. For systems working with R717 the internal heat exchanger is detrimental, which is confirmed in this work. Domanski et al. [41] examined cycle parameters and refrigerant thermodynamic properties to improve the COP and the volumetric heating capacity with liquid-line/suction-line heat exchanger. They found out that fluids performing poorly in basic cycle benefit from internal heat exchange, whereas fluids performing well in basic cycle are marginally affected. Hermes [42] carried out for R134a, R22, R290, R410A, R600a and R717 the positive

and negative effects of the heat exchanger effectiveness, the specific heat ratio, the available heat and working pressures by changing the evaporation temperature.

The requirements for heat pump systems in industrial applications are higher because these systems must reach certain temperature levels. To challenge these requirements, special working fluids must be chosen. For example, Cao et al. [43] investigated six different heat pump systems working with R245fa to produce hot water with a temperature of 95°C. The systems include single-stage vapor compression HP, two-stage HP with external heat exchanger, two-stage HP with refrigerant injection, two-stage HP with refrigeration injection and IHX, two-stage HP with flash tank and a two-stage HP with flash tank and intercooler. Depending on the temperature levels (evaporation temperature: 25 – 35°C, condensation temperature: 98 – 108°C) the COP varies between 2.5 and 4.2. Several research works focus on the development of working fluids with low or even no impact on the environment [44–46]. Palm [47] describes the usage of hydrocarbons as working fluids in small-size heat pumps (< 20 kW cooling). The results showed that the COPs are equal or even higher than those of similar HFC systems. He also describes the benefits of superheating of hydrocarbons, but for R134a and R22 the effect is very small. Kondou and Koyama [48] investigated the performance of heat pump cycles with R717, R365mfc, R1234ze(E) and R1234ze(Z) as working fluids, producing heat with 160°C from waste heat with a temperature level of 80°C. Longo [49] investigated the effect of super-heating on hydrocarbon working fluids depending on their heat transfer coefficient in brazed plate heat exchanger. The results showed that super-heated vapor and saturated vapor show the same trend vs. working fluid mass flow, but the absolute values of the super-heated fluids are between 5% and 10% higher compared to saturated vapor at the same mass flux. Based on the knowledge from these earlier studies, we have tried in the present work to analyze the efficiency increase of selected working fluids for industrial heat pump applications with internal heat exchanger to provide heat at 120°C. Instead of simplified description of the thermodynamic behavior, we have used a modelling environment where the NIST two-phase thermodynamic properties [17] are used for all calculations.

### 5.1.2 Thermodynamic Analysis

The methodology in this chapter is the simulation of a heat pump process with internal heat exchanger (IHX) working with different working fluids. The temperature of the suction gas at the compressor inlet is increased by internal heat exchange. The performance of the heat pump cycles are calculated and compared. The chosen working fluids are described in ???. Isobutane (R600a) is often used in household refrigerators, but the disadvantage is the flammability of Isobutane. The operating pressure and capacity are less than half of R134a. It is also often used in blends with other working fluids [50]. R245fa and R365mfc are hydrofluorocarbons, used as foam blowing agent and applied as fluids for Organic Rankine Cycles. Because of its high critical temperature they can be used in heat pump systems [51, 52]. R236fa is a HFC gas designed to replace R114. It is used in low pressure centrifugal chillers and in some heat pump applications [53]. Ammonia is a well-known working fluid used in large scale industrial applications for more than 120 years. Ammonia has suitable thermodynamic properties, and it belongs to the group of natural working fluids without ODP and GWP. High COP are reached with ammonia machines in spite

of the pronounced superheating of ammonia during compression. The disadvantage of ammonia is its toxicity [54]. Water as a working fluid has several advantages, because it is environmental friendly, neither toxic or harmful, non-flammable, cheap, widely available and efficient. Water has a high phase-change enthalpy and also a high critical pressure and temperature. The disadvantages are the low volumetric heating capacity of the steam, high superheating temperatures after compression and low vapor pressure at environmental conditions.

**Table 5.1:** General properties of the analyzed working fluids for a heat pump process with excess suction gas superheating.

Working fluid	Critical Temperature <sup>1</sup> [°C]	Critical Pressure <sup>1</sup> [bar]	ODP [-]	GWP <sup>2</sup> [-]
R236fa	125	32.0	0	9820
R245fa	154	36.5	0	1050
R365mfc	187	32.7	0	842
R600a	135	36.3	0	20
R717	132	113.3	0	<1
R718	374	220.6	0	0

<sup>1</sup> Lemmon et al. [17]

<sup>2</sup> Daniel et al. [55] and RTOC [50]

The heat pump process is set up with the process simulation software IPSEpro. The process simulation allows the calculation of all specific thermodynamic data, like the NIST two-phase thermodynamic properties based on reference fluid thermodynamic and transport properties [17]. The simulations of the heat pump system are based on the assumption of steady-state conditions in all components and no heat and pressure losses in the heat exchangers. ?? reports further settings for the simulated process: the evaporator temperature is fixed to 60°C and the condenser temperature is fixed to 120°C. The isentropic efficiency  $\eta_{Compr}$  varies in literature in a wide range (e.g.  $0.60 < \eta_{Compr} < 0.85$  [36, 56]), and so a value in the middle range was chosen. The

**Table 5.2:** Parameters for the simulation of the HTHP process with suction gas superheating.

Parameter	Value	Unit
$\eta_{Compr}$	0.75	[-]
$T_{Evap}$	60.0	[°C]
$T_{Cond}$	120.0	[°C]
$\dot{Q}_{in}$	50.0	[kW]

scheme of the simulated heat pump system is shown in ??. The HP consists of an

evaporator (heat source), an internal heat exchanger (recuperator), a compressor, a condenser (heat sink) and an expansion valve. The recuperator exchanges heat from the condensed high pressure fluid to the evaporated low pressure fluid. The evaporated vapor is superheated in the recuperator, whereas the condensed fluid is subcooled. The superheating temperature at the compressor inlet  $T_{Compr,in}$  varies from 60°C to 120°C. ?? illustrates a log(p)-h-diagram of a heat pump process with superheating after

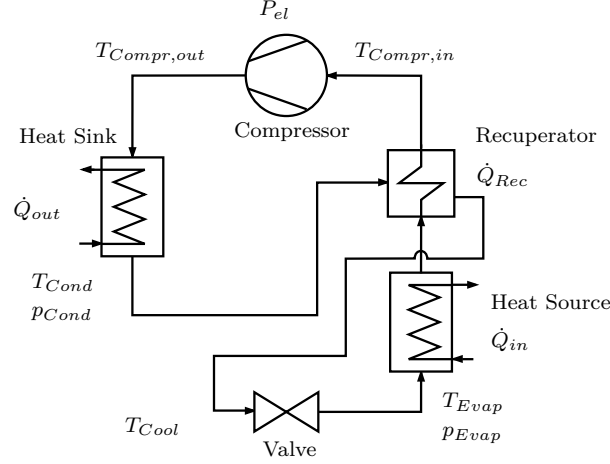


**Figure 5.1:** Simulation scheme of the heat pump system with a recuperator for overheating the suction gas at the compressor inlet.

evaporating the working fluid. The depicted working fluid is R245fa. The evaporation succeeds along the isobaric line from 1-2. 2-3 shows the superheating of the working fluid by the recuperator. 3-4 marks the compression step. The de-superheating (4-5), condensation (5-6) and subcooling (6-7) steps also follow an isobaric line. In the last step (7-1) the isenthalpic expansion of the working fluid closes the process cycle. The

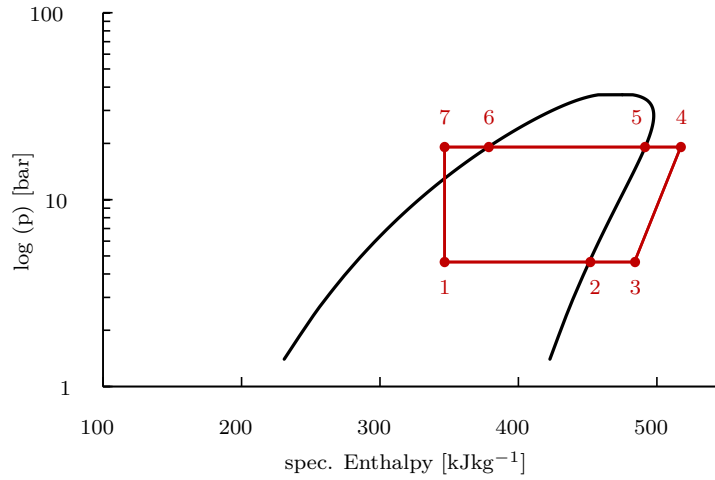


**Figure 5.2:** Log(p)-h-diagram of a heat pump process with superheating after evaporation, working with R245fa.

volumetric heating capacity  $q_{th}$  is the ratio of the heating output to the specific volume

of the vapor at the compressor inlet (see ??). The subcooling step is not considered as part of the volumetric heating capacity because it is only used internally and cannot be used for external heating.

$$q_{th} = \frac{h_4 - h_6}{v_3} \quad (5.2)$$

To describe the amount of superheating, the temperature difference between compressor inlet and evaporator outlet is calculated as described below (5).

$$\Delta T_{SH} = T_{Compr,in} - T_{Evap} \quad (5.3)$$

The specific exergy at standard conditions  $e_0$ , the exergy flow and the exergetic efficiency are calculated compared to ???????. The exergy losses of the internal heat exchanger are calculated as the difference of the sums of ingoing and outgoing exergy streams, as shown in ??.

To evaluate the benefit of superheating to the efficiency of the system, different superheating temperatures, depending on ?? are calculated and compared. To illustrate

**Table 5.3:** Key definitions of  $\Delta T_{SH}$  for cold vapor superheating.

Parameter	Description
$\Delta T_{SH,min}$	minimal necessary superheating temperature difference to avoid condensation along compression
$\Delta T_{SH,max,real}$	maximal possible, real superheating temperature difference, Pinch = 10 K (see ??)
$\Delta T_{SH,max}$	maximal possible, theoretical superheating temperature difference, theoretical optimum with Pinch = 0 K (see ??)

$\Delta T_{SH,max,real}$  and  $\Delta T_{SH,max}$  ??? demonstrate a heat pump process with R245fa. ?? shows a configuration with  $\Delta T_{SH,max,real} = 50$  K and 10 K pinch difference. Compared to this, ?? shows the process design with  $\Delta T_{SH,max} = 60$  K and 0 K pinch difference.

### 5.1.3 Results for optimizing heat pump systems with suction gas superheating

In this section the simulation results of the heat pump cycle with excess cold vapor superheating are reported. A recuperator superheats the working fluid after evaporation. The compressor inlet temperature  $T_{compr,in}$  varies from 60°C ( $\Delta T_{SH} = 0$  K) to 120°C ( $\Delta T_{SH,max} = 60$  K).

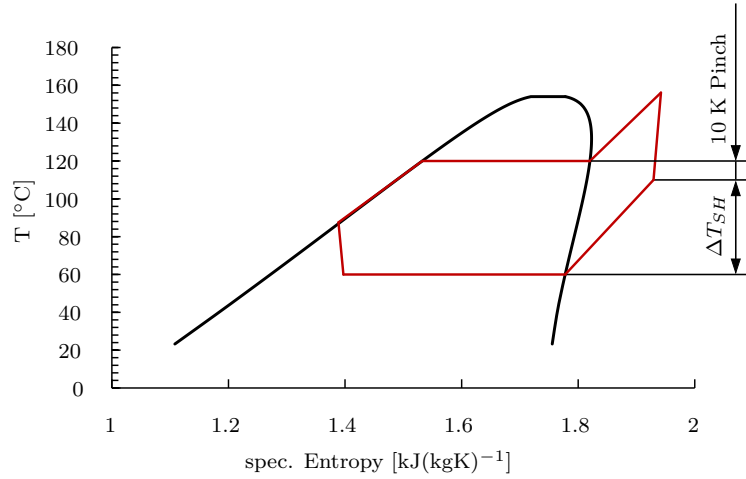


**Figure 5.3:** T-s-diagram of a heat pump process with R245fa and  $\Delta T_{SH,max,real} = 50$  K, with a pinch point difference of 10 K. It shows the real achievable optimum for this process configuration. The evaporation temperature occurs 60 °C, the condensation temperature 120 °C.

#### 5.1.3.1 Graphical comparison of a moderate superheating and an excess superheating heat pump process

In a first step, the different process operations are illustrated in a diagram. Two very important diagrams are the Log(p)-h-diagram and the T-s-diagram. ?? shows a Log(p)-h-diagram of R245fa with two heat pump cycles drawn in. The black cycle represents a heat pump system with a low superheating temperature ( $\Delta T_{SH} = 10$  K) and the red cycle depicts a heat pump with excessive superheating ( $\Delta T_{SH} = 30$  K). For the black cycle, a superheating temperature of 10 K is necessary, because R245fa partially condenses during compression, if the compressor inlet temperature is too low. Because of this effect, the de-superheating step is not applicable.

?? shows a T-s-diagram of R245fa with the same two heat pump processes (black = moderate superheating with  $\Delta T_{SH} = 10$  K; red = excessive superheating with  $\Delta T_{SH} = 30$  K). The COP of the black cycle is 3.17, the red cycle has a performance of 3.44. Raising the compressor inlet temperature from 70 °C to 90 °C, reached with excessive heat recuperation, enlarges the coefficient of performance by about 8.5% for R245fa.

In contrast to this, ???? show a heat pump processes with ammonia, a working fluid that superheats during compression. The simulation bases on the same parameters (evaporation temperature, condensation temperature) as for the cycles with R245fa. The black lines present a cycle without cold vapor superheating. Compared to R245fa the processes with ammonia must be de-superheated, because during the compression step the working fluid is superheated. For ammonia, the performance of the cycle without cold vapor superheating ( $\Delta T_{SH} = 0$  K) reaches a COP of 3.24. Superheating the working fluid after evaporation has no positive effect and decreases the COP.

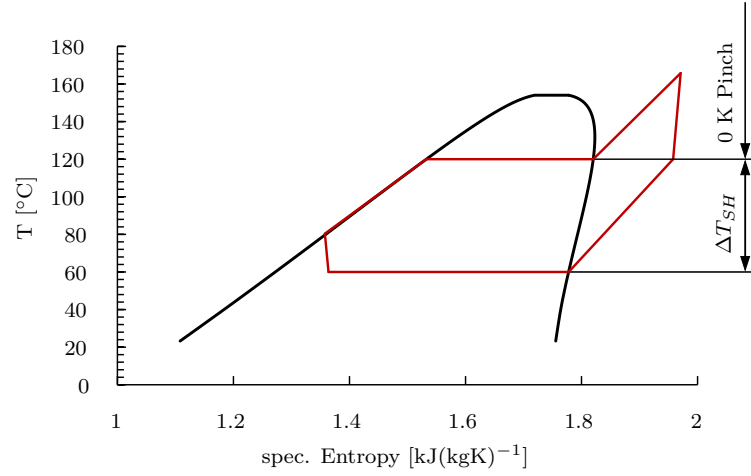


**Figure 5.4:** T-s-diagram of a heat pump process with R245fa and  $\Delta T_{SH,max} = 60$  K, with a pinch point difference of 0 K. It shows the theoretical optimum for this process design. The evaporation temperature occurs 60°C, the condensation temperature 120°C.

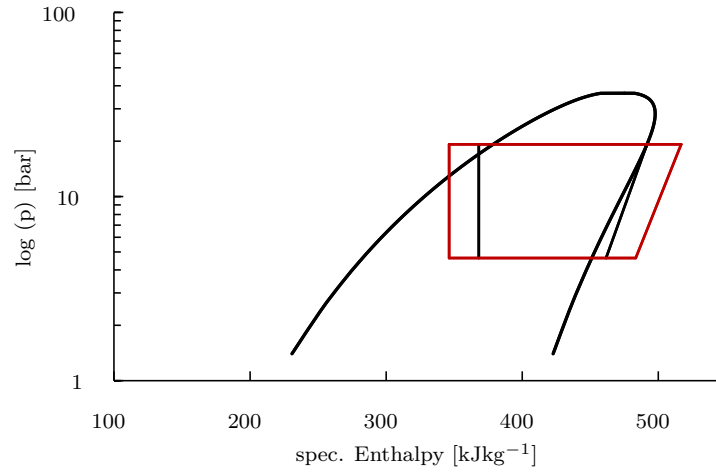


**Figure 5.5:** Log(p)-h-diagram of R245fa with an excessive cold vapor superheating (red line,  $\Delta T_{SH} = 30$  K) and a moderate cold vapor superheating (black line,  $\Delta T_{SH} = 10$  K) heat pump process with an evaporation temperature of 60°C and a condensation temperature of 120°C.

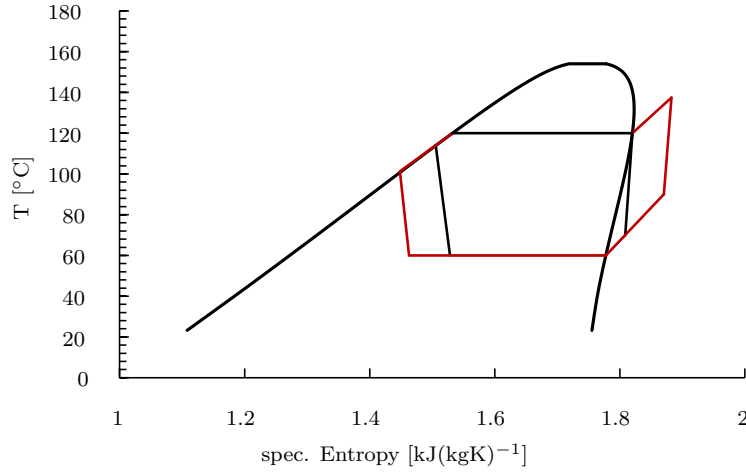


**Figure 5.6:** T-s-diagram of R245fa with an excessive cold vapor superheating (red line,  $\Delta T_{SH} = 30 \text{ K}$ ) and a moderate cold vapor superheating (black line,  $\Delta T_{SH} = 10 \text{ K}$ ) heat pump process with an evaporation temperature of  $60^{\circ}\text{C}$  and a condensation temperature of  $120^{\circ}\text{C}$ .

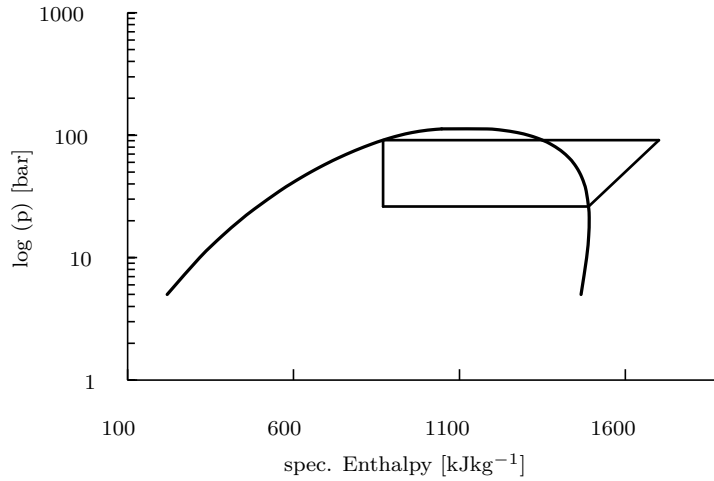


**Figure 5.7:** Log(p)-h-diagram of R717 without cold vapor superheating ( $\Delta T_{SH} = 0 \text{ K}$ ). The heat pump process operates with an evaporation temperature of  $60^{\circ}\text{C}$  and a condensation temperature of  $120^{\circ}\text{C}$ .

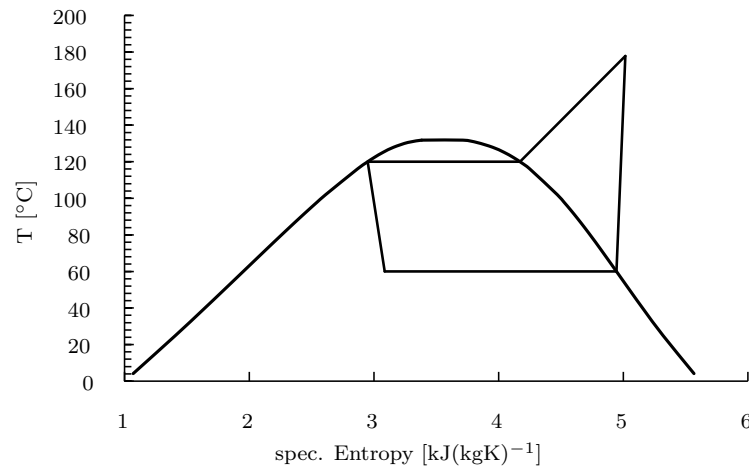


**Figure 5.8:** T-s-diagram of R717 without cold vapor superheating ( $\Delta T_{SH} = 0$  K). The heat pump process operates with an evaporation temperature of 60°C and a condensation temperature of 120°C.

### 5.1.3.2 Comparison of energetic and exergetic efficiencies of a heat pump system with an internal heat exchanger and excess superheating

?? depicts the change in COP with increased superheating temperature at the compressor inlet. The COP for R245fa, R236fa, R365mfc and R600a climbed steadily. For ammonia and water increasing the compressor inlet temperature has no positive effect and declines the efficiency. However, a water heat pump has the highest COP if no cold vapor superheating is applied. The results show that a heat pump, working with R365mfc and a compressor inlet temperature of 120°C has the highest COP compared to the other working fluids ( $\text{COP}_{\text{R365mfc}, \Delta T_{\text{SH}, \text{max}}} = 3.87$ ,  $\text{COP}_{\text{R718}, \Delta T_{\text{SH}, \text{min}}} = 3.74$ ).

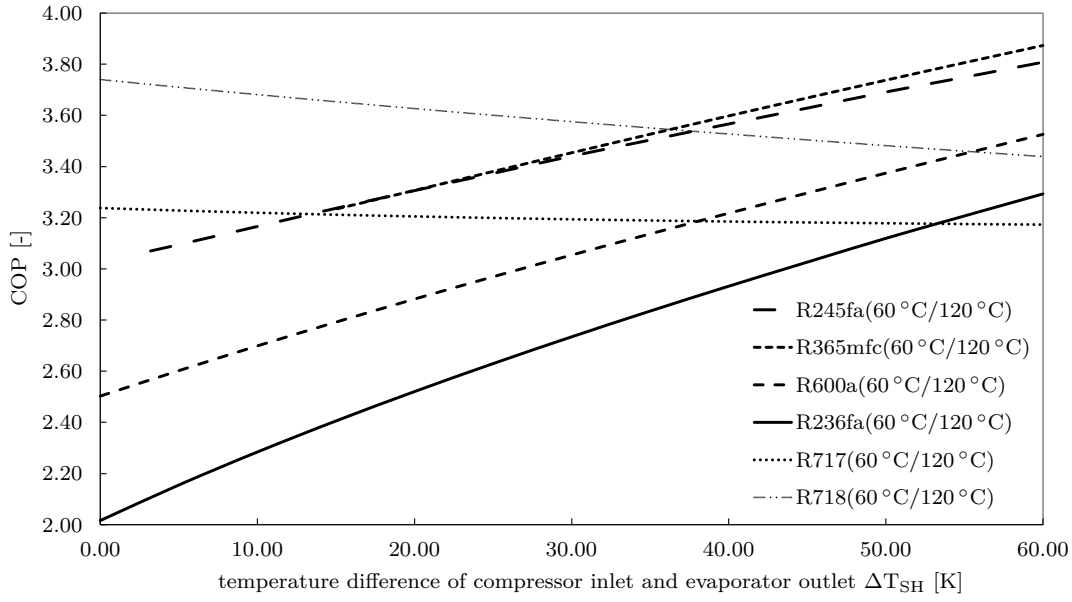


**Figure 5.9:** Behavior pattern of the COP of heat pump systems with different working fluids depending on the state of superheating at compressor inlet. The efficiency of non-superheating (re-entrance) working fluids increases (R245fa, R236fa, R365mfc and R600a). For ammonia and water, excess cold vapor superheating has no positive effect on the efficiency. For all processes the evaporation temperature is 60°C and the condensation temperature is 120°C.

?? shows the exergetic efficiency of heat pump systems with internal heat exchanger and excess superheating. For R245fa, R236fa, R365mfc, and R600a the exergetic efficiency rises with increased suction gas temperature, whereas R717 and R718 show a decreased exergetic efficiency if suction gas superheating is applied. Similar to the behavior of the COP the exergetic efficiency of R365mfc ( $\zeta_{\text{R365mfc}, \Delta T_{\text{SH}, \text{max}}} = 55.0\%$ ) with excess superheating ( $\Delta T_{\text{SH}} = 60$  K) is higher than for water without superheating ( $\zeta_{\text{R718}, \Delta T_{\text{SH}, \text{min}}} = 53.7\%$ ).

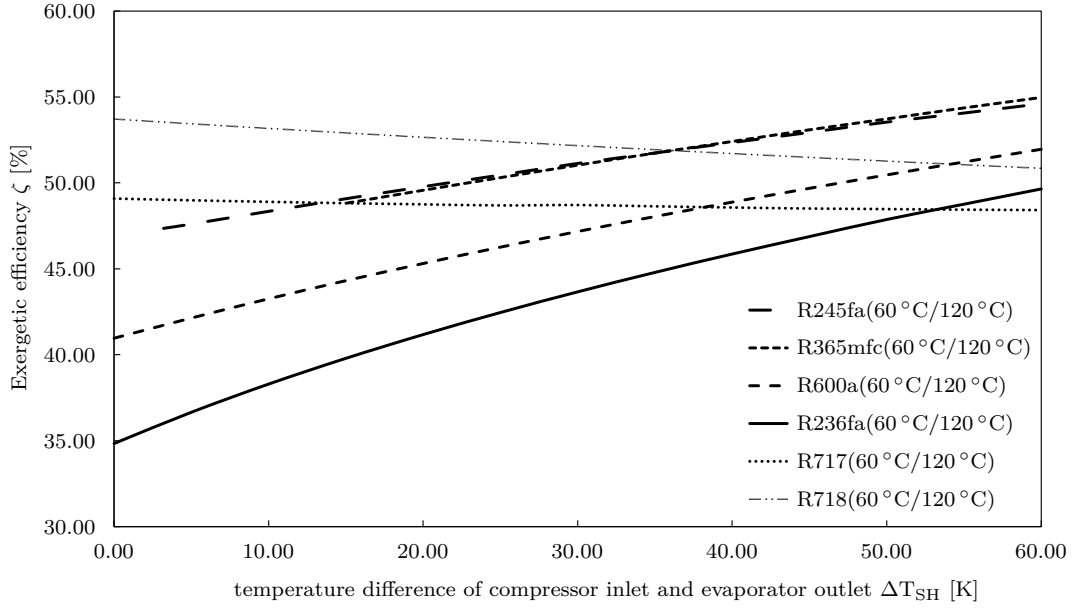


**Figure 5.10:** Exergetic efficiency of a heat pump with IHX and excess superheating.

### 5.1.3.3 Comparison of compressor outlet temperature, volumetric heating capacity and performance data of a heat pump system with an internal heat exchanger and excess superheating

The compressor outlet temperature is an important factor for design and operation of a compressor. With increased  $\Delta T_{SH}$ , the compressor outlet temperatures  $T_{Compr}$  rises. The increase of  $T_{Compr}$  for the different working fluids is shown in ???. With excess superheating ( $\Delta T_{SH} = 60$  K) the compressor inlet temperature of R245fa, R236fa, R365mfc and R600a varies between 164°C(R365mfc) and 173°C(R245fa). In contrast, the compressor outlet temperature of ammonia rises to 270°C and for water to 488°C. The compressor outlet temperature of ammonia and water without superheating are 185°C(R717) and 380°C(R718). These are very high compressor outlet temperatures, but for ammonia and especially for water, a polytrope (intercooled) compressor system lowers the compressor outlet temperature and raises the efficiency. This is described in ??.

The trend of the volumetric heating capacity is shown in ??. The volumetric heating capacity of ammonia and water decrease, whereas the volumetric heating capacities of the other working fluids increase slightly. A look at the absolute values show that ammonia has the highest volumetric heating capacity (17.316 – 17.595 kJm<sup>-3</sup>) and water has the lowest volumetric heating capacity (326 - 356 kJm<sup>-3</sup>).

The detailed simulation results for the recuperation power, the electric power, the heating power and the mass flow for the investigated working fluids are shown in ?????. For R245fa, R236fa, R365mfc and R600a, with excess superheating the recuperation power of the heat pump cycle increases. In contrast, the mass flow of the working fluid, the electric power and the heat rejected to the heat sink decrease. For R245fa and R365mfc minimum superheating temperature of  $\Delta T_{SH,min} = 3.2$  K

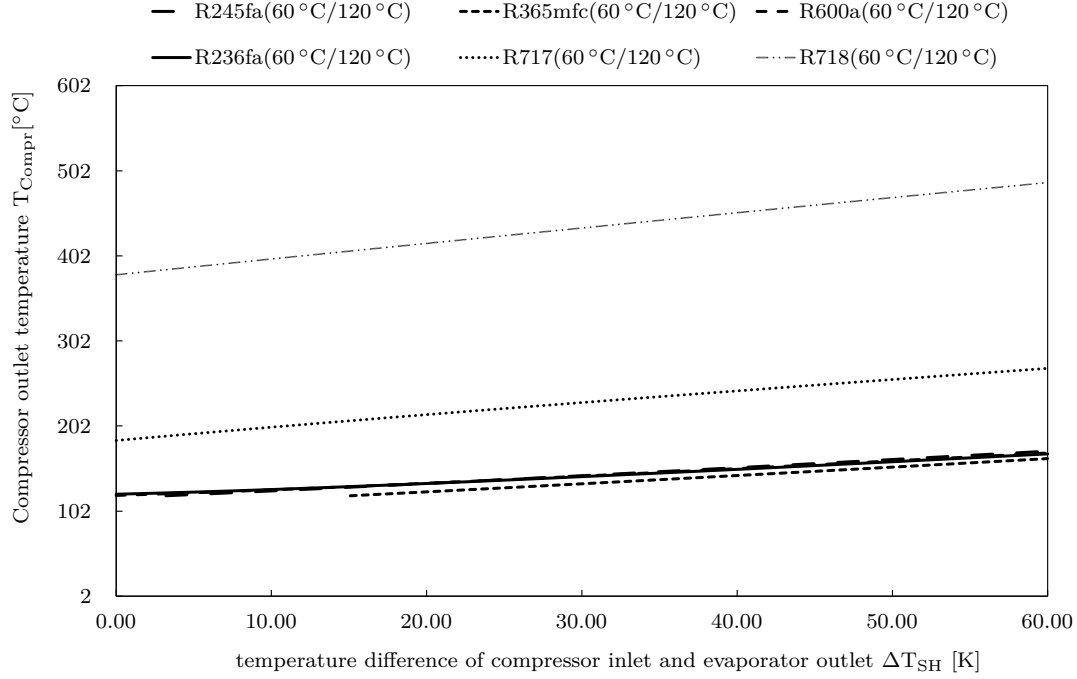


**Figure 5.11:** Rise of the compressor outlet temperature  $T_{Compr}$  with increased  $\Delta T_{SH}$ .

(R245fa) and  $\Delta T_{SH,min} = 15.1$  K (R365mfc) are necessary, to avoid condensation during compression. The results for R236fa and R600a show that for the chosen temperature levels (evaporator 60°C/ condenser 120°C) no superheating is necessary, because no condensation along compression occurs. However, at lower temperature levels, R236a and R600a may condense during compression. The ideal efficiency  $\varepsilon_{Carnot}$  for the simulated evaporation and condensation temperature (see ??), is for all variations 6.55. As a result, the COP of all processes reaches only 31% (R236fa,  $\Delta T_{SH,min}$ ) to 59% (R365mfc,  $\Delta T_{SH,max}$ ) of the ideal Carnot efficiency.

?? contains the absolute pressure levels and the pressure ratio of the investigated working fluids. The pressure ratio ranges from 3.26 (R600a) – 9.96 (R718). Comparing the absolute pressure levels shows that R365mfc has the lowest and ammonia the highest absolute pressure levels. As ?? presents, the percentage increase of R245fa, R236fa and R365mfc and R600a varies from 19.7% to 63.3% for investigated cold vapor superheating. For water and ammonia the efficiency decreases from -2.0 % to -8.1% by raising the superheating temperature from  $\Delta T_{SH,min}$  to  $\Delta T_{SH,max}$ .

**Table 5.4:** Simulated results for the recuperation power, the electric power, the heating power of the heat sink, the factor of COP to Carnot efficiency and the mass flow of the working fluid of a heat pump process with internal heat exchanger operating with R245fa, R236fa and R365mfc.

R236fa				
	$\Delta T_{SH,min}$	$\Delta T_{SH,max,real}$	$\Delta T_{SH,max}$	Unit
$\Delta T_{SH}$	0.0	50.0	60.0	[K]
$\dot{Q}_{Rec}$	0.0	32.3	34.3	[kW]
$P_{el}$	44.9	22.6	20.9	[kW]
$\dot{Q}_{out}$	90.5	70.4	68.9	[kW]
$COP/\varepsilon_{Carnot}$	30.8	47.6	50.3	[%]
$\dot{m}_{Ref}$	1.80	0.64	0.56	[kgs <sup>-1</sup> ]
R245fa				
	$\Delta T_{SH,min}$	$\Delta T_{SH,max,real}$	$\Delta T_{SH,max}$	Unit
$\Delta T_{SH}$	3.2	50.0	60.0	[K]
$\dot{Q}_{Rec}$	2.2	20.8	23.0	[kW]
$P_{el}$	23.1	17.9	17.2	[kW]
$\dot{Q}_{out}$	70.8	66.2	65.5	[kW]
$COP/\varepsilon_{Carnot}$	46.9	56.3	58.1	[%]
$\dot{m}_{Ref}$	0.63	0.39	0.36	[kgs <sup>-1</sup> ]
R365mfc				
	$\Delta T_{SH,min}$	$\Delta T_{SH,max,real}$	$\Delta T_{SH,max}$	Unit
$\Delta T_{SH}$	15.1	50.0	60.0	[K]
$\dot{Q}_{Rec}$	8.2	19.9	22.2	[kW]
$P_{el}$	21.0	17.4	16.6	[kW]
$\dot{Q}_{out}$	68.0	64.9	64.2	[kW]
$COP/\varepsilon_{Carnot}$	49.4	57.0	59.1	[%]
$\dot{m}_{Ref}$	0.49	0.35	0.32	[kgs <sup>-1</sup> ]

**Table 5.5:** Simulated results for the recuperation power, the electric power, the heating power of the heat sink, the factor of COP to Carnot efficiency and the mass flow of the working fluid of a heat pump process with internal heat exchanger operating with R600a, R717 and R718.

R600a				
	$\Delta T_{SH,min}$	$\Delta T_{SH,max,real}$	$\Delta T_{SH,max}$	Unit
$\Delta T_{SH}$	0.0	50.0	60.0	[K]
$\dot{Q}_{Rec}$	0.0	26.2	28.5	[kW]
$P_{el}$	31.2	20.2	19.1	[kW]
$\dot{Q}_{out}$	78.2	68.3	67.2	[kW]
$COP/\varepsilon_{Carnot}$	38.2	51.5	53.8	[%]
$\dot{m}_{Ref}$	0.51	0.24	0.22	[kgs <sup>-1</sup> ]
R717				
	$\Delta T_{SH,min}$	$\Delta T_{SH,max,real}$	$\Delta T_{SH,max}$	Unit
$\Delta T_{SH}$	0.0	50.0	60.0	[K]
$\dot{Q}_{Rec}$	0.0	10.7	12.1	[kW]
$P_{el}$	21.4	22.0	22.0	[kW]
$\dot{Q}_{out}$	69.3	69.8	69.9	[kW]
$COP/\varepsilon_{Carnot}$	49.4	48.5	48.4	[%]
$\dot{m}_{Ref}$	0.08	0.06	0.06	[kgs <sup>-1</sup> ]
R718				
	$\Delta T_{SH,min}$	$\Delta T_{SH,max,real}$	$\Delta T_{SH,max}$	Unit
$\Delta T_{SH}$	0.0	50.0	60.0	[K]
$\dot{Q}_{Rec}$	0.0	2.2	2.6	[kW]
$P_{el}$	17.3	19.1	19.4	[kW]
$\dot{Q}_{out}$	64.9	66.3	66.6	[kW]
$COP/\varepsilon_{Carnot}$	57.1	53.1	52.5	[%]
$\dot{m}_{Ref}$	0.02	0.02	0.02	[kgs <sup>-1</sup> ]

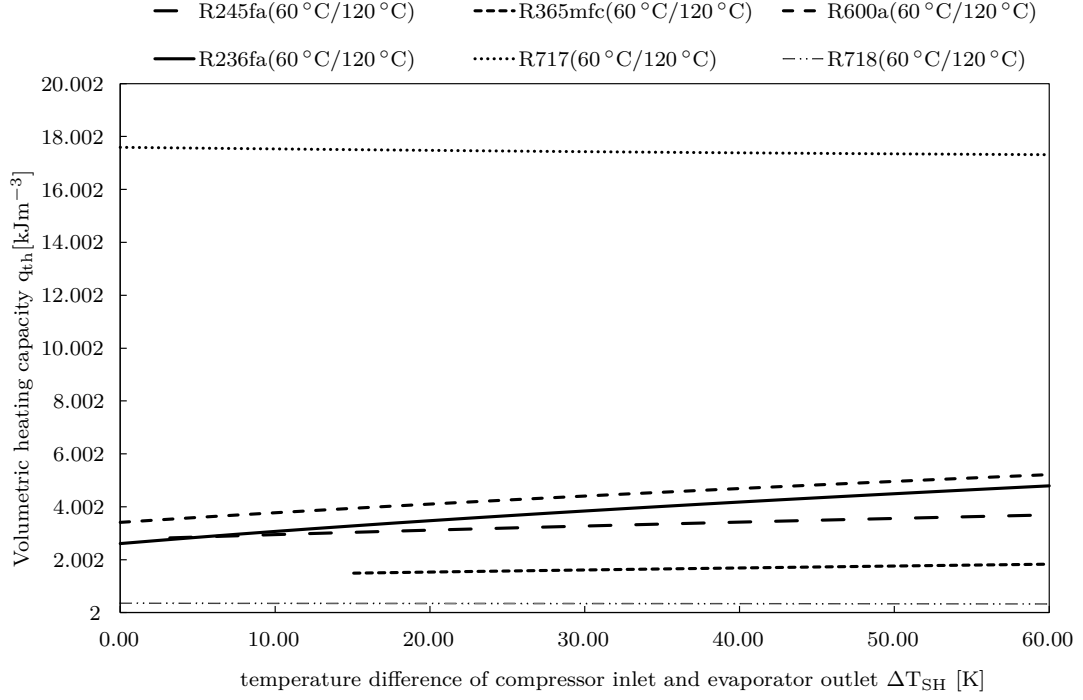


**Figure 5.12:** Behavior of the volumetric heating capacity with increased compressor inlet temperature.

**Table 5.6:** Different pressure levels of evaporation (60°C) and condensation (120°C) of the different working fluids and percental shift  $y_{min_{max}}$  of the COP by raising the superheating temperature from  $\Delta T_{SH,min}$  to  $\Delta T_{SH,max}$ . The table also shows the percentage changes of COP per degree superheating.

	R245fa	R236fa	R365mfc	R600a	R717	R718	Unit
$p_{Evap}$	4.6	7.6	2.0	8.7	26.2	0.2	[bar <sub>abs</sub> ]
$p_{Cond}$	19.3	29.0	9.3	28.4	91.1	2.0	[bar <sub>abs</sub> ]
$p_{Cond}/p_{Evap}$	4.17	3.80	4.71	3.26	3.48	9.96	[-]
$y_{min_{max}}$	24.0	63.3	19.7	40.9	-2.0	-8.1	[%]
$y/T$	0.42	1.10	0.44	0.68	-0.03	-0.13	[%K <sup>-1</sup> ]

## 5.2 Optimization through wet vapor compression

In contrast to ??, the optimization of heat pump processes working with working fluids with bell-shaped saturation line is described below. Typical working fluids with bell-shaped saturation line are water and ammonia. These working fluids superheat during compression. This leads to high compressor outlet temperatures, which causes technical and material problems. An opportunity to lower the compressor outlet temperature is wet vapor compression, where the vapor is not totally evaporated. The vapor quality of the suction gas is  $x < 1$ , as shown in ?. During the compression the temperature rises and the liquid fraction evaporates in the compressor. The evaporation of the remaining liquid chills the compressor and lowers the compressor outlet temperature. This part addresses, if and how much the efficiency can be increased for the chosen working fluids.

### 5.2.1 Thermodynamic analysis

Similar to ?? the simulation is done with IPSEpro. A heat pump process according to ?? is built up and the efficiency for different temperature levels (evaporation and condensation) for water and ammonia are observed. The technological settings for the process simulation are shown in ?. The chosen temperature levels accord to typical application fields of water and ammonia. Ammonia can be used as working fluid for refrigeration and heat pump systems. The investigations varying from  $-20^{\circ}\text{C} - 60^{\circ}\text{C}$  represent refrigeration application, whereas from  $10^{\circ}\text{C} - 130^{\circ}\text{C}$  a heat pump application is assumed. For water a temperature range from  $60^{\circ}\text{C} - 230^{\circ}\text{C}$  was examined. This is because water has very low evaporation pressures in a low temperature field. So only a high temperature heat pump application is assumed.

**Table 5.7:** Thermodynamic settings for the simulation of a wet vapor compression cycle.

Parameter	Value	Unit
Water		
$\eta_{\text{Compr}}$	0.80	[-]
$T_{\text{Evap}}$	60.0 – 180.0	[ $^{\circ}\text{C}$ ]
$T_{\text{Cond}}$	130.0 – 230.0	[ $^{\circ}\text{C}$ ]
Ammonia		
$\eta_{\text{Compr}}$	0.80	[-]
$T_{\text{Evap}}$	-20.0 – 80.0	[ $^{\circ}\text{C}$ ]
$T_{\text{Cond}}$	30.0 – 130.0	[ $^{\circ}\text{C}$ ]

To realize wet vapor compression, several technological settings exist, but for the further examinations only the first point was investigated:

- injection of high pressure liquid (??)

- ultra sonic evaporation to attain wet vapor suction gas
- multi-stage-compressor system: intercooling between the compressors

?? shows a heat pump process with injection. Liquid high pressure fluid from the condenser-outlet is injected into the suction gas stream or directly into the compressor.

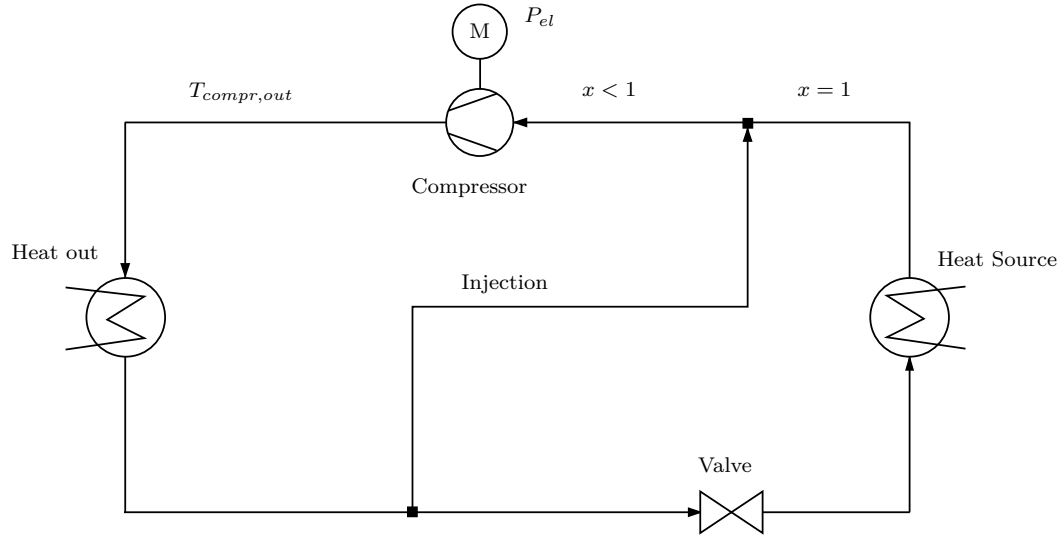


**Figure 5.13:** Scheme of a heat pump process with hot liquid injection for wet vapor compression.

In the following, wet vapor compression of water and ammonia are examined in detail.

### 5.2.2 Wet vapor compression - Water HTHP

Water belongs to the group of superheating working fluids. It shows an extreme degree of superheating, e.g. for a temperature lift from  $90^{\circ}\text{C}$  ( $T_{\text{evap}}$ ) to  $150^{\circ}\text{C}$  ( $T_{\text{cond}}$ ) the compressor outlet temperature reaches temperatures  $>320^{\circ}\text{C}$ . With wet vapor compression, the compressor outlet temperature can be decreased and the efficiency of the system simultaneously increased. ?? illustrates the results of a simulated HTHP systems with water as working fluid and an increased mass content of condensed water in the suction gas ( $0\% \leq \zeta_{\text{inj}} \leq 12\%$ ). The diagram shows that an increase of COP of 5.24%–13.27% can be reached depending on the chosen temperature levels.

?? shows the decrease of the compressor outlet temperature for HTHP systems for water ( $90^{\circ}\text{C}/150^{\circ}\text{C}$ ) and ammonia ( $50^{\circ}\text{C}/100^{\circ}\text{C}$ ). With an increased moisture content in the suction gas the compressor outlet is decreased effectively. ?? shows a summary of the efficiency increase of the observed temperature levels for a water HTHP system.

### 5.2.3 Wet vapor compression - Ammonia HTHP

Ammonia is a natural working fluid and has good thermodynamic properties for large-scale refrigeration systems. Even for heat pump systems with heat sink temperature

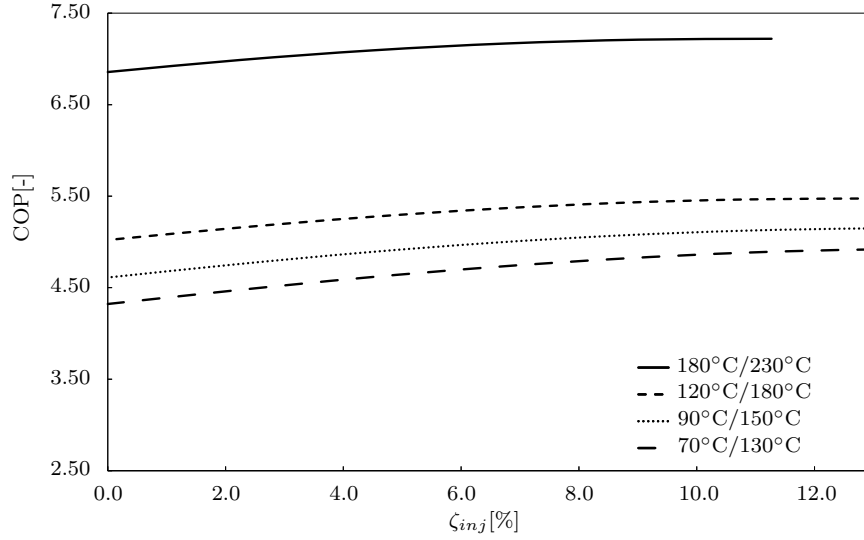


**Figure 5.14:** Water HTHP systems with different temperature lifts. An increased content of condensate in the suction gas increases the COP up to 13.27% (70°C/130°C)

levels up to 110°C ammonia is an applicable working fluid. Beside its toxicity and flammability, ammonia superheats during compression, what causes high compressor outlet temperatures. With wet compression, the COP can be increased, but the effect strongly depends on the temperature levels of heat sink and heat source. In [10], processes with different heat sink and heat source temperatures are shown. The injected mass fraction of water in the suction gas  $\zeta_{inj}$  varies from 0 – 16%.

[10] summarizes the results of the temperature variations of the ammonia heat pump. The results obtained show that the maximum COP increase (+7.42%) is reached at a temperature lift from -20°C to +30°C. As higher the temperature and pressure levels get, as lower gets the COP increase. For the highest examined temperatures (60°C/70°C/80°C to 130°C) even a negative effect of wet suction gas superheating on the COP was obtained.

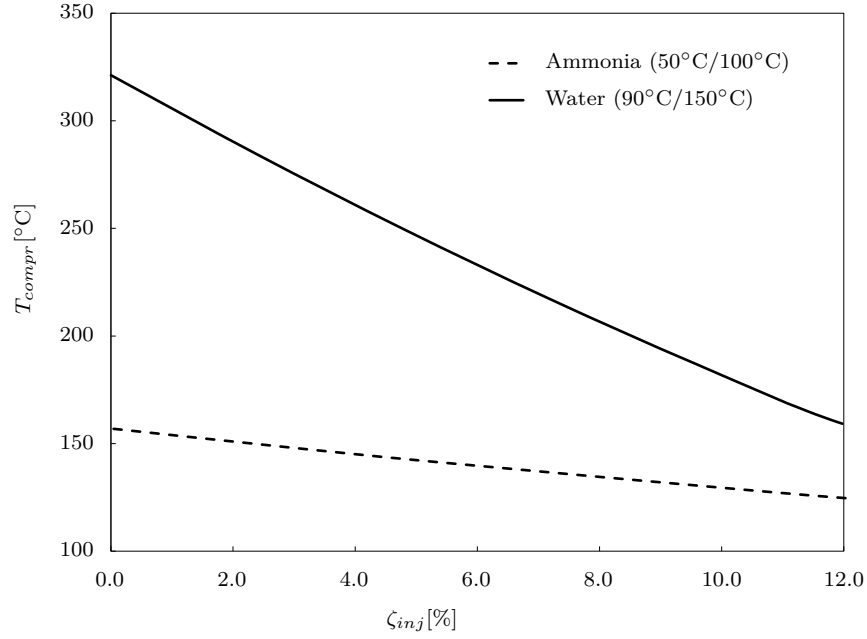


**Figure 5.15:** Decrease of the compressor outlet temperature for a water and ammonia HTHP system with increased water content in the suction gas ( $0\% \leq \zeta_{inj} \leq 12\%$ ).

**Table 5.8:** Variation of different heat source temperatures and heat sink temperatures for a water heat pump with increased mass fraction of water in the suction gas ( $0\% \leq \zeta_{inj} \leq 12\%$ ).

Temperatures [°C]	Temperature difference [K]	Pressures [bar]	Pressure ratio [-]	Effect on COP [%]
70°C/130°C	60	0.3/2.7	8.66	+13.27
90°C/150°C	60	0.7/4.8	6.78	+11.28
120°C/180°C	60	2.0/10.0	5.05	+8.89
180°C/230°C	50	10.0/28.0	2.79	+5.24

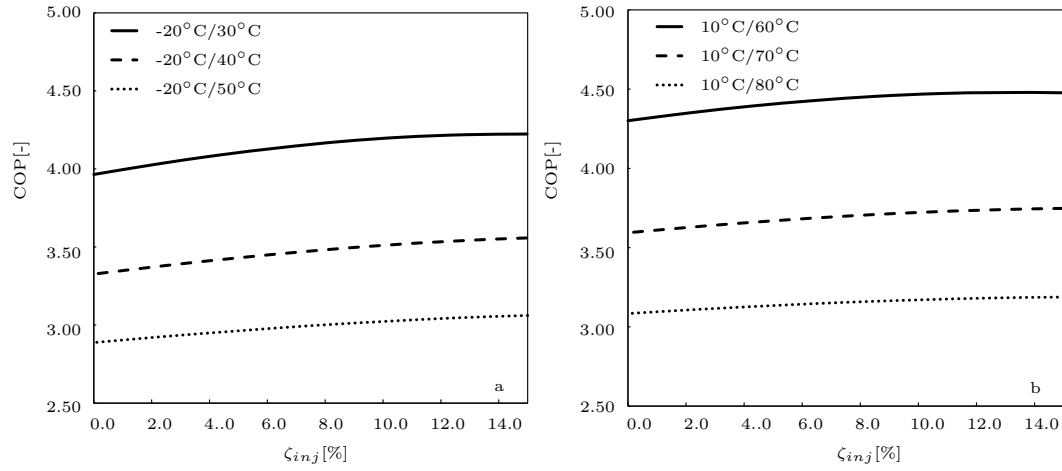


**Figure 5.16:** Performance increase of an ammonia system with increased liquid content in the suction gas. Picture a) depicts a refrigeration system with temperature lifts from  $-20^{\circ}\text{C}$  to  $30^{\circ}\text{C}$ /  $40^{\circ}\text{C}$ /  $50^{\circ}\text{C}$ . Picture b) presents an ammonia heat pump with temperature lifts from  $10^{\circ}\text{C}$  to  $60^{\circ}\text{C}$ /  $70^{\circ}\text{C}$ /  $80^{\circ}\text{C}$ .

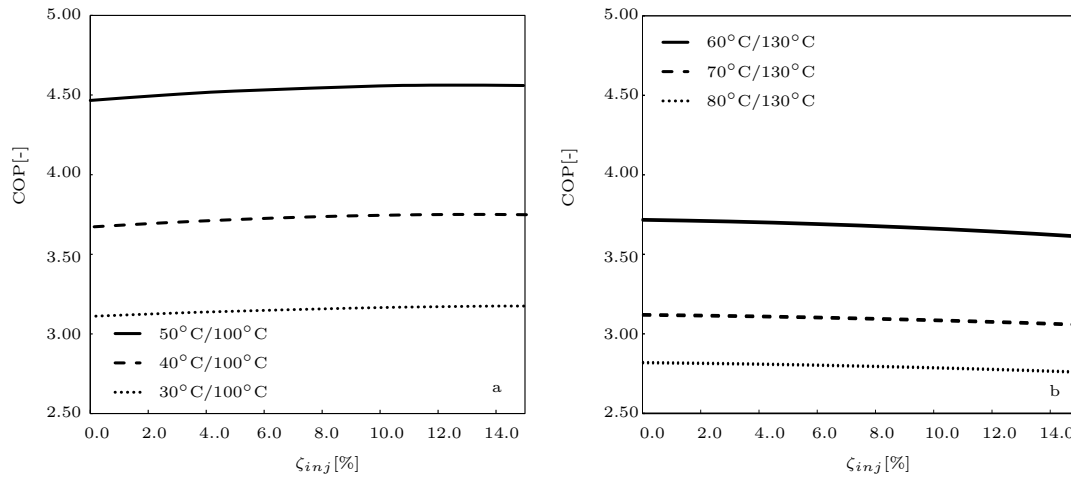


**Figure 5.17:** Effect of increased moisture content in the suction gas on the COP. Picture a) depicts an ammonia heat pump system with temperature lifts from  $30^{\circ}\text{C}$ /  $40^{\circ}\text{C}$ /  $50^{\circ}\text{C}$  to  $100^{\circ}\text{C}$ . A slight increase of COP is shown. Picture b) presents the results for an ammonia heat pump system with temperature lifts from  $60^{\circ}\text{C}$ /  $70^{\circ}\text{C}$ /  $80^{\circ}\text{C}$  to  $130^{\circ}\text{C}$ . For this case no efficiency increase was examined.

**Table 5.9:** Variation of different heat source temperatures and heat sink temperatures for an ammonia heat pump with mass fraction of liquid after the evaporator from  $0\% \leq \zeta_{inj} \leq 16\%$ .

Temperatures [°C]	Temperature difference [K]	Pressures [bar]	Pressure ratio [-]	Effect on COP [%]
-20°C/30°C	50	1.9/11.7	6.14	+7.42
-20°C/40°C	60	1.9/15.6	8.18	+7.18
-20°C/50°C	70	1.9/20.3	10.70	+6.45
10°C/60°C	50	6.2/26.2	4.25	+4.88
10°C/70°C	60	6.2/33.1	5.39	+3.32
10°C/80°C	70	6.2/41.4	6.73	+3.79
30°C/100°C	70	11.7/62.6	5.36	+2.05
40°C/100°C	60	15.6/62.6	4.02	+2.12
50°C/100°C	50	20.3/62.6	3.08	+2.10
60°C/130°C	70	26.2/109.0	4.17	-2.11
70°C/130°C	60	33.1/109.0	3.29	-2.16
80°C/130°C	50	41.4/109.0	2.63	-2.32

## 5.3 Summary

This chapter examines the efficiency improvement of heat pump cycles with excess recuperation and wet vapor compression. Six working fluids (R236fa, R245fa, R600a, R365mfc, R717 and R718) with different behaviour during compression were investigated.

In the first part of this chapter the optimization potential for heat pump systems with suction gas superheating is examined. The degrees of superheating temperature at the compressor inlet was varied from 0 K to 60 K and the heat pump efficiencies for each working fluid were calculated and compared. The results showed that for R236fa, R245fa, R365mfc and R600a the COP increases with higher superheating temperature.

Comparison of the COP shows that without IHX ammonia and water perform better than the other working fluids. But with increased superheating temperature the efficiency of R236fa, R245fa, R365mfc and R600a increase, up to 63.3%. With excess superheating the COP of this working fluids is even higher than the COP of ammonia and water without superheating. For the investigated case ( $T_{Evap} = 60^\circ\text{C}$ ,  $T_{Cond} = 120^\circ\text{C}$ ) an efficiency increase for R236fa, R245fa, R365mfc and R600a from 19.7% to 63.3% was observed. In addition, the volumetric heating capacity of those working fluids increased. According to Selbaş et al. [37], the mass flow of the working fluids decreased for all variations, also for ammonia and water, but no improvement of COP and volumetric heating capacity were obtained for this two working fluids. The results obtained follow the same trends as the results of Klein et al. [40] and Domanski et al. [41].

The exergetic efficiency increases for R236fa, R245fa, R365mfc and R600a with excess superheating up to 55.0% (R365mfc) and is higher, than for water or ammonia systems without superheating ( $\zeta_{R718\Delta T_{SH,min}} = 53.7\%$ ).

The compressor outlet temperatures of R236fa, R245fa, R365mfc and R600a range from  $120^\circ\text{C}$  to  $173^\circ\text{C}$  and were lower than for ammonia and water.  $173^\circ\text{C}$  is close to the upper limit of operation for the current compressor and lubricant design [36]. But comparing the compressor outlet temperatures shows that, even with excess superheating, the compressor outlet temperatures of R236fa, R245fa, R365mfc and R600a are lower than for water and ammonia without superheating.

In addition to increased efficiency, an increased volumetric heating capacity and a decreased mass flow also leads to smaller compressor systems. In conclusion, it can be said that a significant efficiency increase beyond the state of the art is possible for heat pumps if excess recuperative superheating is applied. Proper system design of the heat pump and exact dimensioning of the internal heat exchanger can lead to an efficiency improvement of up to 63.3%.

The second part describes the optimization of heat pump systems working with ammonia and water. These working fluids tend to superheat during compression. Wet vapor compression ( $x_{Suction\ gas} < 1$ ) leads to improvements in the COP up to 13.27% ( $\text{COP}_{Water, 70^\circ\text{C}/130^\circ\text{C}}$ ). Another benefit of wet vapor compression is a decreased compressor outlet temperature with little liquid entrainment. This effect was observed for ammonia and for water.

But for water and ammonia the results differ depending on the observed tem-

perature and pressure range. For ammonia an increase of COP was obtained for a condensation temperature range from 30°C –100°C . For the HTHP application ( $T_{evap} = 60^{\circ}\text{C}$ ,  $70^{\circ}\text{C}$ ,  $80^{\circ}\text{C}$  and  $T_{cond} = 130^{\circ}\text{C}$  ) no positive effect occurred. Whereas for water for all investigations a positive effect was observed.

## **6 Application of high temperature heat pump systems for industrial heat supply**

### **6.1 Current situation of industrial heat supply**

To reduce the CO<sub>2</sub> emissions from combustion of fossil fuels in industry, highly efficient technologies to provide heat and power must be considered. Heat pump systems and combined heat and power plants (CHP) are options to improve the energy efficiency of low temperature heat supply. Already since the oil crises in the 1970-ies, industry has installed combined heat and power plants for low temperature heat production. Concurrently to the heat production, they produce electric power for own use or to sell it to the power grid. However, because of lower electricity prices in the liberalized electricity market, the consumption of electricity from the grid may be more economic than own production from natural gas in CHP units. During the last few years, the mean electricity price at the day-ahead spot market decreased [57]. ?? shows the average hourly selling electricity prices from the EEX from 2013 to 2015. A linear trend of the median shows a negative slope, which is an indication for the decreasing electricity prices. The industrial sector benefits from this development because consuming electricity gets cheaper. But this also means that selling power from CHP plants gets less profitable.

Since heat-driven CHP units effectively provide electricity with boiler efficiency, i.e. about 90% based on the heating value of the additionally consumed fuel, this means that electricity from the grid is also cheaper than heat from fossil fuel in such a situation. However, producing low-temperature heat from electricity can be done much more efficiently if cheap waste heat is available at a reasonable temperature level. Compression heat pump systems provide heat with limited electric energy input. The coefficient of performance (COP) describes the efficiency of the process. As an example, a COP of four means that with one part electric energy and three parts of heat supplied at a lower temperature level (ambient heat, geothermal heat or industrial waste heat), four parts of useful heat at the required temperature level for the industrial process can be produced. Hence, the electric energy input is reduced to a quarter. Low electricity prices favor the operation of a compression heat pump system to provide industrial heat.

#### **6.1.1 Combined heat and power for industrial heat supply**

Many industrial processes need heat and power simultaneously and so CHP offers the opportunity to produce the required energy on site. Even though industry typically uses the produced electricity fully at site, any potential excess of produced power can be supplied to the power grid and sold at market-conditions. Compared to a separate generation of heat and power in boilers and power plants, CHP plants offer higher energy efficiency levels and can achieve fuel savings of 10 - 40%, depending on the used

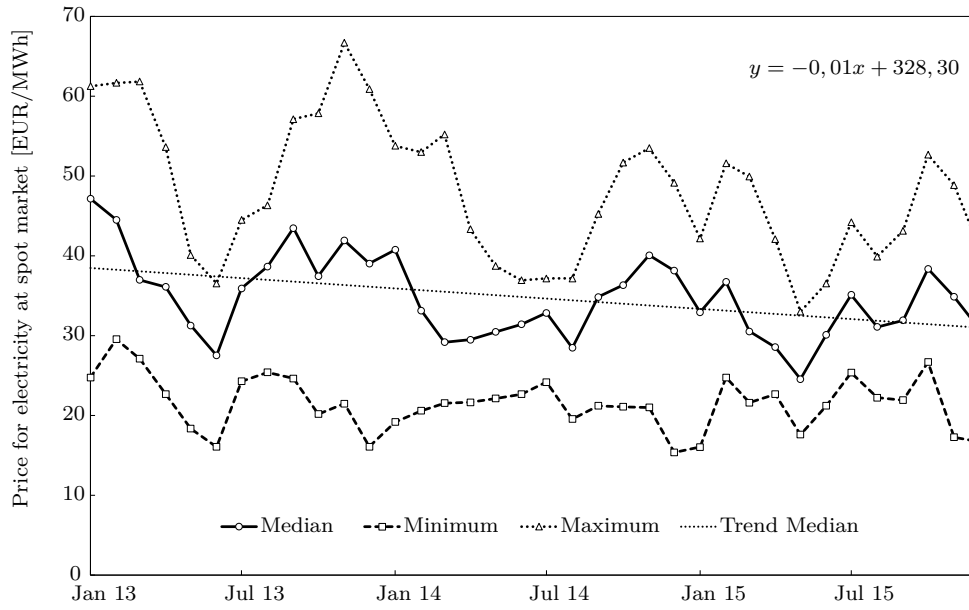


**Figure 6.1:** Price for electricity from January 2013 until December 2015. The diagram illustrates the median, the minimum and the maximum hourly means of the electricity price sold at the European Energy Exchange (EEX) [58]. A linear trend of the median shows a negative slope, so the averaged electricity prices decreased slightly.

technology [59]. Many industrial costumers install CHP plants to satisfy simultaneous thermal and electrical power demands. However, since the economic recession in 2009 many of these plants were under-utilized and the capacity utilization decreased up to 50% [60].

There are many works that focus on the modeling of CHP plants in the industry and the application of CHP units depending on time-sensitive electricity prices to maximize the economic benefits of selling power to the grid [61–64]. Mitra et al. [60] describe a model that addresses the optimization of industrial CHP plants. The model tracks the components of the plant and takes different operation modes into account. Apart from the states of components in terms of operating modes, the transitional behavior and the inherent flexibility of the CHP plant is captured. With this model, a CHP plant in a chemical park was improved and the generated surplus electricity produced during hours of favorable prices is increased. Alipour et al. [65] present the short-term hourly scheduling of industrial and commercial customers with the opportunity of combined heat and power production. A demand-response program deals with the needed heat and power produced by the costumers and serves solutions to minimize the costs. Moradi et al. [66] describe an energy management strategy based on the fuzzy theory to optimize the capacities of CHP systems. The model determines the optimum range for boiler and CHP capacities by maximizing an objective function based on the net present value (NPV). They used hybrid optimization methods involving particle swarm optimization and linear algorithms. Cho et al. [67] present an energy dispatch algorithm that minimizes the cost of energy including cost of electricity from the grid and cost of natural gas to drive the CHP process. Beihong and Weiding [68]

developed an optimal planning method based on mathematical programming theory to handle the problems of cogeneration systems and to minimize annual operating costs. Kong et al. [69] use a linear programming model for optimizing combined cooling, heating and power production. The model minimizes the overall costs of energy considering a gas turbine, an absorption chiller and a heat recovery boiler. Thorin et al. [70] developed a tool for long-term optimization of cogeneration systems based on mixed linear-programming and Lagrangian relaxation. In addition to the possibility of buying and selling electric power at a spot market the provision of secondary reserves is considered. Najafi et al. [71] presents an energy hub management which gives a decision basis whether electricity and gas is procured from the market or whether electricity is supplied to the market by self-generation. The decisions are made under a risk-averse perspective realized with stochastic programming, so called Conditional Value at Risk (CVaR). This models and studies focus the economic production of electricity and heat with CHP plants, depending on electricity prices and operation behavior.

On the background of decreasing electricity prices on the liberalized electricity market the question arises, how process heat should be produced, if CHP plants get uneconomic because using gas to produce power, even with a high efficiency, is more expensive than buying electricity from the grid.

### 6.1.2 High temperature heat pumps for industrial heat supply

An alternative way to provide process heat are heat pump systems. They can provide low temperature heat very efficiently if waste heat is available. Several studies examined the implementation of heat pump systems in industrial processes. Bakthiari et al. [72] analyzed the implementation of an absorption heat pump in a Kraft pulping process. For the integration, two scenarios were examined. Considering to a steam price of 63 USD/MWh, the simple payback times were between 1.7 and 2.7 years for the two case studies.

According to Wolf et al. [73] the latest developments on the market for high temperature heat pump technology (HTHP) allow for heat sink temperatures up to 160°C, although further developments are foreseen [74, 75].

A promising working fluid for industrial applications at increased heat sink temperatures above 120°C is water. On the one hand, water is environmentally friendly and safe but, on the other hand, it also has favorable thermodynamic properties in terms of high phase-change enthalpy and high critical temperature. Lachner et al. [76] investigated the economic feasibility of water-based vapor compression chillers. They identified a baseline cycle with the most attractive configurations for a water-based refrigeration and compared it to state-of-the-art technologies for chillers that use R134a as working fluid. Chamoun et al. [74] designed a heat pump that uses water as working fluid and developed a new dynamic model of the used twin screw compressor and of the used flash evaporation. To describe the thermodynamic processes in the twin screw compressor Chamoun et al. [77] developed a mathematical model with a special discretization method in order to study the dry compression cycle of this machine. In addition to the technological requirements for industrial heat pumps also the implementation into processes is a challenge to solve.

Based on technological developments, several studies examined application cases

for industrial heat pumps. Ammar et al. [78] identified potentials for integration of low grade heat into industrial processes. The paper addresses the potential for low-grade heat recovery with regard to new incentives and technologies, but they also illustrate organizational, financial and economic barriers. Wolf et al. [73] analysed the industrial heat demand of the German industry and the technical potential of industrial heat pumps. The potential for process heat with a temperature level up to 160 °C is about 611 PJ and promising sectors are the food and beverages industry, the chemical industry and the pulp and paper industry.

## 6.2 Integration of HTHP in industrial processes

### 6.2.1 Heat sources for HTHP systems

Generally several types of heat sources for heat pump systems exist:

- geothermal heat
- heat from groundwater
- ambient heat
- waste heat

Geothermal heat, ambient heat and heat from groundwater are used for heat pumps for building applications, whereas waste heat is used for industrial applications. The temperature range of heat sources for HTHP is higher than for heat pumps for domestic heating and the time depending occurrence of waste heat is very important. Several points for an ideal implementation of an HTHP into an industrial process can be summarized:

- Existence of usable waste heat: amount, temperature level, quality and occurrence of a usable waste heat stream
- Suitable heat sink: amount, temperature level and demand for heat
- Infrastructure: space requirements and integration facilities for a HTHP, heat distribution system, etc.

For the implementation of HTHP in industrial processes a simultaneous demand for process heat and occurrence of waste heat are necessary. Industrial sectors, like the food and beverages industry, the pulp and paper industry and the chemical industry, often meet these requirements. For the use of waste heat the quality is of importance. The heat utilization of a hot water stream happens in another way than utilizing humid hot air, where the partial pressure, the content of water and the saturation point must be considered.

For an optimum use of the waste heat the use of cascading systems can perform better than using a fixed temperature level. In a cascading system, evaporation temperatures are adjusted to the occurring waste heat temperature level. ?? shows the a cascading waste heat utilization in a  $\dot{Q}$ -T-Diagram. The black line shows the temperature curve of the heat source versus the exchanged heat, where the dashed line shows the temperature curve of three evaporation steps in the evaporator of the heat pump. The

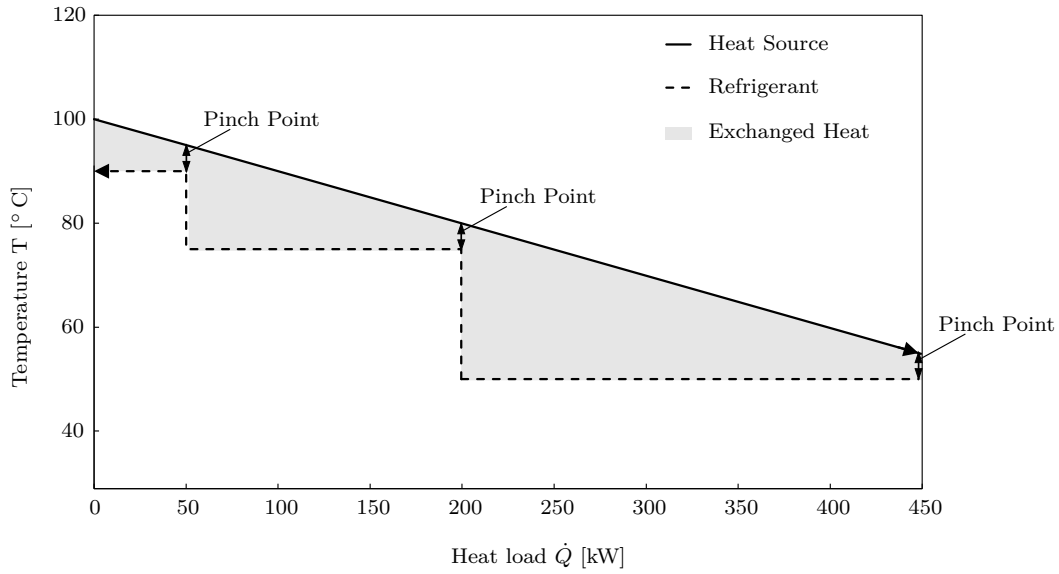


**Figure 6.2:** Description of a cascading heat utilization system with different evaporation temperatures (90°C, 75°C, 50°C) in a  $\dot{Q}$ -T-Diagram.

evaporation temperature levels are 90°C, 75°C and 50°C. The grey area shows the exchanged heat from the heat source to the heat sink.

For an ideal waste heat utilization the pinch point is very important. The pinch point is a crucial point between the heat delivering and the heat absorbing medium and describes the minimal temperature difference, which is necessary for heat exchange between the two media. The theory bases on the second law of thermodynamics and determines that heat flows in response to a temperature gradient only from a hot to a cold medium. The pinch temperature for the heat exchange in ?? is chosen with  $T_{pinch} = 5K$ , which is used for liquid media. For gaseous media a higher pinch temperature must be chosen ( $T_{pinch} = 20K$ ).

The chosen evaporator temperature levels refer to typical waste heat temperature levels for food processing and pulp and paper industry. ?? summarizes usable waste heat streams in this sectors.

### 6.2.2 Heat sink integration

On the one hand, the integration of high temperature heat pumps needs suitable waste heat sources to operate the system. On the other hand the heat of the heat pump should supply processes with heat. ?? summarizes industrial processes, where the process temperature levels are ideal for the integration of HTHP. Besides suitable temperature limits an adjusted implementation of a HTHP to the whole process is essential for a trouble-free application.

**Table 6.1:** Chosen waste heat sources in the processing industry.

Industrial sector	Process Description	Medium Composition	Temperature level [°C]
Pulp and Paper	Bleaching	Warm water	64.6 <sup>1</sup>
Pulp and Paper	Pulp machine	Warm water	62.1 <sup>1</sup>
Pulp and Paper	Grinding	Warm water	60.0 – 70.0 <sup>1</sup>
Pulp and Paper	Dryer	Humid hot air	50.0 – 62.0 <sup>2</sup>
Food and beverages	Refrigerator	Brine/ Refrigerant	30.0 – 50.0
Food and beverages	Dryer	Humid air	50.0 – 60.0
Textile	Drying	Humid air	60.0 – 70.0 <sup>3</sup>
Textile	Washing	Warm water	50.0 – 55.0 <sup>3</sup>

<sup>1</sup> Bakhtiari et al. [72]<sup>2</sup> Jung and Hutter [79]<sup>3</sup> Hloch and Bohnen [80]

### 6.2.3 Application field for HTHP: Pulp and paper industry

An example to analyze the economic viability of the heat production systems is the pulp and paper industry. On the one hand, it is a very energy- intensive sector and for the production of one tonne of paper, 5-17 GJ of process heat are necessary [85]. On the other hand, the process heat is required at a relatively low temperature level, typically below 200°C. Combined heat and power systems are common heat production technologies in the whole field of wood processing industry [86], but also heat pump systems could operate in the required temperature range. Beside the moderate temperature levels for process heat, also suitable heat sources for heat pump systems are available. Especially moist air from drying processes or waste water from bleaching processes can be used as heat source. ?? shows a simplified flow diagram of processes in the pulp and paper industry.

While the production of paper still needs large amounts of energy, there is a huge efficiency increase potential which is currently not exploited. For the German pulp and paper industry, Fleiter et al. [81] calculated an energy saving potential of 34 TJ/a for fuels and 12 TJ/a for electricity based on the evaluation of 17 process technologies. The most effective improvements are expected from heat recovery systems and innovative paper drying technologies. They noted that processes in the pulp and paper industry are not expected to change radically, but significant energy saving potential exists. In 2013 the fuel consumption of the European pulp and paper industry amounted 159 470 TJ. A big amount is provided by biomass (57.1 %), but also natural gas plays an important role with 34.6 % of the total fuel energy input. Because of high demands of electricity and heat, CHP is an established technology to produce heat and electric power simultaneously. 96.4% of total on-site electricity generation in the European pulp and paper industry is produced through CHP. The total electricity consumption

**Table 6.2:** Chosen processes for the integration of HTHP.

Industrial sector	Process Description	Temperature level [°C]
Pulp and Paper	Process water heating	130.0 – 150. <sup>1</sup>
Pulp and Paper	Drying	100.0 – 120. <sup>2</sup>
Petroleum refining	Destillation <sup>*1</sup>	150.0 – 200.0 <sup>3</sup>
Pharmaceuticals	Process steam	120.0 – 170.0 <sup>3</sup>
Food and Beverage	Drying	120.0 – 240.0 <sup>3</sup>
Food and Beverage	Concentration <sup>*2</sup>	35.0 – 95.0. <sup>3</sup>
Food and Beverage	Heating, cooking	100.0 – 140.0 <sup>4</sup>
Food and Beverage	cleaning	40.0 – 80.0 <sup>4</sup>
Food and Beverage	pasteurization	80.0 – 100.0 <sup>4</sup>
Textile	Wash-water heating	40.0 – 70.0 <sup>5</sup>
Textile	Process steam	150.0 – 190.0 <sup>5</sup>

<sup>\*1</sup> Butane, Propane

<sup>\*2</sup> e.g. sugar, milk, whey, juice, syrup

<sup>1</sup> Fleiter [81]

<sup>2</sup> Sappi Austria Produktions-GmbH & Co.KG [82]

<sup>3</sup> Chua et al. [83]

<sup>4</sup> Schmitt et al. [84]

<sup>5</sup> Hloch and Bohnen [80]

in 2013 was 101 528 GWh, 40.2% (40 791 GWh) were covered with electricity produced on site. The total amount of electricity production on site accounted 51 704 GWh and so 10 913 GWh of electricity were sold at spot market in 2013. This means that 21.1% of produced electricity on-site were sold [87].

As a consequence of the developments at the EEX and political sanctions to counteract climate change, there is a tendency towards decreasing electricity prices. The so-called merit-order effect shifts the profit from the power generation companies to the consumers, what several scientific works confirm [88–90]. This trend motivates industrial plant operators operate CHP systems in heat-only mode and buy electricity from the grid.

It is now to match, which technology is the best way of heat production for this sector depending on prevailing gas- and electricity prices. This chapter analyzes the thermodynamic efficiency of each heat production system (gas turbine, gas and steam turbine combined cycle and high temperature heat pump systems) with focus on exergetic losses as well as the economic performance of such systems considering energy prices and investment costs. For a tentative industrial setup including all three heat generation options, an optimization calculation has been carried out with the target function of minimized heat supply costs for the period between January 2013

and June 2016 based on real energy price data.

The outcome gives indications whether investing in a flexible heat generation setup may make sense in the framework of volatile electricity markets. It can be used as decision aid, whether to produce power in times of high electricity prices to supply the industrial process or to consume electricity to produce heat with heat pumps. In times with low electricity prices with a high amount of renewable electricity in the electricity supply, the application of heat pump system may get useful.

As another potential benefit for industrial operators in view of future restrictions of greenhouse gas emissions, heat pumps can be considered as CO<sub>2</sub>-free heat-supply systems if they are operated with green electricity [91, 92]. Since there is a high temperature demand in industry in the range 100°C to 150°C, the CO<sub>2</sub> emission reduction potential is high in this field.

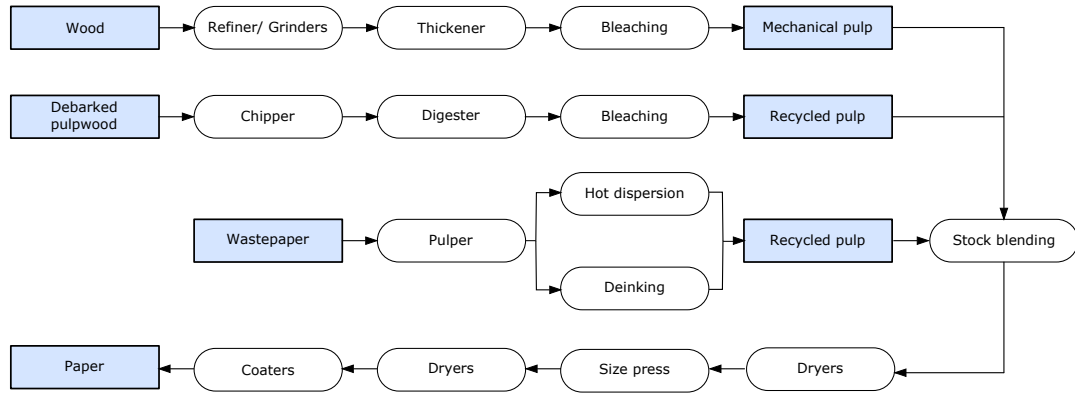


**Figure 6.3:** Simple flow scheme of a paper production process.

### 6.3 Process types for industrial heat supply

Heat plays an important role in many processes, for example drying, cooking, separation, absorption and adsorption. The following chapter explains the considered process types of thermodynamically efficient low-temperature heat generation, which will be further analysed in the present study.

#### 6.3.1 Fuel fired boiler system

The traditional way to provide heat is to combust fuel in a combustion chamber, as shown in ???. This is a process with a rather low thermodynamic efficiency if the required heat is at a low temperature level, because of high exergy losses in the combustion chamber and in the boiler. The losses in the boiler are caused by partially incomplete combustion and heat losses of the exhaust gas [12]. The boiler efficiency  $\eta_B$  describes the losses of a fuel fired boiler system ???.

$$\eta_B = \frac{\dot{Q}_{Process}}{\dot{m}_{Fuel} * H_L} \quad (6.1)$$

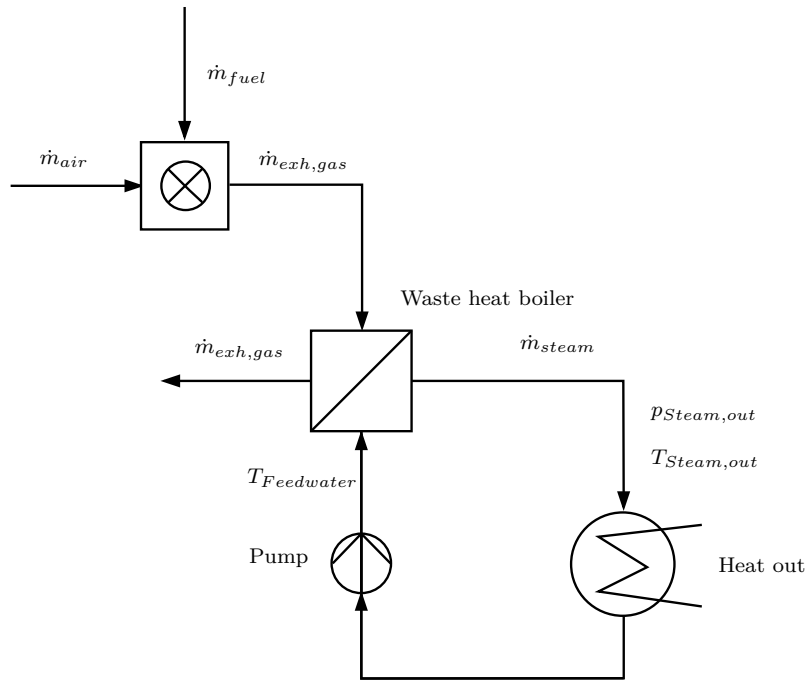


**Figure 6.4:** Simplified scheme of a fuel fired boiler system.

### 6.3.2 Gas turbine process

The open gas turbine process (GT) is a simple power cycle and converts the chemical energy of a fuel into electricity and heat. With combined heat and power (CHP) units, the waste heat in the exhaust gas of the gas turbine may be used to supply industrial processes. ?? shows a simplified scheme of such a process, consisting of a compressor, a combustion chamber, a gas turbine, a waste heat boiler, a pump and a heat sink. In the first step, air is compressed, then, fuel is combusted in the pressurized air stream to increase the temperature and the hot exhaust gas is expanded in a gas turbine. The exergy in the exhaust gas is partly converted into electric power and the remaining enthalpy in the turbine off gas can be used to produce steam in a heat recovery boiler. The heat recovery boiler works with a superheater, an evaporator, a steam drum and an economizer. This produced steam is used in the heat sink to supply industrial processes. The efficiency of the gas turbine process is evaluated with some key figures, especially the electric efficiency, the thermal efficiency and the exergetic efficiency. The electric efficiency ?? describes the conversion efficiency of the used fuel into electricity. For all calculations, complete combustion is assumed.

$$\eta_{el,GT} = \frac{P_{el,GT}}{\dot{m}_{Fuel} * H_L} \quad (6.2)$$

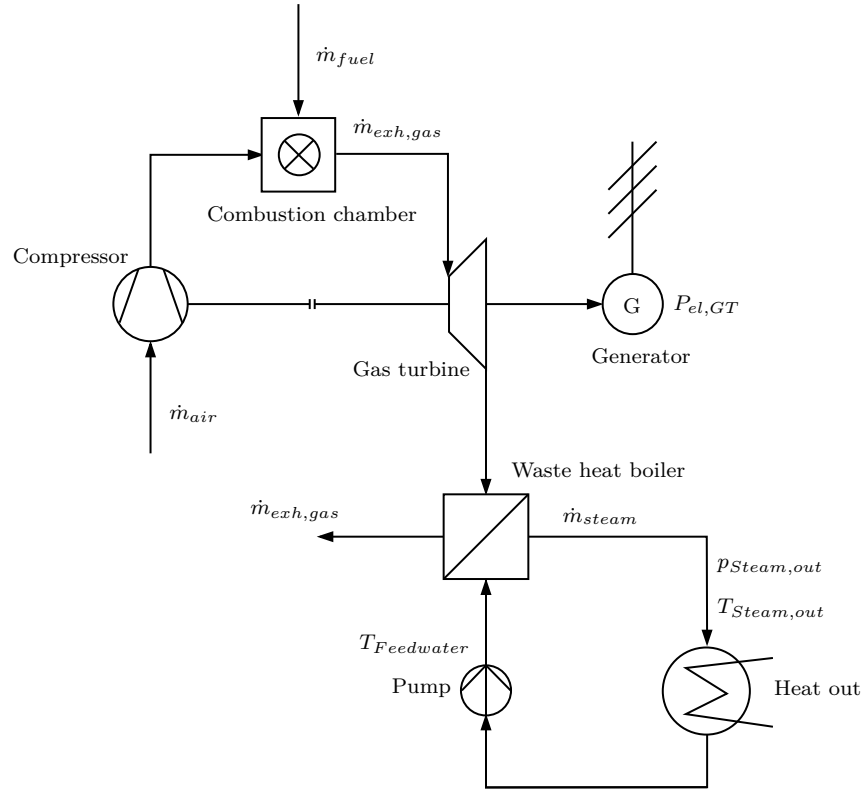


**Figure 6.5:** Simplified scheme of a gas turbine process (GT) with a heat-recovery boiler.

The heat utilization efficiency  $\eta_{heat}$  relates the produced heat of the gas turbine process, which is used to supply other processes.

$$\eta_{heat} = \frac{\dot{Q}_{Process}}{\dot{m}_{Fuel} * H_L} \quad (6.3)$$

$$\eta_{total} = \eta_{el,GT} + \eta_{heat} = \frac{P_{el,GT} + \dot{Q}_{Process}}{\dot{m}_{Fuel} * H_L} \quad (6.4)$$

The total fuel utilization efficiency is shown in ???. Because mixing up heat and electricity as in ??? neglects the thermodynamic value of the energy forms, we introduce an exergy-based comparison in the following. The exergetic efficiency describes the conversion of input exergy into useful exergy. For combined heat and power plants, the exergetic efficiency includes, apart from the produced electric power, also the exergy stream of the usable process heat. ??? shows the exergetic efficiency definition for the process in ???. Work and electricity represent pure exergy. The exergy flow of the heat ??? and the specific exergy ??? are calculated as described in ???, whereas the exergetic efficiency is described below in ???. The specific exergy at standard conditions ( $e_0$  and  $e_{Fuel}$ ) is calculated based on the chemical exergy formulation according to Baehr and Kabelac[34] based on the equilibrium environment by Ahrendts [5].

$$\zeta_{GT} = \frac{P_{el,GT} + \dot{E}_Q}{\dot{m}_{Fuel} * e_{Fuel}} \quad (6.5)$$

### 6.3.3 Gas and steam turbine process

Compared to a GT process, a gas and steam turbine combined cycle (GT-CC) works with a steam turbine (ST) cycle as a second power cycle (see ??). The hot exhaust gas after the gas turbine operates a heat recovery steam generator. A two pressure stage heat recovery system to produce high-pressure steam and low-pressure steam with additional enthalpy utilization of the exhaust gas is chosen. The system is composed of two sets of economizers, evaporators and superheaters, one for each pressure stage, and additional heat exchangers to optimize the heat utilization of the exhaust gas. The high-pressure and low-pressure steam is supplied to a two pressure level back-pressure steam turbine to generate electric power. The GT-CC is optimized on the supply of heat at required temperature and pressure level and secondary to produce electric power. So a back-pressure steam turbine is chosen. With a condensation steam turbine, the electric efficiency would be higher, but the produced process steam would not fit to the requirements of the industrial processes. In the back pressure system the steam is condensed in the heat sink at a suitable pressure level to supply the required heat to the industrial processes. The electric output and the electric efficiency of the gas and steam turbine process are shown in ?? and ?. The total fuel utilization efficiency is calculated again as the sum of electric efficiency and the heat utilization efficiency ?? according to ??.

$$P_{el,GT-CC} = P_{el,GT} + P_{el,ST} \quad (6.6)$$

$$\eta_{el,GT-CC} = \frac{P_{el,GT-CC}}{\dot{m}_{Fuel} * H_L} \quad (6.7)$$

$$\eta_{total} = \eta_{el,GT-CC} + \eta_{heat} \quad (6.8)$$

The exergetic efficiency is calculated similarly to the gas turbine process (??).

$$\zeta_{GT-CC} = \frac{P_{el,GT-CC} + \dot{E}_Q}{\dot{m}_{Fuel} * e_{Fuel}} \quad (6.9)$$

### 6.3.4 High temperature heat pump system

Heat pumps take up heat at a lower temperature level and release heat at a higher temperature level. This process, according to thermodynamics, requires addition of exergy. In the common case of compression heat pump system, the exergy is added in the form of compression work, i.e. mechanical work efficiently generated from electric energy. The possible temperature increase generally depends on the specific exergy input. Practically, for compression heat pump systems, it mainly depends on the

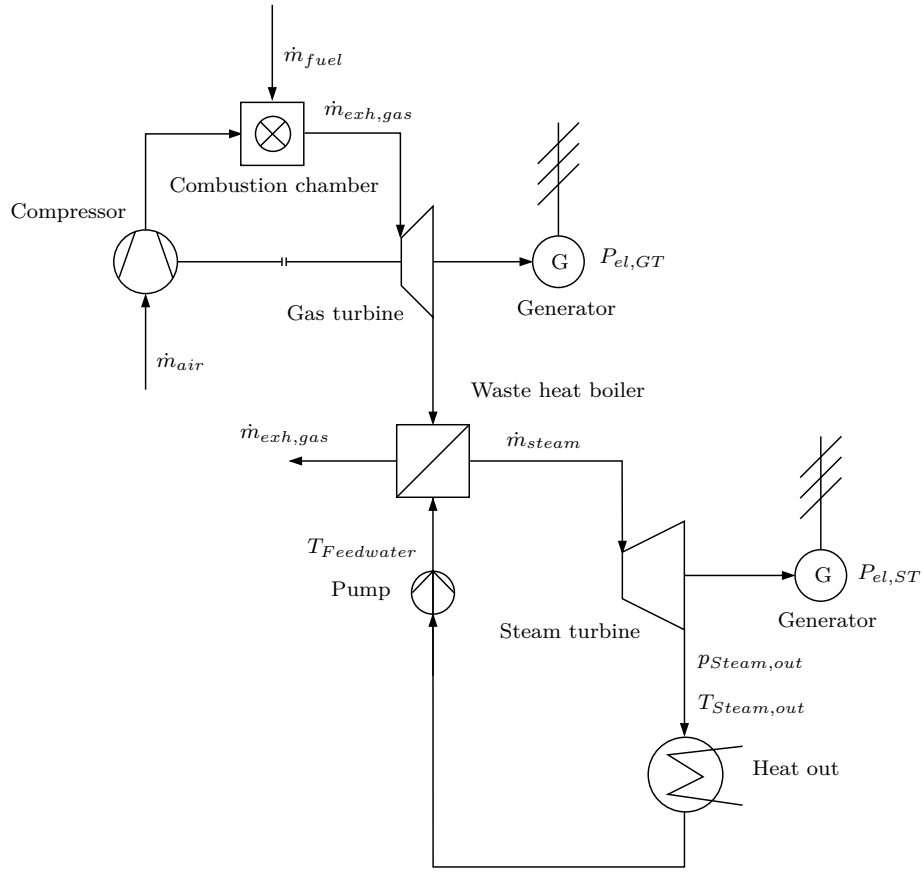


**Figure 6.6:** Simplified scheme of a gas turbine combined cycle process (GT-CC) with heat recovery boiler and a back-pressure steam turbine.

exergetic efficiency of the compression step and on the thermodynamic properties of the used working fluid. In this work, an electrical heat pump system working with a polytrope (intercooled) compression system and water as working fluid is analyzed. ?? shows a simplified scheme of the calculated process that works with two heat exchangers for heat source and heat sink, a compressor and a valve to expand the refrigerant. The efficiency of electrically driven heat pump systems is determined by the quotient of produced heating power to applied electrical power, called coefficient of performance (COP) as shown in ??. The exergetic efficiency includes the exergy stream of the heat sink, the incoming exergy stream of the heat source and the electric power ??.

$$COP = \frac{\dot{Q}_{Process}}{P_{el}} \quad (6.10)$$

$$\zeta_{HP} = \frac{\dot{E}_Q}{P_{el} + \dot{E}_{Heat\ source}} \quad (6.11)$$

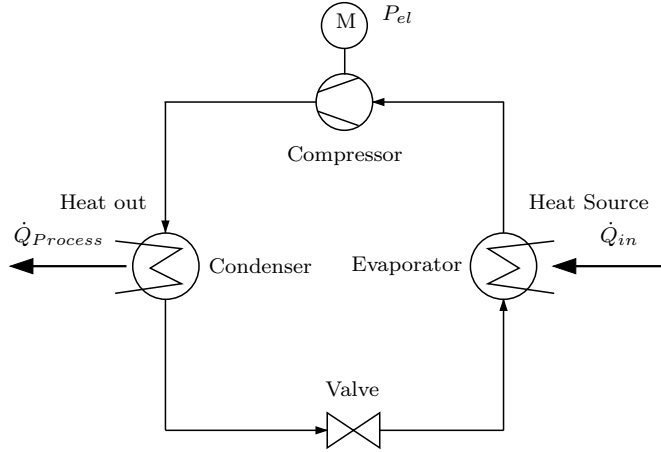


**Figure 6.7:** Simplified scheme of a high temperature heat pump system for process heat supply

## 6.4 Economic factors of industrial process heat supply

The economic calculations were made to compare the economic performance of the heat supply processes. The calculations include, firstly, the variable costs of the three systems. Secondly, investment costs for a newly installed HTHP are to be considered, because in our methodological approach we assume that either a GT or a GT-CC system is already in operation while the HTHP system requires installation of additional technology. The resulting setup comprises two parallel heat generation options and the operator can flexibly choose between a gas-powered and an electricity-powered heat supply system dependent on the energy price situation.

### 6.4.1 Consumption related costs of heat production

The variable costs of heat for the GT and the GT-CC processes are shown in ??-??. The formulation in ?? and ?? hold for the pre-existing gas-turbine based systems and ?? reflects the variable costs of the HTHP system.  $P_{therm}$  describes the fuel power based on the lower heating value, as shown in ??. Compared to the CHP process, the costs of heat for the heat pump only depend on the COP and the electricity price.

$$CoH_{GT} = \frac{P_{therm} * C_{Gas} - P_{el,GT} * C_{El}}{\dot{Q}_{Process}} \quad (6.12)$$

$$CoH_{GT-CC} = \frac{P_{therm} * C_{Gas} - P_{el,GT-CC} * C_{El}}{\dot{Q}_{Process}} \quad (6.13)$$

$$CoH_{v,HTHP} = \frac{C_{El}}{COP} \quad (6.14)$$

The collected industrial energy prices for both, electricity and gas prices, refer to E-Control ([93], [58]) and serve as foundation for the calculated consumption related costs.

#### 6.4.2 Investment and operation costs of a HTHP

In order to get a precise picture of the economic performance of an HTHP, the investment costs are converted into EUR/kW<sub>Q</sub> and include capital costs as well as internal fixed costs. When it comes to investment, capital costs  $C_{\text{Capital}}$ , are to be considered as well. The approach therefore considers costs for depreciation  $D_C$ , shown in ?? and interest costs  $I_C$  shown in ?. Costs for annual interests are calculated with the average cost method according to Schneider [94]. Since the costs for investment are very high, we assume total debt financing and chose an interest rate of 5%p.a.

$$D_C = \frac{I_0 - R_W}{n} \quad (6.15)$$

$$I_C = \frac{I_0 + R_W}{2} * i \quad (6.16)$$

$$C_{\text{Capital}} = D_C + I_C \quad (6.17)$$

For allocating the total costs into EUR per MWh, additional costs for capital, salary and service are to be summed up and divided by  $Q_{\text{Process}}$ , like it is shown in ?. Finally, levelized costs for heat production in EUR per MWh can be calculated for the HTHP system (??).

$$CoH_{f,HTHP} = \frac{C_{\text{Capital}} + C_{\text{Personnel}} + C_{\text{Service}}}{Q_{\text{Process}}} \quad (6.18)$$

$$CoH_{HTHP} = CoH_{v,HTHP} + CoH_{f,HTHP} \quad (6.19)$$

?? gives an overview of the included parameters. With respect to uncertainties about precise investment costs, we consider four levels of specific investment costs and study the impact of HTHP system erection costs on the total CoH.

According to Zhang et al. [96] and data from several manufacturers, the estimated installation costs of HTHP range between 250 EUR/kW<sub>Q</sub> and 750 EUR/kW<sub>Q</sub>, although further decline in the future due to serial production is expected.

**Table 6.3:** Assumptions and calculations for modelling the economic model of the capital related costs of heat production.

Parameter	A	B	C	D	Unit
Spec. acquisition costs	1.000	750	500	250	[EUR/kW <sub>Q</sub> ]
I <sub>0</sub>	100.000.000	75.000.000	50.000.000	25.000.000	[EUR]
R <sub>W</sub>		0			[EUR]
n		20 <sup>1</sup>			[a]
t		6.000			[h]
i		5.0			[%]
Q <sub>Process</sub>		600.000			[MWh/a]
Q <sub>Personnel</sub>		40.000			[EUR/a]
Q <sub>Service</sub>		10.000			[EUR/a]
D <sub>C</sub>	5.000.000	3.750.000	2.500.000	1.250.000	[EUR/a]
I <sub>C</sub>	2.500.000	1.875.000	1.250.000	625.000	[EUR]
CoH <sub>f,HTHP</sub>	12.58	9.46	6.33	3.21	[EUR/MWh]

<sup>1</sup> Verein deutscher Ingenieure [95]

## 6.5 Technological settings for the observed heat supply process

In the first step, a process simulation of the chosen heat supply processes is set up with the process simulation software IPSEpro. For the simulation of the heat supply processes, some assumptions are necessary. ?? shows the assumed parameters. Heat exchanger pressure drops are not considered in the calculations. The parameters of the gas turbine depend on the performance data of the Siemens SGT-800 (53.0 MW) gas turbine [97].

**Table 6.4:** General performance assumptions for key process components.

Parameter	Value	Unit
$\eta_{\text{Compr}}$	0.80	[–]
$\eta_{\text{Motor}}$	0.97	[–]
$\eta_{\text{SGT-800}}$	21.4 : 1	[–]
$T_{\text{SGT-800,out}}$	551	[°C]

Apart from the general efficiency assumptions in ??, the process and working parameters have to be fixed in order to compare the alternatives on a fair basis. The scope of all technologies is to produce heat for an industrial production process. ?? shows the minimum technological requirements for the processes. These are typical values needed for many industrial processes, especially in the pulp and paper industry. The minimum outlet temperature to the heat sink is assumed with 141.8°C and a pressure level of 3.8 bar<sub>abs</sub>. This parameters are also chosen, to make the simulation results of the three heat supply processes comparable.

**Table 6.5:** Technological setting for the heat supply processes.

Parameter	Value	Unit
$T_{\text{Feedwater}}$	120	[°C]
$T_{\text{Steam,out}}$	142	[°C]
$p_{\text{Steam,out}}$	3.8	[bar <sub>abs</sub> ]
$\Delta h$	2232	[kJ/kg]
$\dot{m}_{\text{Steam}}$	44.8	[kg/s]
$\dot{Q}_{\text{Heat out}}$	100	[MW]

## 6.6 Thermodynamic analysis

### 6.6.1 Gas turbine process with heat recovery boiler

The designed gas turbine process operates with a turbine inlet temperature of 1270°C and an outlet temperature of 551°C to meet the technological settings (see ??). The gas leaves the waste heat boiler with a temperature of 142°C. ?? shows the calculated results, especially the input fuel power, the produced electric power and the useful process heat.

**Table 6.6:** Simulated results of the gas turbine process with CHP and a gas and steam turbine combined cycle with back-pressure steam turbine.

Parameter	GT	GT-CC	Unit
$P_{\text{Fuel}}$	221	282	[MW]
$P_{\text{ST-HP}}$	-	74.6	[bar <sub>abs</sub> ]
$T_{\text{ST-HP}}$	-	520	[°C]
$P_{\text{ST-LP}}$	-	12.0	[bar <sub>abs</sub> ]
$T_{\text{ST-LP}}$	-	190	[°C]
$T_{\text{exh,gas}}$	142	162	[°C]
$P_{\text{el,GT}}$	86	110	[MW]
$P_{\text{el,ST}}$	-	21	[MW]
$P_{\text{el,GT-CC}}$	-	131	[MW]
$\dot{Q}_{\text{Heat out}}$	100	100	[MW]
$\eta_{\text{heat}}$	45.21	35.44	[%]
$\eta_{\text{net,el}}$	39.01	46.49	[%]
$\eta_{\text{total}}$	84.22	81.93	[%]
$\zeta$	49.82	53.44	[%]

?? shows the energy flow diagram of the gas turbine process. With an input fuel power of 221 MW, the generation of 86 MW<sub>el</sub> electric power and 100 MW<sub>therm</sub> of process heat can be achieved. Losses in the shaft and the generator of 8 MW can be identified in the simulation. The simulation shows that 27 MW of heat are released to the environment with the exhaust gas through the chimney.

Compared to the energy flow diagram in ??, the exergy flow diagram in ?? reveals more detailed information about conversion losses. The diagram shows the inefficiencies of the combustion process, with exergy losses of 66 MW. Relevant exergy losses occur also in the gas turbine (10 MW), in the waste heat boiler (22 MW) and in the compressor of the GT (7 MW). The relative losses, compared to the input exergy stream of each conversion step, are 20.0% in the combustion chamber, 3.8% in the gas turbine, 6.5% in the compressor and 36.7% in the waste heat boiler.

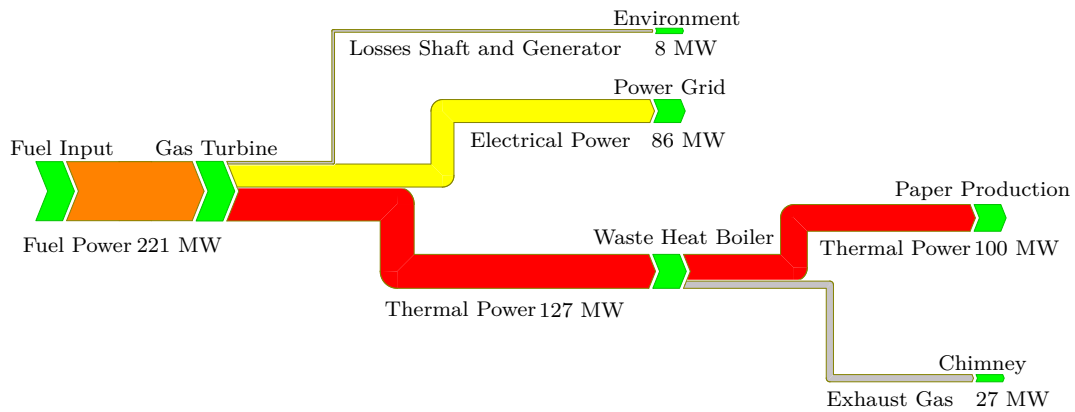


**Figure 6.8:** Energy flow of a gas turbine process including shaft and generator losses.

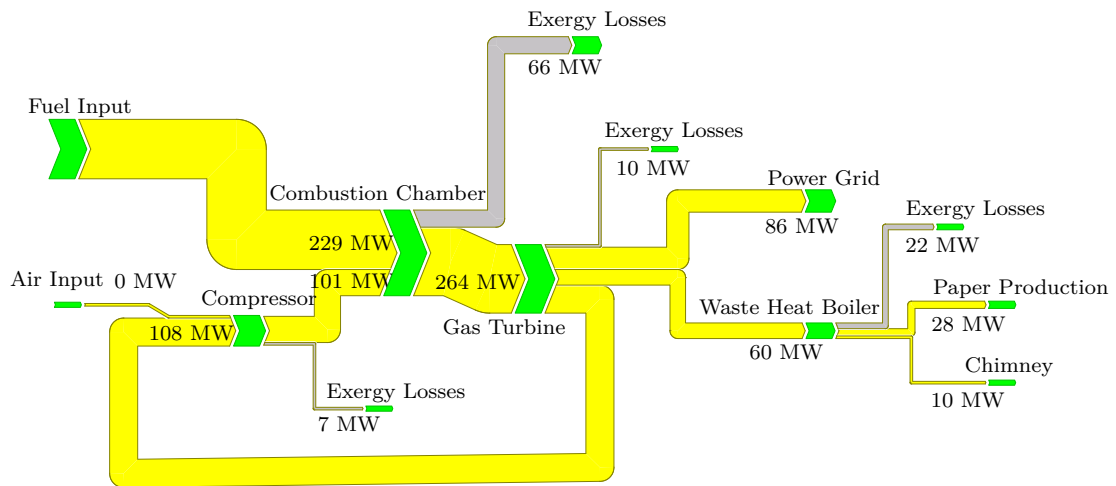


**Figure 6.9:** Exergy flow diagram of gas turbine process with heat-recovery boiler.

### 6.6.2 Gas and steam turbine combined cycle with back-pressure steam turbine

To achieve the required amount of process heat for the production process, the fuel input of the GT-CC is higher than in the GT process (??). With a fuel input of 282 MW the gas turbine produces 110 MW<sub>el</sub> and the steam turbine 21 MW<sub>el</sub> electric power. The gas temperature at the turbine inlet is 1270°C and the outlet temperature of the gas turbine is 551°C. A first waste heat boiler produces steam with a temperature of 520°C and a pressure level of 74.6 bar<sub>abs</sub> to operate the high-pressure steam turbine. A second heat-recovery boiler produces steam with a temperature of 190°C and a pressure level of 12 bar<sub>abs</sub> and supplies the low-pressure steam turbine. The steam turbine produces 21 MW<sub>el</sub> electrical power and so with the combined cycle 131 MW<sub>el</sub> electrical power can be produced. The outlet steam of the steam turbine is used as process heat with a pressure level of 3.8 bar<sub>abs</sub> and a temperature of 142°C. The optimization of the process considers the maximum pressure and temperature levels

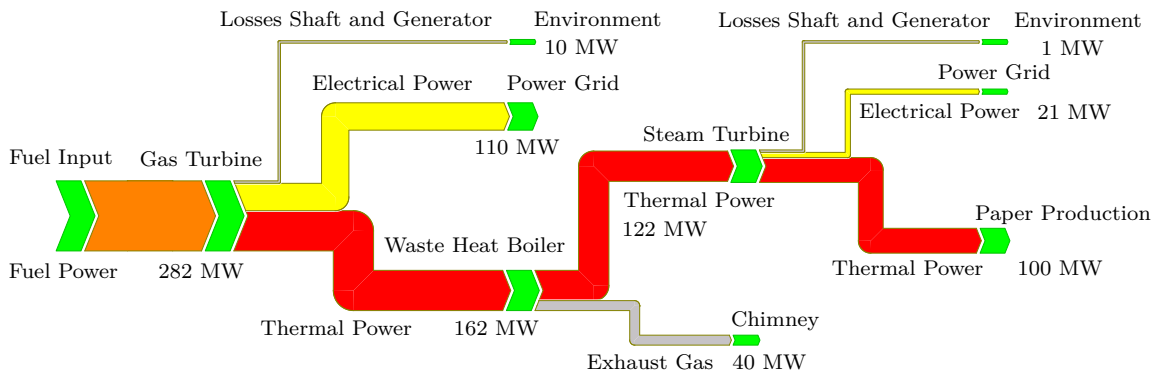


**Figure 6.10:** Energy flow diagram of gas turbine combined cycle GT – CC.

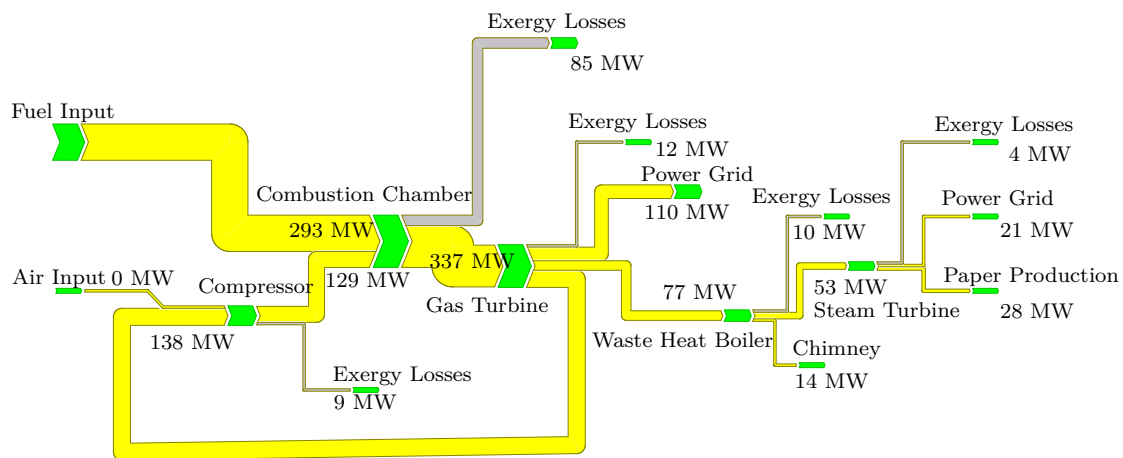


**Figure 6.11:** Exergy flow of a gas turbine combined cycle process GT - CC.

and the minimum pinch point. As a consequence of the pinch point between the gas leaving the evaporator, and the temperature of the saturated steam, the exhaust gas has a temperature level of 162°C after the waste heat boiler. The heat output efficiency of the GT-CC process is lower than that of the GT process because of the higher share of generated electricity. The total fuel utilization of the GC-CC is slightly lower, mainly because of the higher exhaust gas temperature and the operation of two more pumps to operate the two-pressure level steam turbine. ?? shows the energy streams of the GT-CC process.

The exergy streams and exergy losses are illustrated in ??. Exergy losses occur in the combustion chamber, the gas turbine, the waste heat boiler, the compressor and the steam turbine. The relative exergy losses compared to the input exergy streams are 20.1% in the combustion chamber, 3.6% in the gas turbine, 13.0% in the waste heat boiler, 6.5% in the compressor and 7.5% in the steam turbine.

**Table 6.7:** Process specific data and results for the simulated high temperature heat pump process.

Parameter	Variation			Unit
	1	2	3	
$T_{\text{Evap}}$	50	75	90	[°C]
$p_{\text{Evap}}$	0.1	0.4	0.7	[bar <sub>abs</sub> ]
$T_{\text{Cond}}$	152	152	152	[°C]
$p_{\text{Cond}}$	5.0	5.0	5.0	[bar <sub>abs</sub> ]
$p_{\text{Cond}}/p_{\text{Evap}}$	40.3	13.0	7.1	[-]
$P_{\text{el}}$	33	25	20	[MW]
$\dot{Q}_{\text{Heat source}}$	69	77	82	[MW]
COP	3.0	4.0	5.0	[-]
$\zeta_{\text{HP}}$	59.57	70.15	78.35	[%]

### 6.6.3 High temperature heat pump process

The heat pump uses waste heat from the production process to generate process steam. The calculation of the heat pump systems were varied for three different evaporation temperatures (50°C, 75°C and 90°C) and so the calculated COP also varies between 3.0 and 5.0. ?? shows the detailed results of the variation. Depending on the technical requests (see ??) the produced heat of the heat pump systems amounts to 100 MW<sub>therm</sub>. The system is designed to provide saturated steam at 3.8 bar<sub>abs</sub> and 142°C from 120°C feedwater. However, even though water was assumed as working fluid in the present study, an indirect heat exchanger between working fluid and process steam is considered with a temperature difference of 10 K. Still, the exergetic efficiency of the system lies between 59.57% and 78.35%, which is higher than for the GT and the GC-CC process.

?? shows the energy flow diagram of the heat pump process with a COP of 4.0. With 77 MW waste heat power and 25 MW electric power 100 MW process heat is generated at the required temperature level of 142°C considering 10 K temperature difference in the heat pump condenser / steam generator apparatus. Mechanical losses only occur in the compressor.

The exergy flow diagram (??) shows the exergy losses in the heat pump process. Exergy losses occur in the heat exchangers (evaporator and condenser) and in the compressor and amount to 26.7% in the evaporator, 16.7% in the compressor and 6.7% in the condenser compared to the exergy input to the respective apparatus.

To answer the question, which heat supply technology is exergetically most efficient, ?? shows a summary of the calculated results. Even with the lowest COP of three, the exergetic efficiency of the heat pump process is the highest one compared to GT and GT-CC. This neglects exergy losses of the electricity generation and distribution, what should be acceptable since excess electricity is used in times of low electricity prices. Then, also a high share of renewable electricity, caused by wind and photovoltaic

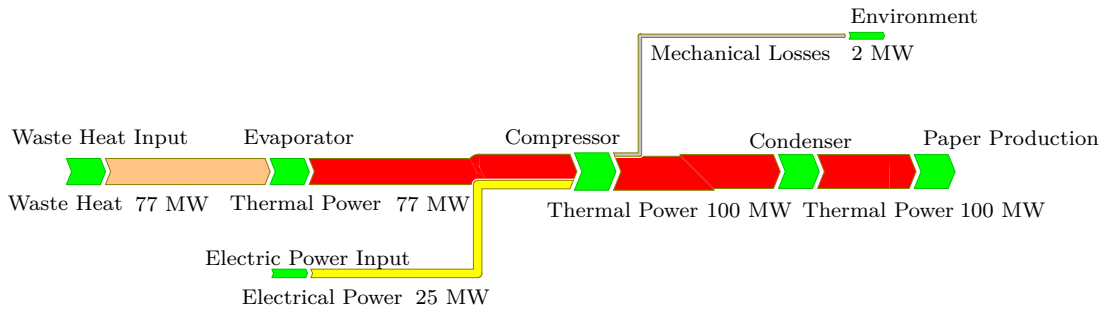


**Figure 6.12:** Energy flow diagram of a heat pump system. The diagram shows the results of variation 3.

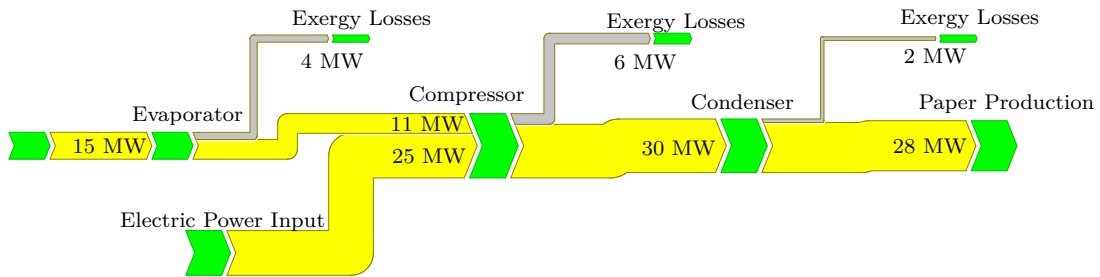


**Figure 6.13:** Exergy flow diagram of a heat pump.

plants, can be expected. The calculation bases on the assumption that heat pump systems are operated in this times with a high share of renewable energy. The power for the heat pump is not generated in thermal power plants.

**Table 6.8:** Summary of the exergetic efficiencies of the simulated heat supply processes.

$\zeta_{GT}$	$\zeta_{GT-CC}$	$\zeta_{HP,50^{\circ}C}$	$\zeta_{HP,75^{\circ}C}$	$\zeta_{HP,90^{\circ}C}$	Unit
49.82	53.44	59.57	70.15	78.35	[%]

## 6.7 Economic evaluation

Apart from thermodynamic efficiencies, economic factors play an important role for the implementation and application of energy efficiency measures. With respect to our chosen methodological approach described above, the following results have been obtained. Firstly, the outcome of the modeled heat supply systems is presented and, secondly, followed by economic analyses using real-life European energy market prices 2013 – 2016 (see Figure 3).

### 6.7.1 Consumption related costs of heat production

A first overview on the economic situation is obtained from the operation and consumption costs to produce the needed industrial heat. The costs of generated heat are calculated for the GT, the GT-CC and the HP process as shown in ??????. For the GT and the GT-CC process, the costs of heat relate to the gas and electricity price ?????, the costs of heat of the HP process only depend on the electricity price ?? ?? shows the relation of the costs of heat and the electricity price. For the GT and the GT-CC process, a gas price of 25.0 EUR/MWh (LHV-based) is adopted and for the heat pump process, a variation with three different working efficiencies is shown. The diagram shows that, if the electricity price is lower than 42.8 EUR/MWh at a gas price of 25.0 EUR/MWh, the heat pump process has the lowest costs of heat at about 15 EUR/MWh and the costs of heat production decrease below this value for lower electricity prices. Contrasting to this, the costs of heat production for the GT and the GT-CC raises with lower electricity prices. At the intersections of the curves, the costs of heat production are equal. This points mark the economic break-even of the heat production processes. If the occurring electricity price is higher than the electricity price at break-even, the GT or the GT-CC process is economic. If the electricity price is lower, the heat production with heat pumps is cheaper. Additionally, we have added a line for the costs of heat generation with a simple gas boiler working at 90% boiler efficiency. It can be seen that for electricity prices lower than about 32 EUR/MWh, the simple boiler operates cheaper than the GT-cycles. This is the reason, why some GT units have at least temporarily been switched off by industry during the last three years in Europe. The process steam was generated with the afterburners and the heat recovery boilers in these cases.

The data of the line-intersections are summarized in ??. Depending on the efficiency (COP) of the heat pump system, the electricity price at break-even rises with higher COP. This means that, with a higher efficiency, the heat production with heat pumps is cheaper despite higher electricity prices.

To answer the second question, the results show that the performance of the heat pump system, the gas price and the electricity price are very important factors. For example, a heat pump system, operating with a COP of 4, is an economic heat production way as long as the electricity price is lower than 45.1 EUR/MWh compared to a GT-CC (operating with a gas price of 25 EUR/MWh). Compared to a GT process, the heat pump system is economic, when the electricity price is lower than 49.7 EUR/MWh.

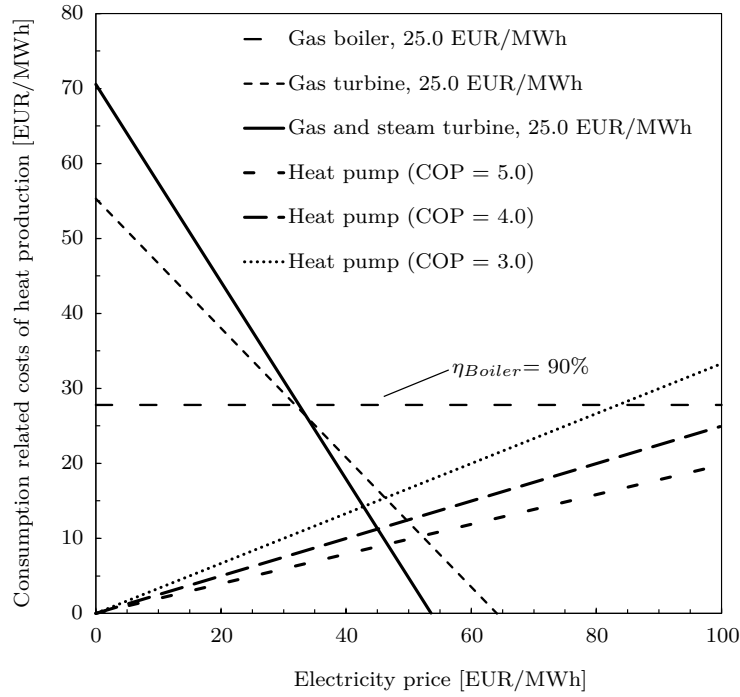


**Figure 6.14:** Relation of electricity price and costs for heat production depending on the used technology. The gas price for the GT and the GT-CC is assumed with 25.0 EUR/MWh according to E-control [58].

**Table 6.9:** Illustration of the electricity price and the costs of heat production at the points of break-even. This point is the intersection of the curves, when the costs of heat production of the heat pump system and the gas turbine process resp. gas and steam turbine process are equally.

	COP=3	COP=4	COP=5	Unit
Electricity price at break-even $C_{el, \text{ Break Even}}$				
HP – GT	46.2	49.7	52.1	[EUR/MWh]
HP – GT-CC	42.8	45.1	46.6	[EUR/MWh]
Costs of heat generation at break-even $CoH_{\text{ Break Even}}$				
HP – GT	15.4	12.4	10.3	[EUR/MWh]
HP – GT-CC	14.3	11.3	9.2	[EUR/MWh]

### 6.7.2 Capital and operation costs of heat production

Beside consumption related costs, investment costs and costs for capital are crucial for an overall economic consideration. According to ?? the costs of heat production depending on capital and investment costs for an HTHP system are calculated. For all further investigations it is assumed that a gas turbine or a gas turbine combined cycle system for industrial heat supply is installed at production site and a HTHP system would need to be installed additionally.

?? shows the levelized costs of heat production of a newly installed HTHP in comparison to other available heat supply systems for a period from January 2013 to June 2016 (with energy prices as shown in ??). The graphs of the conventional systems are based on ?????. The graph of the HTHP is calculated at a COP of 4 and investment costs of 500 EUR/kW<sub>Q</sub> are assumed. The results show that in the period between February 2013 and May 2014, as well as in the period between August 2014 and September 2015, economic conditions for replacing conventional heat supply systems would have been favorable. From October 2015 onwards, CHP-based CoH decrease as a result of decreasing natural gas prices and increasing electricity prices. Generally, the CoH from the HTHP system are less influenced by volatile electricity prices than the CoH from the CHP systems. The CoH of HTHP range in the considered time window between 12 EUR/MWh and 18 EUR/MWh.

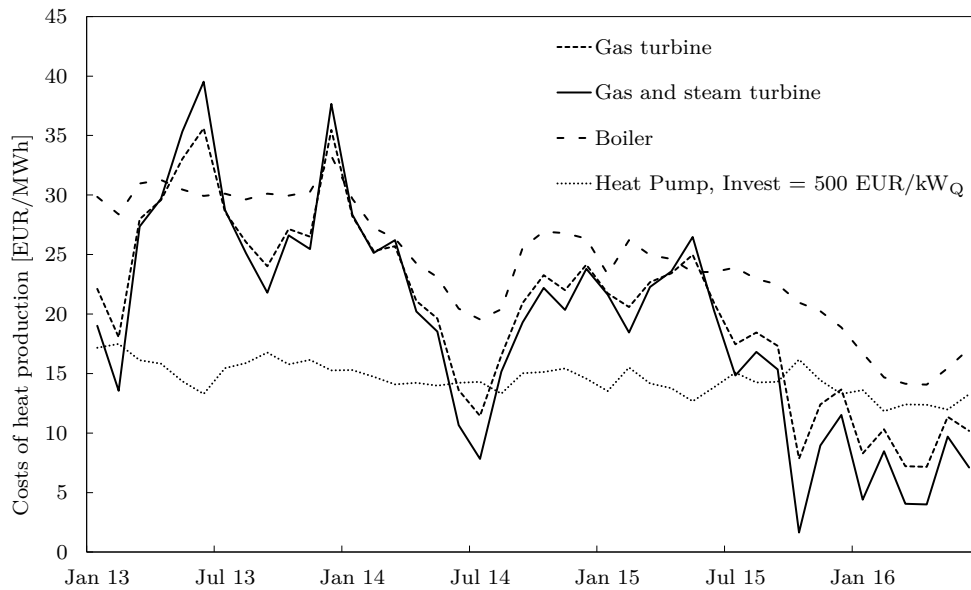


**Figure 6.15:** Cumulative costs of heat for a gas turbine, a gas and steam turbine, a boiler and a heat pump system working with a COP of 4 from January 2013 until June 2016. The costs of heat of the heat pump system includes the investment costs, assumed with 500 EUR/kW<sub>Q</sub> and the consumption related costs.

It is evident from ?? that the GT-CC system is in direct competition to the HTHP system. In price situations where the GT system would be superior to the GT-CC system, the HTHP system is always more economic than GT. ?? shows the switching schedule between GT-CC and HTHP operation in a tentative plant where both

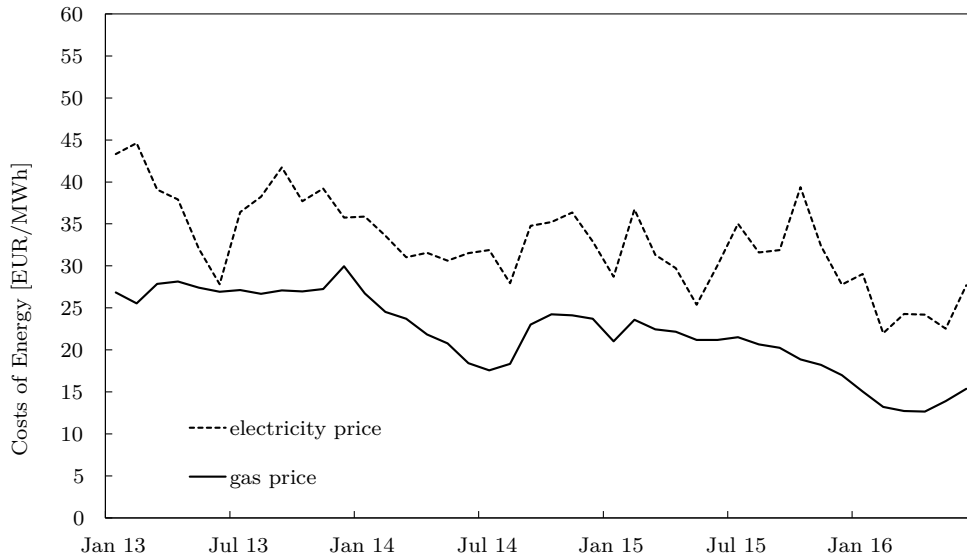


**Figure 6.16:** Electricity and gas prices from January 2013 until June 2016 according to E-control [58, 93].

**Table 6.10:** Share of each heat production technology depending on the specific investment costs for the HTHP system in the period January 2013 – June 2016.

Specific investment	1.000	750	500	250	[EUR/kW <sub>Q</sub> ]
B	0.0	0.0	0.0	0.0	[%]
GT	0.0	0.0	0.0	0.0	[%]
GT-CC	54.8	42.9	31.0	23.8	[%]
HTHP	45.2	57.1	69.0	76.2	[%]

technologies are available in the investigated time window. The CoH of the HTHP system depend on operation costs as well as on investment costs. Therefore the calculation is done for four different levels of specific erection costs of the HTHP system.

The share of the heat production technologies, based on the examination of ?? , is shown in ??. The results obtained show again that the HTHP and the GT-CC process are most economic. The share of the heat pump system on heat production varies from 45%-76% depending on the specific investment costs. Lower investment costs favor the operation of the HTHP, and the share of heat production for HTHP with specific investments of 750 EUR/kW<sub>Q</sub>, 500 EUR/kW<sub>Q</sub>, and 250 EUR/kW<sub>Q</sub>, is higher than 50%. For the investment costs a very broad range is assumed. Currently HTHP is no common technology, so the investment costs are quite high. If the technology gets state of the art, like gas and steam turbine systems, the investment costs will decrease to the lower limit of the assumed range or even lower.

A sensitivity analysis of the consumption related costs is done for these two tech-

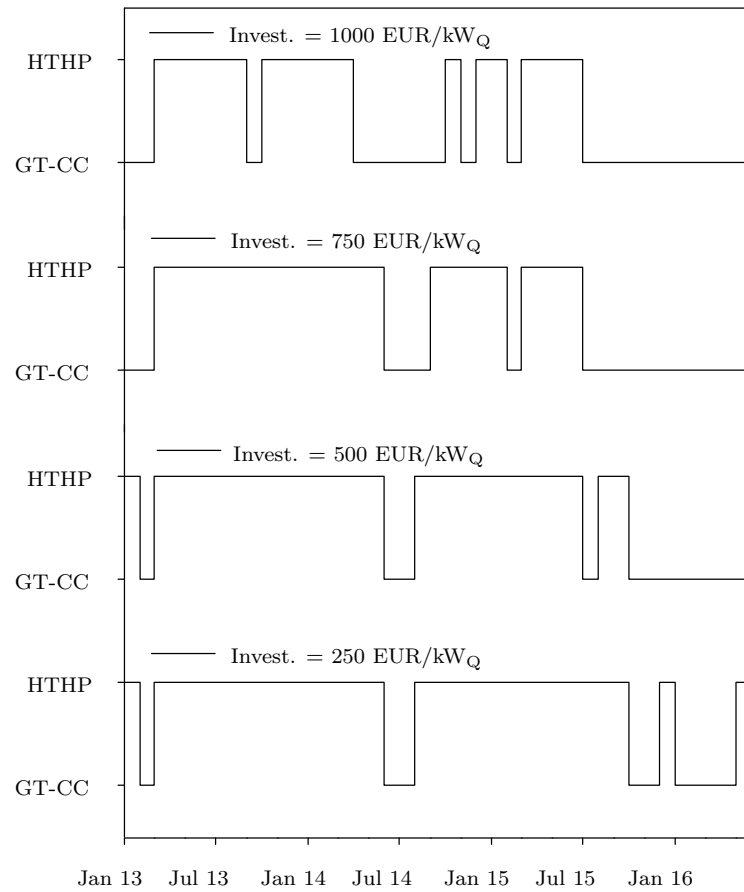


**Figure 6.17:** Economically best technology for industrial heat production depending on the cumulative costs of heat for the period from January 2013 until June 2016 according to different investment costs. The graph shows that HTHP and GT-CC were economic best, the gas turbine and the boiler had in this period higher costs for heat production.

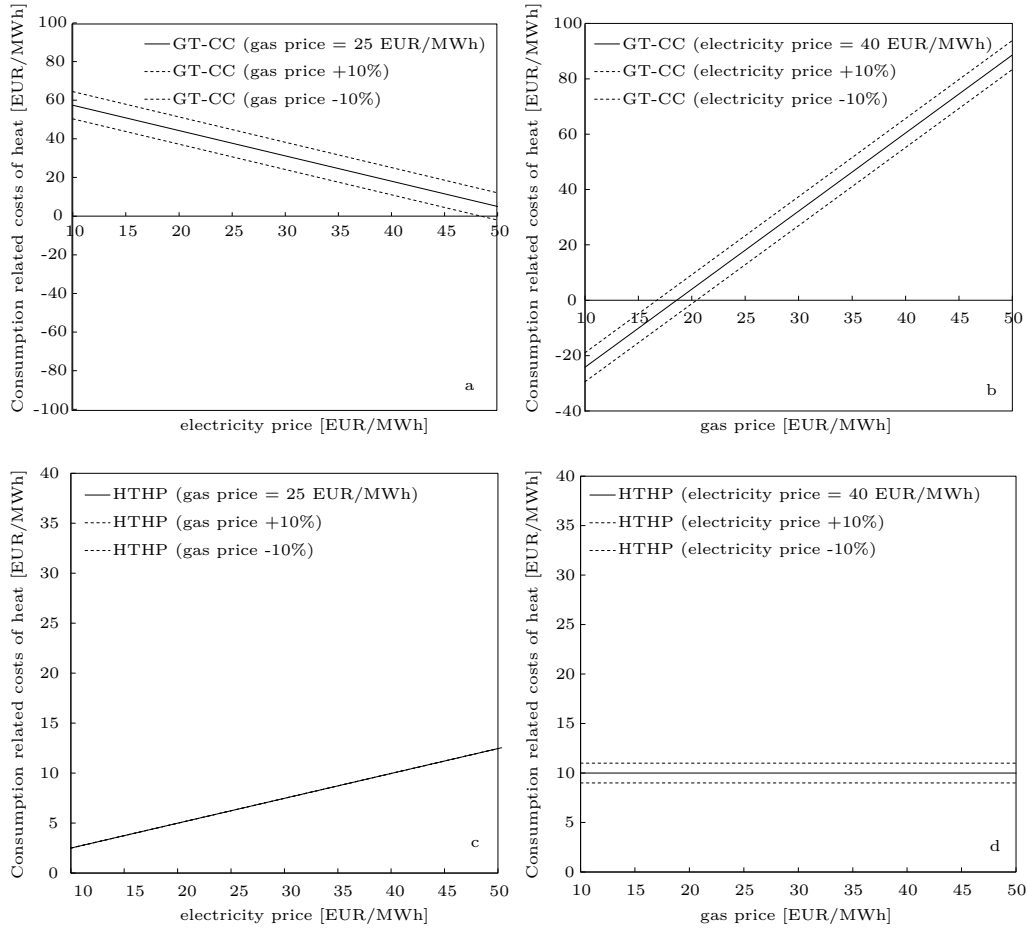


**Figure 6.18:** Sensitivity analysis of the consumption related costs of a GT-CC and the HTHP with a COP of 4 depending on different electricity and gas prices.

nologies. ?? depicts the effects of changing electricity and gas prices on the costs. The first picture (a) shows the correlation of the CoH of a GT-CC process by varying the electricity price  $\pm 10\%$ . In the second picture (b) the gas price is varied  $\pm 10\%$ . Picture (c) and (d) show the correlation of costs of heat and energy prices for the HTHP process. The change of the consumption related costs for the GT-CC process in connection with changing energy prices is more distinct than for the HTHP. The diagrams for the gas-fired systems show that changing gas prices have more impact on the costs of heat production than changing electricity prices. For HTHP systems changing gas prices are not relevant.

Since economic considerations in industry always include the pay-back time, a breakdown of it for the four considered levels of investment is brought into play and illustrated in ?. The payback time for every case of investment heights is shown for every month and refer to the left axis. It is calculated under the assumption of the given price conditions and are expected to be constant, which of course is not accurate for reality. The outcome of the graph shows that in case of low investment costs, thus 250 EUR/kW<sub>Q</sub> or 500 EUR/kW<sub>Q</sub>, payback time would have been clearly

below ten years the most of the time.

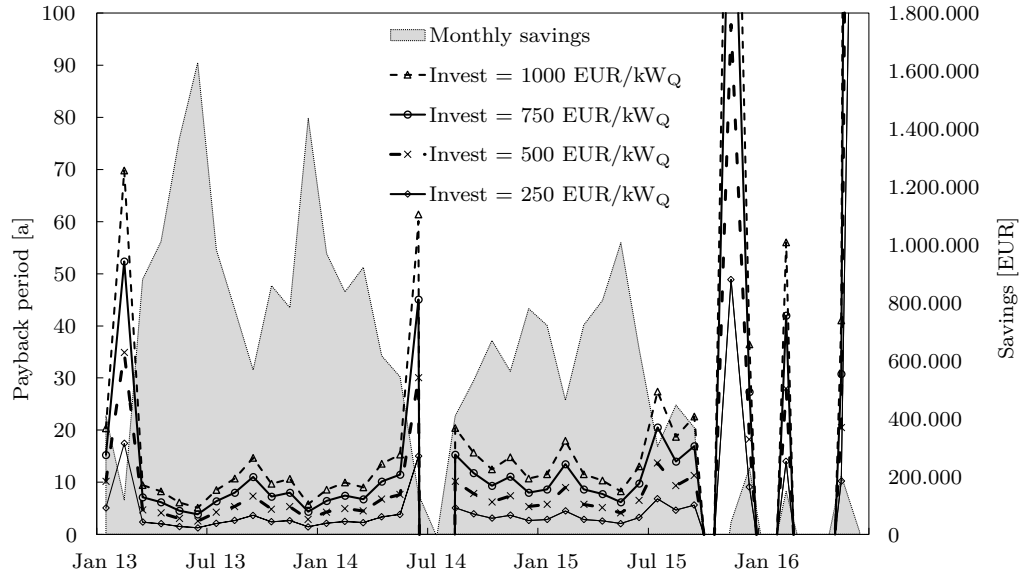


**Figure 6.19:** Pay-back time of a heat pump system working with a  $COP = 4$  substituting a gas and steam turbine process according to different investment costs over a period from January 2013 until June 2016. The diagram also shows the monthly savings by using a HTHP for industrial heat production instead of a GT-CC.

## 6.8 Summary

The focus of this chapter is to assess the thermodynamic efficiency and variable costs of industrial heat supply depending on natural gas and electricity prices for an application in the pulp and paper industry. The exergetic efficiency shows that even with the lowest COP the HP system is thermodynamically most efficient. For the economic analysis the heat generation costs of the individual heat supply processes are calculated and compared. The intersections of the heat generation costs of each heat recovery technology, depending on the electricity price, give information on whether a current production or a current consumption is economically sensible. It is remarkable to see that for the recent European situation of natural gas and electricity prices, the operating cost optimum is clearly on the heat-pump side. Based on consumption related costs, the HTHP system (working with a COP of 4) is the most economic heat production technology, if a gas price of 25 EUR/MWh (basis lower heating value) is assumed and the electricity price is lower than 45 EUR/MWh<sub>el</sub>. Considering capital, operation and service costs, the cumulative costs for the period from January 2013 until June 2016 are calculated on a monthly basis. The results show that, depending on the occurred energy prices, either the GT-CC or the HTHP system were most economic. Based on a monthly analysis, the share of heat supply through the HTHP varies between 45% and 76% and for the GT-CC between 24% and 55%, depending on the assumed investment costs for the HTHP system. For the investigated period, the GT or gas boiler solutions were not economic compared to the combination of GT-CC and HTHP. The sensitivity analysis shows that the fuel-based heat production technologies depend more on the gas price than on the electricity price. This means, gas prices have a higher influence on the costs of heat than electricity prices. An overview of the theoretical amortization time shows that, depending on real electricity prices, the expected pay-back time is subject to intense fluctuations. For investments of 250 EUR/kW<sub>Q</sub> or 500 EUR/kW<sub>Q</sub>, pay-back times would have been below ten years for the energy price situation between January 2013 and May 2014 and between September 2014 and August 2015. The recent development after September 2015 clearly discourages investment in HTHP systems. It should be generally noted that the methodological approach for the economic calculation can be considered conservative with a high interest rate of 5% p.a.

Also the investment costs of the HTHP are considered conservative. At the moment, HTHP systems are no common technology, so the investment costs are quite high. If the technology gets a state of the art technology, like gas and steam turbines, the investment costs can be expected to decrease. This will lead to lower costs of heat and so the HTHP can get an efficient alternative to the common heat production systems. For example a specific investment of 100 EUR/ kW<sub>Q</sub> would increase the share of heat supply of HTHP up to 83%.

The results obtained may serve as a first decision aid for plant operators, whether to provide electricity under economic conditions to the grid or to better consume electricity under favorable conditions from the grid. In general the results of this work can serve as decision aid for industrial plant and electricity grid operators, as electricity can be flexibly produced with CHP in times of high electricity prices, or electricity is purchased from the grid for heat supply using HTHP systems when electricity prices are low. This way, industrial players can contribute to balancing supply and demand

mismatches in the electricity grid both on a daily and on a seasonal basis.

However, political sanctions in the future to raise the climate goals will lead to stricter measures to reduce CO<sub>2</sub> emissions. Potential CO<sub>2</sub> emission penalties would add to the price of fossil fuels and help to shift economics towards the HTHP solution. Currently, electricity prices decrease at EEX. It also can be assumed the prices for fossil fuels (especially oil and gas) will decrease, because of decreased demand caused by their partial substitution with renewable energy. To avoid a relapse to a high share of fossil energy production, stricter measures and adjusted penalties for CO<sub>2</sub> emissions are indispensable.

However, industrial heat pump systems can benefit from the developments in the European energy market, because especially the industrial sector can earn high benefits from favorable electricity prices on the spot market. On the other hand, the already installed gas turbines and steam turbines in the industry can act as decentralized back-up capacities to provide electricity in times when the amount of renewable energy is insufficient to cover the demand.

## 7 Discussion and Conclusion

### 7.1 Discussion

Currently the industrial heat demand is mainly covered with fossil fuels. High temperature heat pumps can contribute to reduce industrial CO<sub>2</sub> emissions. Therefore, one aim of this work was the development of test bench for high temperature heat pump systems to determine efficiency parameters of these systems. The first measurements of the station showed that the cyclic concept of the test bench works in an efficient way. The evaluation of the test station was made with a common heat pump for hot water and space heating. The comparison of COP's, obtained with the test station, correlates with manufacturers data.

To optimize high temperature heat pump systems, several investigations were made. The investigations distinguish between the used working fluid. The obtained results showed clearly that system design influences the efficiency of the system, and an adapted process according to the used type of working fluid can increase the efficiency significant.

For working fluids with a re-entrant saturation line, an excessive suction gas superheating with an internal heat exchanger was examined. The IHX makes it possible to increase the COP of those system up to 63.3% (COP<sub>R236fa</sub>). Comparable results were found in the literature [37, 40, 41].

For working fluids with a bell-shaped saturation line, wet-steam compression is an option. For working fluids, such as ammonia and water, an efficiency increase up to 13.27% was achieved. Furthermore, the compressor discharge temperature drops. This positive effect is confirmed in the literature [98, 99].

The implementation of the wet steam compression still causes technical difficulties. Beside direct injection of condensate into the compressor or into the suction gas, other possibilities exist to decrease the steam quality to  $x < 1$ . In the case of a multi-stage compression process, the working fluid can be intercooled between the compression steps until the two-phase region is reached.

A further possibility is ultrasonic evaporation, in which mist with atomized droplets is generated by an ultrasonic sensors direct in the evaporator unit. These fine moisture enters the compressor and thus leads to the desired cooling effect. Studies on this type of wet steam compaction are currently ongoing and a patent entitled "Kompressionskälteprozess mit Kondensateinspritzung" (A 50684/2016) has been submitted.

In general, for wet vapor compression the compressor type must be chosen carefully. Scroll or screw compressors, which operate in a continuous compression process, are more suitable for wet operation than piston compressors. For piston compressors the probability of damage because of slugging during liquid compression is significantly increased. However, practical tests show that it is possible to operate compressors with a small amount of liquid in the suction gas [100, 101].

In the third part, the implementation of HTHP to an industrial plant, according to thermodynamic and economic factors, was examined. When comparing the exergetic efficiencies, the heat pump technology was, compared to gas turbines and gas and steam turbine combined cycles, the thermodynamically best way. For the observed period from January 2013 to June 2016, amortization times less than 10 years could be achieved, if moderate investment costs ( $<500 \text{ EUR/kW}_{\text{therm}}$ ) were assumed. Between February 2013 and May 2014, as well as in the period between August 2014 and September 2015, the ratio of electricity price to gas price would have favoured the implementation of HTHP. Recent developments, especially the sinking gas prices after September 2015 clearly discourages investment in HTHP systems. For further considerations renewed calculations, with prognostic data for energy prices, need to be carried out. Especially the development of compensation of  $\text{CO}_2$ -emissions could have an economic impact on the implementation of HTHP and future energy systems.

### 7.2 Conclusion

The use of HTHP for industrial process heat production can make an important contribution to the achieved international climate goals. However, the use of this technology is currently restricted to the building sector. In order to drive a broad application in the industrial sector, on the one hand optimized and efficient systems are required. On the other hand, the focus must also be placed on the economic conditions. The present work addresses these topics and shows possibilities for increasing the efficiency of these systems. Based on the obtained results, an efficiency increase through optimizing process design is possible.

In addition, an application case for HTHP is presented, in which an efficient process heat supply is examined, but also economic factors and investment costs of such systems are considered. In conclusion, the results show that the implementation of a HTHP would have been economic for the observed period. Based on this knowledge, plant operators should be motivated to consider about the implementation of HTHP. In addition the outcome of this thesis may serve as a first decision aid for plant operators, whether to provide electricity under economic conditions to the grid or to better consume electricity under favorable conditions from the grid. On the one hand, plant operators can use the results to choose the most economical method for process heat production. On the other hand, the heat pump technology allows an efficient coupling of the heat and electricity sectors. Therefore, HTHP systems, in the case of an broad application, allow for balancing the supply and demand situation in the power grid.

Energy efficiency and renewable energy will play an important role in the future. Electricity may get cheaper on the electricity exchange, so the use of heat pumps may get more economic in the future. Industrial heat pump systems will benefit from this development, because especially the industrial sector can earn high benefits from favorable electricity prices on the spot market. In contrast, it is to be assumed that prices for fossil fuels will also decrease due to falling demand. In order to counteract a rise in fossil fuels, adapted political conditions will be necessary. Finally it is to say that HTHP is no state of the art technology. The assumed investment costs are in a quite high range, but if the technology gets common, also these costs may sink. This, and adopted political conditions, can lead to an broad application of heat pumps in

the industrial sector.

## 7.3 Outlook

The outcome of this work is that HTHP contribute to switch to an efficient and renewable energy system. Therefore, further examinations according to the technical realization of the observed optimization measures is suggested. From the current point of view, a investigation of different compressor systems for wet compression usage is recommended. Especially the suitability of turbo compressors for wet vapor compression should be investigated. From the current perspective, this technology seems promising for wet vapor application.

In addition, the application fields of HTHP are expandable. Novel processes are under development and represent potential applications for HTHP. Especially absorption and desorption processes, using different temperature levels, enable the implementation of heat pump systems.



## References

- [1] Y. Kaya and K. Yokobori. *Environment, energy, and economy: Strategies for sustainability*. Tokyo: United Nations Univ. Press, 1997, X, 381 S. ISBN: 92-808-0911-3.
- [2] EUROSTAT. *Energy balance (June 2017 edition)*. Online Database. Aug. 8, 2017. URL: <http://ec.europa.eu/eurostat/>.
- [3] T. Naegler et al. “Quantification of the European industrial heat demand by branch and temperature level”. In: *International Journal of Energy Research* 39.15 (2015), pp. 2019–2030. ISSN: 1099-114X. DOI: 10.1002/er.3436. URL: <http://dx.doi.org/10.1002/er.3436><http://onlinelibrary.wiley.com/store/10.1002/er.3436/asset/er3436.pdf?v=1&t=j63ktmkc&s=6c6362a6b6b7b23413fd0aaade7e0a390cec2dc4>.
- [4] H. D. Baehr and S. Kabelac. “Der 2. Hauptsatz der Thermodynamik”. In: *Thermodynamik: Grundlagen und technische Anwendungen*. Berlin, Heidelberg: Springer Berlin Heidelberg, 2016, pp. 89–170. ISBN: 978-3-662-49568-1. DOI: 10.1007/978-3-662-49568-1\_3. URL: [https://doi.org/10.1007/978-3-662-49568-1\\_3](https://doi.org/10.1007/978-3-662-49568-1_3).
- [5] J. Ahrendts. “Reference states”. In: *Energy* 5.8-9 (1979), pp. 667–677.
- [6] C. Diederichsen. *Referenzumgebungen zur Berechnung der chemischen Exergie*. Vol. 50. VDI. Düsseldorf: VDI-Verlag, 1991.
- [7] T. Maurer. *Kältetechnik für Ingenieure*. Kältetechnik für Ingenieure. Berlin, VDE Verlag, [2016], 2016. ISBN: 978-3-8007-3935-6.
- [8] H. D. Baehr and S. Kabelac. “Gemische und chemische Reaktionen”. In: *Thermodynamik: Grundlagen und technische Anwendungen*. Berlin, Heidelberg: Springer Berlin Heidelberg, 2012, pp. 235–374. ISBN: 978-3-642-24161-1. DOI: 10.1007/978-3-642-24161-1\_5. URL: [http://dx.doi.org/10.1007/978-3-642-24161-1\\_5](http://dx.doi.org/10.1007/978-3-642-24161-1_5).
- [9] T. Pröll and H. Hofbauer. “Simulation Tool for Biomass Gasification Based Processes”. In: *The Berkeley Electronic Press* (2008).
- [10] SimTech Simulation Technology. *IPSEpro*. June 13, 2017. URL: <http://www.simtechnology.com/CMS/index.php/ipsepro>.
- [11] F. C. Dargam and E. W. Perz. “A decision support system for power plant design”. In: *European Journal of Operational Research* 109.2 (1998), pp. 310–320. ISSN: 0377-2217. DOI: [https://doi.org/10.1016/S0377-2217\(98\)00059-9](https://doi.org/10.1016/S0377-2217(98)00059-9). URL: <http://www.sciencedirect.com/science/article/pii/S0377221798000599>.

- [12] H. D. Baehr and S. Kabelac. “Verbrennungsprozesse und Verbrennungskraftmaschinen”. In: *Thermodynamik: Grundlagen und technische Anwendungen*. Berlin, Heidelberg: Springer Berlin Heidelberg, 2016, pp. 443–526. ISBN: 978-3-662-49568-1. DOI: 10.1007/978-3-662-49568-1\_7. URL: [http://dx.doi.org/10.1007/978-3-662-49568-1\\_7](http://dx.doi.org/10.1007/978-3-662-49568-1_7).
- [13] W. Pohlmann. *Taschenbuch der Kältetechnik*. Vol. 21., überarb. u. erw. Aufl. Berlin [u.a.]: VDE Verlag, 2013, p. 1269. ISBN: 978-3-8007-3393-4.
- [14] European Parliament. *Regulation (EU) Nr. 517/2014 of the European Parliament and of the Council of 16 April 2014 on fluorinated greenhouse gases and repealing Regulation (EC) No 842/2006*. Legal Rule or Regulation. 2014. URL: <http://data.europa.eu/eli/reg/2014/517/oj>.
- [15] K. Reisner. *Fachwissen Kältetechnik eine Einführung für die Aus- und Weiterbildung mit Aufgaben und Lösungen*. 5., überarb. u. erw. Aufl. Berlin [u.a.]: VDE Verl., 2013, X, 310 S. URL: <http://d-nb.info/1031888705/04>.
- [16] P. Linstrom and W. Mallard. *NIST Chemistry WebBook, NIST Standard Reference Database Number 69*. Gaithersburg MD, 20899: National Institute of Standards and Technology, 2017. DOI: doi:10.18434/T4D303.
- [17] E. Lemmon, M. Huber, and M. O. McLinden. *NIST Reference Fluid Thermodynamic and Transport Properties-REFPROP, Version 9.1*. Gaithersburg, 2013.
- [18] H. D. Baehr and R. Tillner-Roth. “Working equations”. In: *Thermodynamische Eigenschaften umweltverträglicher Kältemittel / Thermodynamic Properties of Environmentally Acceptable Refrigerants: Zustandsgleichungen und Tafeln für Ammoniak, R 22, R 134a, R 152a und R 123 / Equations of State and Tables for Ammonia, R 22, R 134a, R 152a and R 123*. Berlin, Heidelberg: Springer Berlin Heidelberg, 1995, pp. 22–37. ISBN: 978-3-642-79400-1. DOI: 10.1007/978-3-642-79400-1\_3. URL: [http://dx.doi.org/10.1007/978-3-642-79400-1\\_3](http://dx.doi.org/10.1007/978-3-642-79400-1_3) [https://link.springer.com/chapter/10.1007/978-3-642-79400-1\\_3](https://link.springer.com/chapter/10.1007/978-3-642-79400-1_3).
- [19] W. Wagner and A. Pruß. “The IAPWS Formulation 1995 for the Thermodynamic Properties of Ordinary Water Substance for General and Scientific Use”. In: *Journal of Physical and Chemical Reference Data* 31.2 (2002), pp. 387–535. DOI: 10.1063/1.1461829. URL: <http://aip.scitation.org/doi/abs/10.1063/1.1461829> <http://aip.scitation.org/doi/10.1063/1.1461829>.
- [20] R. Span and W. Wagner. “A New Equation of State for Carbon Dioxide Covering the Fluid Region from the Triple Point Temperature to 1100 K at Pressures up to 800 MPa”. In: *Journal of Physical and Chemical Reference Data* 25.6 (1996), pp. 1509–1596. DOI: 10.1063/1.555991. URL: <http://aip.scitation.org/doi/abs/10.1063/1.555991> <http://aip.scitation.org/doi/10.1063/1.555991>.
- [21] D. Bücker and W. Wagner. “Reference Equations of State for the Thermodynamic Properties of Fluid Phase n-Butane and Isobutane”. In: *Journal of Physical and Chemical Reference Data* 35.2 (2006), pp. 929–1019. DOI: 10.1063/1.1901687. URL: <http://aip.scitation.org/doi/abs/10.1063/1.1901687> <http://aip.scitation.org/doi/10.1063/1.1901687>.

- [22] E. W. Lemmon, M. O. McLinden, and W. Wagner. “Thermodynamic Properties of Propane. III. A Reference Equation of State for Temperatures from the Melting Line to 650 K and Pressures up to 1000 MPa”. In: *Journal of Chemical & Engineering Data* 54.12 (2009), pp. 3141–3180. ISSN: 0021-9568. DOI: 10.1021/je900217v. URL: <http://dx.doi.org/10.1021/je900217v>.
- [23] R. Tillner-Roth and H. D. Baehr. “An International Standard Formulation for the Thermodynamic Properties of 1,1,1,2 Tetrafluoroethane (HFC 134a) for Temperatures from 170 K to 455 K and Pressures up to 70 MPa”. In: *Journal of Physical and Chemical Reference Data* 23.5 (1994), pp. 657–729. DOI: 10.1063/1.555958. URL: <http://aip.scitation.org/doi/abs/10.1063/1.555958> <http://aip.scitation.org/doi/10.1063/1.555958>.
- [24] E. W. Lemmon and R. Span. “Short Fundamental Equations of State for 20 Industrial Fluids”. In: *Journal of Chemical & Engineering Data* 51.3 (2006), pp. 785–850. ISSN: 0021-9568. DOI: 10.1021/je050186n. URL: <http://dx.doi.org/10.1021/je050186n> <http://pubs.acs.org/doi/pdfplus/10.1021/je050186n>.
- [25] J. Pan et al. “An equation of state for the thermodynamic properties of 1,1,1,3,3,3-hexafluoropropane (HFC-236fa)”. In: *Fluid Phase Equilibria* 321 (2012), pp. 10–16. ISSN: 0378-3812. DOI: <http://dx.doi.org/10.1016/j.fluid.2012.02.012>. URL: <http://www.sciencedirect.com/science/article/pii/S0378381212000830> [http://ac.els-cdn.com/S0378381212000830/1-s2.0-S0378381212000830-main.pdf?\\_tid=491e251e-6723-11e7-8143-00000aacb361&acdnat=1499878871\\_be6f4199dee2f692438abcfa341bbc8e](http://ac.els-cdn.com/S0378381212000830/1-s2.0-S0378381212000830-main.pdf?_tid=491e251e-6723-11e7-8143-00000aacb361&acdnat=1499878871_be6f4199dee2f692438abcfa341bbc8e).
- [26] E. W. Lemmon and R. Span. “Thermodynamic Properties of R-227ea, R-365mfc, R-115, and R-13I1”. In: *Journal of Chemical & Engineering Data* 60.12 (2015), pp. 3745–3758. ISSN: 0021-9568. DOI: 10.1021/acs.jced.5b00684. URL: <http://dx.doi.org/10.1021/acs.jced.5b00684> <http://pubs.acs.org/doi/pdfplus/10.1021/acs.jced.5b00684>.
- [27] M. Richter, M. O. McLinden, and E. W. Lemmon. “Thermodynamic Properties of 2,3,3,3-Tetrafluoroprop-1-ene (R1234yf): Vapor Pressure and  $p$ – $\rho$ – $T$  Measurements and an Equation of State”. In: *Journal of Chemical & Engineering Data* 56.7 (2011), pp. 3254–3264. ISSN: 0021-9568. DOI: 10.1021/je200369m. URL: <http://dx.doi.org/10.1021/je200369m> <http://pubs.acs.org/doi/pdfplus/10.1021/je200369m>.
- [28] M. Thol and E. W. Lemmon. “Equation of State for the Thermodynamic Properties of trans-1,3,3,3-Tetrafluoropropene [R-1234ze(E)]”. In: *International Journal of Thermophysics* 37.3 (2016), p. 28. ISSN: 1572-9567. DOI: 10.1007/s10765-016-2040-6. URL: <http://dx.doi.org/10.1007/s10765-016-2040-6>.
- [29] M. E. Mondéjar, M. O. McLinden, and E. W. Lemmon. “Thermodynamic Properties of trans-1-Chloro-3,3,3-trifluoropropene (R1233zd(E)): Vapor Pressure, ( $p$ ,  $\rho$ ,  $T$ ) Behavior, and Speed of Sound Measurements, and Equation of State”. In: *Journal of Chemical & Engineering Data* 60.8 (2015), pp. 2477–2489. ISSN: 0021-9568. DOI: 10.1021/acs.jced.5b00348. URL: <http://dx.doi.org/10.1021/acs.jced.5b00348>.

- [30] G. Morrison. “The shape of the temperature-entropy saturation boundary”. In: *International Journal of Refrigeration* 17.7 (1994), pp. 494–504. ISSN: 0140-7007. DOI: [http://dx.doi.org/10.1016/0140-7007\(94\)90011-6](http://dx.doi.org/10.1016/0140-7007(94)90011-6). URL: <http://www.sciencedirect.com/science/article/pii/0140700794900116>.
- [31] S. Riepl et al. “Innovative heat pump generates up to  $-100^{\circ}\text{C}$  of coldness and up to  $200^{\circ}\text{C}$  of heat”. In: *Euroheat and Power/Fernwärme International* 44.6 (2015), pp. 28–33. ISSN: 0949166X (ISSN). URL: <https://www.scopus.com/inward/record.uri?eid=2-s2.0-84937426171&partnerID=40&md5=9b7cd1f7635765e1afabe3c7e4253f72>.
- [32] T. Fleckl, M. Hartl, and F. Helminger. “Performance testing of a lab-scale high temperature heat pump with HFO-1336mzz-Z as the working fluid”. In: *European Heat Pump Summit*, p. 25.
- [33] Ochsner Energie Technik GmbH. *Höchsttemperaturwärmepumpe*. Web Page. URL: <http://ochsner-energietechnik.com>.
- [34] H. D. Baehr and S. Kabelac. *Thermodynamik Grundlagen und technische Anwendungen*. 15. Aufl. Berlin [u.a.]: Springer Vieweg, 2012, XIX, 667 S. ISBN: 978-3-642-24160-4. URL: [http://deposit.d-nb.de/cgi-bin/dokserv?id=3949750&prov=M&dok\\_var=1&dok\\_ext=htm%20http://media.obvsg.at/AC09024494-1001](http://deposit.d-nb.de/cgi-bin/dokserv?id=3949750&prov=M&dok_var=1&dok_ext=htm%20http://media.obvsg.at/AC09024494-1001).
- [35] R. Radermacher and Y. Hwang. *Vapor compression heat pumps with refrigerant mixes*. 2005, 307 Seiten. ISBN: 0-8493-3489-6.
- [36] A. A. Kiss and C. A. Infante Ferreira. *Heat pumps in chemical process industry*. 2017, xx, 422 Seiten. ISBN: 978-1-4987-1895-0.
- [37] R. Selbaş, Ö. Kızılkın, and A. Şencan. “Thermoeconomic optimization of subcooled and superheated vapor compression refrigeration cycle”. In: *Energy* 31.12 (2006), pp. 2108–2128. ISSN: 0360-5442. DOI: <http://dx.doi.org/10.1016/j.energy.2005.10.015>. URL: <http://www.sciencedirect.com/science/article/pii/S0360544205002161>.
- [38] N. Felbab. “Condensation of saturated vapours on compression and estimation of minimum suction superheating”. In: *Applied Thermal Engineering* 52.2 (2013), pp. 527–530. ISSN: 1359-4311. DOI: <http://dx.doi.org/10.1016/j.applthermaleng.2012.12.026>. URL: <http://www.sciencedirect.com/science/article/pii/S1359431112008459>.
- [39] R. Mastrullo et al. “A chart for predicting the possible advantage of adopting a suction/liquid heat exchanger in refrigerating system”. In: *Applied Thermal Engineering* 27.14–15 (2007), pp. 2443–2448. ISSN: 1359-4311. DOI: <http://dx.doi.org/10.1016/j.applthermaleng.2007.03.001>. URL: <http://www.sciencedirect.com/science/article/pii/S1359431107000816>.
- [40] S. A. Klein, D. T. Reindl, and K. Brownell. “Refrigeration system performance using liquid-suction heat exchangers”. In: *International Journal of Refrigeration* 23.8 (2000), pp. 588–596. ISSN: 0140-7007. DOI: [http://dx.doi.org/10.1016/S0140-7007\(00\)00008-6](http://dx.doi.org/10.1016/S0140-7007(00)00008-6). URL: <http://www.sciencedirect.com/science/article/pii/S0140700700000086>.

- [41] P. A. Domanski, D. A. Didion, and J. P. Doyle. "Evaluation of suction-line/liquid-line heat exchange in the refrigeration cycle". In: *International Journal of Refrigeration* 17.7 (1994), pp. 487–493. ISSN: 0140-7007. DOI: [http://dx.doi.org/10.1016/0140-7007\(94\)90010-8](http://dx.doi.org/10.1016/0140-7007(94)90010-8). URL: <http://www.sciencedirect.com/science/article/pii/S0140700794900108>.
- [42] C. J. L. Hermes. "Alternative evaluation of liquid-to-suction heat exchange in the refrigeration cycle". In: *International Journal of Refrigeration* 36.8 (2013), pp. 2119–2127. DOI: 10.1016/j.ijrefrig.2013.06.007.
- [43] X.-Q. Cao et al. "Performance analysis of different high-temperature heat pump systems for low-grade waste heat recovery". In: *Applied Thermal Engineering* 71.1 (2014), pp. 291–300. ISSN: 1359-4311. DOI: <http://dx.doi.org/10.1016/j.applthermaleng.2014.06.049>. URL: <http://www.sciencedirect.com/science/article/pii/S1359431114005298>.
- [44] Y. S. Chang, M. S. Kim, and S. T. Ro. "Performance and heat transfer characteristics of hydrocarbon refrigerants in a heat pump system". In: *International Journal of Refrigeration* 23.3 (2000), pp. 232–242. ISSN: 0140-7007. DOI: [http://dx.doi.org/10.1016/S0140-7007\(99\)00042-0](http://dx.doi.org/10.1016/S0140-7007(99)00042-0). URL: <http://www.sciencedirect.com/science/article/pii/S0140700799000420>.
- [45] K.-J. Park and D. Jung. "Performance of heat pumps charged with R170/R290 mixture". In: *Applied Energy* 86.12 (2009), pp. 2598–2603. ISSN: 0306-2619. DOI: <http://dx.doi.org/10.1016/j.apenergy.2009.04.009>. URL: <http://www.sciencedirect.com/science/article/pii/S0306261909001408>.
- [46] Z. Sagia and C. Rakopoulos. "Alternative refrigerants for the heat pump of a ground source heat pump system". In: *Applied Thermal Engineering* 100 (2016), pp. 768–774. ISSN: 1359-4311. DOI: <http://dx.doi.org/10.1016/j.applthermaleng.2016.02.048>. URL: <http://www.sciencedirect.com/science/article/pii/S1359431116301910>.
- [47] B. Palm. "Hydrocarbons as refrigerants in small heat pump and refrigeration systems – A review". In: *International Journal of Refrigeration* 31.4 (2008), pp. 552–563. ISSN: 0140-7007. DOI: <http://dx.doi.org/10.1016/j.ijrefrig.2007.11.016>. URL: <http://www.sciencedirect.com/science/article/pii/S0140700707002216>.
- [48] C. Kondou and S. Koyama. "Thermodynamic assessment of high-temperature heat pumps using low-GWP HFO refrigerants for heat recovery". In: *International Journal of Refrigeration* 53 (2015), pp. 126–141. DOI: 10.1016/j.ijrefrig.2014.09.018. URL: <http://www.sciencedirect.com/science/article/pii/S0140700714002576>.
- [49] G. A. Longo. "The effect of vapour super-heating on hydrocarbon refrigerant condensation inside a brazed plate heat exchanger". In: *Experimental Thermal and Fluid Science* 35.6 (2011), pp. 978–985. DOI: 10.1016/j.expthermflusci.2011.01.018. URL: <https://www.scopus.com/inward/record.uri?eid=2-s2.0-79957598145&partnerID=40&md5=338c00b8ae6f32d1022064b53e686167>.

- [50] RTOC. *UNEP 2014 Report Of The Refrigeration, Air Conditioning And Heat Pumps Technical Options Committee*. Report 978-9966-076-09-0. 2015. URL: <http://conf.montreal-protocol.org/>.
- [51] X. Wu et al. "Performance evaluation of a capacity-regulated high temperature heat pump for waste heat recovery in dyeing industry". In: *Applied Thermal Engineering* 93 (2016), pp. 1193–1201. DOI: 10.1016/j.applthermaleng.2015.10.075. URL: <https://www.scopus.com/inward/record.uri?eid=2-s2.0-84946605472&partnerID=40&md5=3c5159c2f8857060c7369a487e6c5deb>.
- [52] L. Pan et al. "Theoretical and experimental study on several refrigerants of moderately high temperature heat pump". In: *Applied Thermal Engineering* 31.11–12 (2011), pp. 1886–1893. ISSN: 1359-4311. DOI: <http://dx.doi.org/10.1016/j.applthermaleng.2011.02.035>. URL: <http://www.sciencedirect.com/science/article/pii/S1359431111001165>.
- [53] Linde Group. *Linde Industrial Gases*. Web Page. 2016. URL: [www.linde-gas.com/](http://www.linde-gas.com/).
- [54] B. O. Bolaji and Z. Huan. "Ozone depletion and global warming: Case for the use of natural refrigerant – a review". In: *Renewable and Sustainable Energy Reviews* 18 (2013), pp. 49–54. ISSN: 1364-0321. DOI: <http://dx.doi.org/10.1016/j.rser.2012.10.008>. URL: <http://www.sciencedirect.com/science/article/pii/S1364032112005503>.
- [55] J. Daniel et al. *A focus on information and options for policymakers, Chapter 5 in Scientific Assessment of Ozone Depletion: 2010*. Report. World Meteorological Organization, 2011. URL: <https://www.esrl.noaa.gov/csd/assessments/ozone/2010/citations.html>.
- [56] J. Schiffmann and D. Favrat. "Experimental investigation of a direct driven radial compressor for domestic heat pumps". In: *International Journal of Refrigeration* 32.8 (2009), pp. 1918–1928. ISSN: 0140-7007. DOI: <http://dx.doi.org/10.1016/j.ijrefrig.2009.07.006>. URL: <http://www.sciencedirect.com/science/article/pii/S0140700709001686>.
- [57] M. Dillig, M. Jung, and J. Karl. "The impact of renewables on electricity prices in Germany - An estimation based on historic spot prices in the years 2011-2013". In: *Renewable and Sustainable Energy Reviews* 57 (2016), pp. 7–15. DOI: 10.1016/j.rser.2015.12.003. URL: <https://www.scopus.com/inward/record.uri?eid=2-s2.0-84952777508&partnerID=40&md5=2c4d8a570ba058b45ec92e2f215df520>.
- [58] E-Control. *E-Control*. Web Page. 2016. URL: <https://www.e-control.at/statistik/strom/marktstatistik/stromboersen>.
- [59] R. Madlener and C. Schmid. "Combined Heat and Power Generation in Liberalised Markets and a Carbon-Constrained World". In: *GAIA - Ecological Perspectives for Science and Society* 12.2 (2003), pp. 114–120. URL: <http://www.ingentaconnect.com/content/oekom/gaia/2003/00000012/00000002/art00008>.

- [60] S. Mitra, L. Sun, and I. E. Grossmann. “Optimal scheduling of industrial combined heat and power plants under time-sensitive electricity prices”. In: *Energy* 54 (2013), pp. 194–211. ISSN: 0360-5442. DOI: <http://dx.doi.org/10.1016/j.energy.2013.02.030>. URL: <http://www.sciencedirect.com/science/article/pii/S0360544213001448>.
- [61] S. Soltani et al. “A comparative exergoeconomic analysis of two biomass and co-firing combined power plants”. In: *Energy Conversion and Management* 76 (2013), pp. 83–91. ISSN: 01968904 (ISSN). DOI: 10.1016/j.enconman.2013.07.030. URL: <https://www.scopus.com/inward/record.uri?eid=2-s2.0-84882323688&doi=10.1016%2fj.enconman.2013.07.030&partnerID=40&md5=0115403c76811f50bd1bca9987bc03d2>.
- [62] P. K. Sahoo, B. Wolduamlak, and K. M. Singh. “Exergoeconomic optimisation of a cogeneration system using exergy splitting method”. In: *26th International Conference on Efficiency, Cost, Optimization, Simulation and Environmental Impact of Energy Systems, ECOS 2013*. China International Conference Center for Science and Technology. URL: <https://www.scopus.com/inward/record.uri?eid=2-s2.0-84903643303&partnerID=40&md5=0873990240b1bedf71b9910585766d0e>.
- [63] A. G. Kaviri et al. “Modelling and exergoeconomic based design optimisation of combined power plants”. In: *International Journal of Exergy* 13.2 (2013), pp. 141–158. ISSN: 17428297 (ISSN). DOI: 10.1504/IJEX.2013.056130. URL: <https://www.scopus.com/inward/record.uri?eid=2-s2.0-84883591556&doi=10.1504%2fIJEX.2013.056130&partnerID=40&md5=b6164c7b42367823d206e7d0d2f9c124>.
- [64] A. Atmaca and R. Yumrutaş. “Thermodynamic and exergoeconomic analysis of a cement plant: Part i - Methodology”. In: *Energy Conversion and Management* 79 (2014), pp. 790–798. ISSN: 01968904 (ISSN). DOI: 10.1016/j.enconman.2013.11.053. URL: <https://www.scopus.com/inward/record.uri?eid=2-s2.0-84896317050&doi=10.1016%2fj.enconman.2013.11.053&partnerID=40&md5=c21569ae70dfdc6eabf0181d20d99b1>.
- [65] M. Alipour, K. Zare, and B. Mohammadi-Ivatloo. “Short-term scheduling of combined heat and power generation units in the presence of demand response programs”. In: *Energy* 71 (2014), pp. 289–301. ISSN: 0360-5442. DOI: <http://dx.doi.org/10.1016/j.energy.2014.04.059>. URL: <http://www.sciencedirect.com/science/article/pii/S0360544214004721>.
- [66] M. H. Moradi et al. “An energy management system (EMS) strategy for combined heat and power (CHP) systems based on a hybrid optimization method employing fuzzy programming”. In: *Energy* 49 (2013), pp. 86–101. ISSN: 0360-5442. DOI: <http://dx.doi.org/10.1016/j.energy.2012.10.005>. URL: <http://www.sciencedirect.com/science/article/pii/S0360544212007670>.
- [67] H. Cho et al. “Cost-optimized real-time operation of CHP systems”. In: *Energy and Buildings* 41.4 (2009), pp. 445–451. ISSN: 0378-7788. DOI: <http://dx.doi.org/10.1016/j.enbuild.2008.11.011>. URL: <http://www.sciencedirect.com/science/article/pii/S0378778808002454>.

- [68] Z. Beihong and L. Weiding. “An optimal sizing method for cogeneration plants”. In: *Energy and Buildings* 38.3 (2006), pp. 189–195. ISSN: 0378-7788. DOI: <http://dx.doi.org/10.1016/j.enbuild.2005.05.009>. URL: <http://www.sciencedirect.com/science/article/pii/S0378778805000897>.
- [69] X. Q. Kong, R. Z. Wang, and X. H. Huang. “Energy optimization model for a CCHP system with available gas turbines”. In: *Applied Thermal Engineering* 25.2–3 (2005), pp. 377–391. ISSN: 1359-4311. DOI: <http://dx.doi.org/10.1016/j.applthermaleng.2004.06.014>. URL: <http://www.sciencedirect.com/science/article/pii/S1359431104001784>.
- [70] E. Thorin, H. Brand, and C. Weber. “Long-term optimization of cogeneration systems in a competitive market environment”. In: *Applied Energy* 81.2 (2005), pp. 152–169. ISSN: 0306-2619. DOI: <http://dx.doi.org/10.1016/j.apenergy.2004.04.012>. URL: <http://www.sciencedirect.com/science/article/pii/S0306261904000984>.
- [71] A. Najafi et al. “Medium-term energy hub management subject to electricity price and wind uncertainty”. In: *Applied Energy* 168 (2016), pp. 418–433. ISSN: 0306-2619. DOI: <http://dx.doi.org/10.1016/j.apenergy.2016.01.074>. URL: <http://www.sciencedirect.com/science/article/pii/S0306261916300617>.
- [72] B. Bakhtiari et al. “Opportunities for the integration of absorption heat pumps in the pulp and paper process”. In: *Energy* 35.12 (2010), pp. 4600–4606. DOI: [10.1016/j.energy.2010.03.047](http://dx.doi.org/10.1016/j.energy.2010.03.047).
- [73] S. Wolf et al. *Analyse des Potenzials von Industrierärmepumpen in Deutschland*. Report. Universität Stuttgart Institut für Energiewirtschaft und Rationelle Energieanwendung, 2014. URL: [http://www.ier.uni-stuttgart.de/publikationen/veroeffentlichungen/forschungsberichte/downloads/141216\\_Abschluss%20bericht\\_FKZ\\_0327514A.pdf](http://www.ier.uni-stuttgart.de/publikationen/veroeffentlichungen/forschungsberichte/downloads/141216_Abschluss%20bericht_FKZ_0327514A.pdf).
- [74] M. Chamoun et al. “Dynamic model of an industrial heat pump using water as refrigerant”. In: *International Journal of Refrigeration* 35.4 (2012), pp. 1080–1091. DOI: [10.1016/j.ijrefrig.2011.12.007](http://dx.doi.org/10.1016/j.ijrefrig.2011.12.007). URL: <https://www.scopus.com/inward/record.uri?eid=2-s2.0-84861231176&partnerID=40&md5=b745853ade01783f483fac0da33ce717>.
- [75] M. Chamoun et al. “Experimental and numerical investigations of a new high temperature heat pump for industrial heat recovery using water as refrigerant”. In: *International Journal of Refrigeration* 44 (2014), pp. 177–188. ISSN: 0140-7007. DOI: <http://dx.doi.org/10.1016/j.ijrefrig.2014.04.019>. URL: <http://www.sciencedirect.com/science/article/pii/S0140700714000954>.
- [76] B. F. Lachner Jr, G. F. Nellis, and D. T. Reindl. “The commercial feasibility of the use of water vapor as a refrigerant”. In: *International Journal of Refrigeration* 30.4 (2007), pp. 699–708. ISSN: 0140-7007. DOI: <http://dx.doi.org/10.1016/j.ijrefrig.2006.09.009>. URL: <http://www.sciencedirect.com/science/article/pii/S0140700706002039>.

- [77] M. Chamoun et al. "Modelica-based modeling and simulation of a twin screw compressor for heat pump applications". In: *Applied Thermal Engineering* 58.1–2 (2013), pp. 479–489. ISSN: 1359-4311. DOI: <http://dx.doi.org/10.1016/j.applthermaleng.2013.04.020>. URL: <http://www.sciencedirect.com/science/article/pii/S1359431113002901>.
- [78] Y. Ammar et al. "Low grade thermal energy sources and uses from the process industry in the UK". In: *Applied Energy* 89.1 (2012), pp. 3–20. ISSN: 0306-2619. DOI: 10.1016/j.apenergy.2011.06.003. URL: [http://www.sciencedirect.com/S0306261911003734/1-s2.0-S0306261911003734-main.pdf?\\_tid=df2e98b2-0dde-11e6-9fd6-00000aacb35d&acdnat=1461916336\\_6cbf34ef30bbf3d2bb559e23c2711aee](http://www.sciencedirect.com/S0306261911003734/1-s2.0-S0306261911003734-main.pdf?_tid=df2e98b2-0dde-11e6-9fd6-00000aacb35d&acdnat=1461916336_6cbf34ef30bbf3d2bb559e23c2711aee).
- [79] H. Jung and A. Hutter. *Energierückgewinnung in der Papierindustrie*. Report. n.s. URL: [http://www.ptspaper.de/fileadmin/PTS/PTSPAPER/01\\_Ueber\\_uns/Dokumente/Veroeffentlichungen/2010\\_HIT\\_Energierueckgewinnung.pdf](http://www.ptspaper.de/fileadmin/PTS/PTSPAPER/01_Ueber_uns/Dokumente/Veroeffentlichungen/2010_HIT_Energierueckgewinnung.pdf).
- [80] H. Hloch and J. Bohnen. *Ganzheitliche energetische Betrachtung einer Wäscherei als Lösungsansatz für prozessintegrierte Energieeinsparung zur nachhaltigen Steigerung der Energieeffizienz von Wäschereien*. Report. 2012.
- [81] T. Fleiter. *Energieverbrauch und CO<sub>2</sub>-Emissionen industrieller Prozesstechnologien Einsparpotenziale, Hemmnisse und Instrumente*. ISI-Schriftenreihe "Innovationspotenziale". Stuttgart: Fraunhofer-Verl., 2013, III, 562 S. ISBN: 9783839605158. URL: <http://www.gbv.de/dms/tib-ub-hannover/741216000.pdf>.
- [82] Sappi Austria Produktions-GmbH & Co.KG. *Papier erleben*. 2011. URL: <http://www.papiermachtschule.at>.
- [83] K. J. Chua, S. K. Chou, and W. M. Yang. "Advances in heat pump systems: A review". In: *Applied Energy* 87.12 (2010), pp. 3611–3624. ISSN: 0306-2619. DOI: <http://dx.doi.org/10.1016/j.apenergy.2010.06.014>. URL: <http://www.sciencedirect.com/science/article/pii/S030626191000228X>.
- [84] B. Schmitt et al. *SolFood Leitfaden zur Nutzung solarer Prozesswärme in der Ernährungsindustrie*. Report. 2015.
- [85] L. Szabó et al. "A world model of the pulp and paper industry: Demand, energy consumption and emission scenarios to 2030". In: *Environmental Science & Policy* 12.3 (2009), pp. 257–269. ISSN: 1462-9011. DOI: <http://dx.doi.org/10.1016/j.envsci.2009.01.011>. URL: <http://www.sciencedirect.com/science/article/pii/S1462901109000227>.
- [86] V. Uran. "Optimization system for combined heat and electricity production in the wood-processing industry". In: *Energy* 31.14 (2006), pp. 2996–3016. ISSN: 0360-5442. DOI: <http://dx.doi.org/10.1016/j.energy.2005.10.037>. URL: <http://www.sciencedirect.com/science/article/pii/S0360544205002331>.

- [87] Confederation of European Paper Industries. *Key Statistics 2014 European Pulp and Paper Industry*. Web Page. Brussels: Confederation of European Paper Industries, 2015. URL: <http://www.cepi.org/system/files/public/documents/publications/statistics/2015/Key%20Statistics%202014%20FINAL.pdf>.
- [88] F. Sensfuß, M. Ragwitz, and M. Genoese. “The merit-order effect: A detailed analysis of the price effect of renewable electricity generation on spot market prices in Germany”. In: *Energy Policy* 36.8 (2008), pp. 3086–3094. ISSN: 03014215. DOI: 10.1016/j.enpol.2008.03.035.
- [89] K. Würzburg, X. Labandeira, and P. Linares. “Renewable generation and electricity prices: Taking stock and new evidence for Germany and Austria”. In: *Energy Economics* 40, Supplement 1 (2013), S159–S171. ISSN: 0140-9883. DOI: <http://dx.doi.org/10.1016/j.eneco.2013.09.011>. URL: <http://www.sciencedirect.com/science/article/pii/S0140988313002065>.
- [90] R. Green and N. Vasilakos. “Market behaviour with large amounts of intermittent generation”. In: *Energy Policy* 38.7 (2010), pp. 3211–3220. ISSN: 0301-4215. DOI: <http://dx.doi.org/10.1016/j.enpol.2009.07.038>. URL: <http://www.sciencedirect.com/science/article/pii/S0301421509005461>.
- [91] J. Lambauer et al. *Industrielle Großwärmepumpen - Potenziale, Hemmnisse und Best-Practice Beispiele*. Report. Universität Stuttgart Institut für Energiewirtschaft und Rationelle Energieanwendung, 2008.
- [92] I. H. P. Centre. *Annex 35 Application of Industrial Heat Pumps*. Report. IEA Heat Pump Centre, 2014.
- [93] E-Control. *E-Control*. Web Page. 2016. URL: <https://www.e-control.at/de/industrie/gas/gaspreis/industriegaspreise>.
- [94] W. Schneider. *BWL-Crash-Kurs Kosten- und Leistungsrechnung*. Kosten- und Leistungsrechnung. Konstanz: UVK-Verl.-Ges., 2006, 363 S. ISBN: 978-3-8252-2781-4.
- [95] Verein deutscher Ingenieure. “Richtlinienreihe VDI 2067 - Wirtschaftlichkeit gebäudetechnischer Anlagen”. In: *Bauphysik* 25.6 (2003), pp. 408–409. ISSN: 1437-0980. DOI: 10.1002/bapi.200301760. URL: <http://dx.doi.org/10.1002/bapi.200301760>.
- [96] J. Zhang et al. “A comprehensive review on advances and applications of industrial heat pumps based on the practices in China”. In: *Applied Energy* 178 (2016), pp. 800–825. ISSN: 0306-2619. DOI: <http://dx.doi.org/10.1016/j.apenergy.2016.06.049>. URL: <http://www.sciencedirect.com/science/article/pii/S0306261916308248>.
- [97] Siemens. *Siemens Gas Turbines*. Web Page. 2016. URL: <http://www.energy.siemens.com/hq/pool/hq/power-generation/gas-turbines/downloads/gas-turbines-siemens-interactive.pdf>.

- [98] P. P. J. Vorster and J. P. Meyer. “Wet compression versus dry compression in heat pumps working with pure refrigerants or non-azeotropic binary mixtures for different heating applications”. In: *International Journal of Refrigeration* 23.4 (2000), pp. 292–311. ISSN: 0140-7007. DOI: [http://dx.doi.org/10.1016/S0140-7007\(99\)00050-X](http://dx.doi.org/10.1016/S0140-7007(99)00050-X). URL: <http://www.sciencedirect.com/science/article/pii/S014070079900050X>[http://ac.els-cdn.com/S014070079900050X/1-s2.0-S014070079900050X-main.pdf?\\_tid=eb8f4d7c-696d-11e7-bb92-00000aacb360&acdnat=1500130828\\_11709f5188b67091f5987237004bfcd3](http://ac.els-cdn.com/S014070079900050X/1-s2.0-S014070079900050X-main.pdf?_tid=eb8f4d7c-696d-11e7-bb92-00000aacb360&acdnat=1500130828_11709f5188b67091f5987237004bfcd3).
- [99] C. Wu et al. “Study on the characteristics of incomplete wet compression”. In: *Kung Cheng Je Wu Li Hsueh Pao/Journal of Engineering Thermophysics* 37.6 (2016), pp. 1329–1334. URL: <https://www.scopus.com/inward/record.uri?eid=2-s2.0-84975784655&%20partnerID=40&md5=f138d549cf6991e7bfa3ca9a3ef5d515>.
- [100] L. N. Fan, L. R. Tao, and L. H. Yang. “Influence of decreasing suction vapor quality on volumetric efficiency of variable speed rotary compressor”. In: *Shanghai Ligong Daxue Xuebao/Journal of University of Shanghai for Science and Technology* 36.4 (2014), pp. 312–316. DOI: 10.13255/j.cnki.jusst.2014.04.002. URL: <https://www.scopus.com/inward/record.uri?eid=2-s2.0-84908059235&doi=10.13255%2fj.cnki.jusst.2014.04.002&partnerID=40&md5=a5f7c560160c3638e8875edc87ad27d1>.
- [101] J. Yang et al. “Study on mechanical vapor recompression system with wet compression single screw compressor”. In: *Applied Thermal Engineering* 103 (2016), pp. 205–211. DOI: 10.1016/j.applthermaleng.2016.04.053. URL: <https://www.scopus.com/inward/record.uri?eid=2-s2.0-84964462333&doi=10.1016%2fj.applthermaleng.2016.04.053&partnerID=40&md5=3e4314d22ce64cae432084dac319fdd5>.



## List of Tables



## List of Figures



## **A Appendix**

## Curriculum Vitae Dipl.- Ing. Magdalena Wolf

### Personal and contact information

---

Office: Institute of Chemical and Energy Engineering  
BOKU-University of Natural Resources and Life  
Sciences, Vienna  
Peter Jordan Straße 82  
1190 Vienna

Phone: +43 1 47654 89315  
Email: magdalena.wolf@boku.ac.at  
Internet: www.boku.ac.at/ivet

Date of birth: May 01, 1988  
Nationality: Austrian



### Schulische Ausbildung

---

2002 - 2007 Höhere technische Bundeslehranstalt, HTBLA Braunau  
Schwerpunkt Elektronik: Technische Informatik und Bionik

2007 Graduation with excellent outcome

### Academic curriculum

---

2007 - 2011 Bachelor programme Food Science and Biotechnology at University of Natural Resources and Life Science, Vienna

2011 Graduation as Bakk.techn. in Food Science and Biotechnology

Bachelor thesis:  
„Versuche zur Erhöhung der Aussagekraft mikrobiologischer Standardparameter“

2011 – 2013 Master programme Food Science and Technology at University of Natural Resources and Life Science, Vienna

2013 Graduation as Diplomingenieur in Food Science and Technology

Master thesis:  
Nutzung von vertikalen Geokollektoren zum Einsatz für Wärmepumpen

2013 - present PhD studies at Institute of Chemical and Energy Engineering at University of Natural Resources and Life Science, Vienna

PhD thesis:  
Application potential and optimization of high temperature heat pump systems for process heat supply

### Career history and functions (selection)

---

2013 - present Junior researcher  
Institute of Chemical and Energy Engineering, University of Natural Resources and Life Science, Vienna

2011 - 2013 Student assistant  
Institute of Chemical and Energy Engineering, University of Natural Resources and Life Science, Vienna

## Publications

---

1. Wolf, M., Pröll, T., 2016, "Energieoptimierte, industrielle Prozesswärmebereitstellung am Beispiel der Papierindustrie, in Science Research Pannonia Nachhaltige Technologien, S. 277, Pinkafeld, ISBN: 978-3-7011-0372-0
2. Wolf, M., Pröll, T., "Thermodynamic analysis of refrigerants for operation in high temperature heat pump systems" 11th Minisymposium VT, S.115, 2015, Wien, ISBN: 978-3-200-04069-4.
3. Göbl, C., Wolf, M., Pröll, T., Wöss, D., Schumergruber, A., 2015, " Utilisation of waste heat of refrigerating plants through high-temperature heat pumps", BWK 67(10), 44-48.

## Conferences

---

4. Wolf, M., Pröll, T., 2016, "Energieoptimierte, industrielle Prozesswärmebereitstellung am Beispiel der Papierindustrie", enova International Congress, Pinkafeld, 24.-25. November 2016.
5. Wolf, M., Pröll, T., "Operation of a Testing Station for High Temperature Heat Pumps", European Heat Pump Summit, Nuremberg, Germany, October 2015.

## Ongoing projects (selection)

---

1. "Waste heat potentials in the central region of Salzburg and Hallein", principal: Salzburg AG (November 2013 – October 2015)

## Teaching (selection)

---

- team-teaching in lecture "refrigeration Engineering"
- practical courses in energy engineering and chemical engineering
- serval master thesis under supervision

## Master thesis

---

1. Kalthoff, T. (2016): Analysis of part-load performances of a plate heat exchanger in district heating transfer stations
2. Kogler, B. (2016): Bau und Inbetriebnahme eines Hochtemperatur-Wärmepumpenprüfstandes
3. Leitner, A. (2015): Potentiale und Grenzen für den Einsatz von Hochtemperaturwärmepumpen in Fernwärmenetzen, am Beispiel der Fernwärme im Zentralraum Hallein - Salzburg

## Main research areas

---

- Heat pump systems
- District heating systems
- Energy- efficiency and technical heat management
- Refrigeration Engineering